

QUASIELASTIC LIGHT SCATTERING STUDIES OF THE FORMATION
OF MICELLES OF HUMAN APOLIPOPROTEINS A-I AND A-II,
LECITHINS AND BILE SALTS

by

JOANNE MARIE DONOVAN

S.B., Massachusetts Institute of Technology
(1977)

S.M., Massachusetts Institute of Technology
(1980)

SUBMITTED IN PARTIAL FULFILLMENT OF THE
REQUIREMENTS FOR THE DEGREE OF
DOCTOR OF PHILOSOPHY

at the

MASSACHUSETTS INSTITUTE OF TECHNOLOGY

September, 1984

Signature of Author:
Department of Medical Engineering
August 24, 1984

Certified by:
Thesis Supervisor

Accepted by:
Chairman, Departmental Committee

~~SCIENCE~~

MASSACHUSETTS INSTITUTE
OF TECHNOLOGY
SEP 26 1984
LIBRARIES

SCHERING-
PLOUGH LIBRARY

QUASIELASTIC LIGHT SCATTERING STUDIES OF THE FORMATION
OF MICELLES OF HUMAN APOLIPOPROTEINS A-I AND A-II,
LECITHINS AND BILE SALTS

by

Joanne Marie Donovan

Submitted to the Department of Medical Engineering on August 24, 1984, in partial fulfillment of the requirements for the degree of Doctor of Philosophy.

ABSTRACT

In man, high density lipoproteins (HDL) play a crucial role in cholesterol transport. The novel properties of these lipoproteins are largely determined by their protein components, apolipoproteins A-I and A-II (apo A-I and apo A-II). This thesis provides a systematic study of the self association of apo A-I and apo A-II and their interactions with the major membrane lipids of HDL, lecithins, and with bile salts, physiological amphiphiles also associated with HDL and which also play an important role in cholesterol transport in bile. A series of lipid-protein systems of increasing complexity was studied, beginning with apolipoprotein self-interactions and progressing to the interactions of apolipoproteins with lecithins and bile salts. Quasielastic light scattering was used to non-invasively measure mean hydrodynamic radius (\bar{R}_h) of the particles formed as functions of physiologically important variables including apolipoprotein concentration, relative apolipoprotein and lecithin composition, temperature and ionic strength.

The self association of apo A-I in aqueous solution is promoted by increases in protein concentration and ionic strength, and decreases in temperature and guanidine HCl concentration. \bar{R}_h ranges from 28 Å to a maximum of 68 Å. A mathematical model of apo A-I self association is proposed which involves the association of monomers to dimers, progressing stepwise to a limit of octamers. The free energy change for the interaction of four dimers to form an octamer is estimated under various solution conditions, and comparison of these values suggests that hydrophobic forces favor self association, and are weakly counteracted by electrostatic repulsive forces. Apo A-II self association is also promoted by increases in protein concentration and decreases in guanidine HCl concentration, but is unaffected by temperature changes. Understanding apolipoprotein self association provides a basis for further studies on more complex systems.

Apo A-I self association was largely unaffected by bile salts below their critical micellar concentration (CMC),

although by equilibrium dialysis small amounts of bile salts were protein bound. Above the CMC, additional bile salt molecules were bound, and apo A-I dissociated to dimers. This suggests that bile salt binding to native HDL is a consequence of interactions with other HDL components, and that apo A-I present in bile should have no major effect on the size or structure of simple bile salt micelles.

The phase diagram of apo A-I and apo A-II with dimyristoylphosphatidylcholine (DMPC), a synthetic lecithin, was found to consist of three regions: at low lipid/protein ratios, simple apolipoprotein micelles coexist with mixed apolipoprotein/DMPC micelles; at intermediate ratios, mixed micelles exist; and at high ratios, apolipoprotein/DMPC vesicles form. These aggregated species coexist with low concentrations of apolipoprotein monomers. The phase limit (~80% DMPC by weight) shifts to lower % DMPC with decreases in total amphiphile concentration, and increases in temperature. These data are consistent with a model in which a ring of apolipoprotein surrounds a lecithin bilayer. Apo A-I/egg yolk phosphatidylcholine (EYPC) mixed micelles were prepared by diluting a bile salt/EYPC mixed micellar solution to bile salt concentrations below their CMC. The resulting phase diagram with dilute bile salts was very similar to that obtained with DMPC in the absence of bile salts. Therefore, apo A-I and apo A-II/lecithin mixed micelles form in all proportions up to the phase limit. This interaction is spontaneous with DMPC, and is catalyzed by bile salts with EYPC. Previously observed sizes and compositions of native and synthetic HDL particles are explained by the dependence of the phase diagram on different relative compositions of apolipoproteins and lecithin. This suggests that nascent HDL formation may be physiologically catalyzed by bile salts or other detergent amphiphiles found at the sites of HDL synthesis.

Low concentrations of apo A-I affect the micelle to vesicle transition observed upon dilution of bile salt/EYPC mixed micelles: (1) the size of the resultant vesicles increased; (2) with the occurrence of the micelle to vesicle transition at lower total lipid concentrations, the micellar phase was expanded; and (3) the transition from micelles to vesicles was kinetically delayed. At high apo A-I concentrations, this transition was completely abolished, suggesting that bile salts and apo A-I bind interchangeably to the mixed micelles. These findings suggest that apo A-I may be important in determining the physical state of biliary lipids at physiological biliary concentrations of apo A-I.

These studies provide new insights into the physical chemistry of HDL formation, and suggest that not only does apo A-I play an important role in the physical chemistry of HDL, but also influences the physical chemistry of biliary lipids in health and in disease.

Thesis Supervisor: George B. Benedek

Title: Alfred H. Caspary Professor of Physics and Biological Physics

TABLE OF CONTENTS

	PAGE
CHAPTER ONE: INTRODUCTION	10
I. BACKGROUND.....	12
A. HDL.....	12
B. Apo A-I.....	14
C. Apo A-II.....	15
D. Bile Salts.....	15
E. Quasielastic Light Scattering.....	16
II. SUMMARY.....	17
 CHAPTER TWO: THE SELF ASSOCIATION PATTERNS OF HUMAN APOLIPOPROTEINS A-I AND A-II AND INTERACTIONS WITH BILE SALTS: A QUANTITATIVE ANALYSIS BASED ON QUASIELASTIC LIGHT SCATTERING	
I. INTRODUCTION.....	20
II. EXPERIMENTAL.....	22
A. Materials.....	22
1. Bile Salts.....	22
2. Reagents.....	22
3. Apo A-I and Apo A-II.....	22
B. Methods.....	24
1. Solution Preparation.....	24
2. Sample Clarification.....	24
3. Quasielastic Light Scattering.....	24
4. Mean Scattered Light Intensity.....	26
5. Equilibrium Dialysis.....	27
6. High Pressure Experiments.....	28
III. RESULTS.....	29
A. Self Association of Apo A-I.....	29
1. Concentration Dependence.....	29
2. Temperature Dependence.....	31
3. Ionic Strength Effects.....	31
4. Effect of Guanidine HCl.....	35
5. Pressure Effects.....	35
B. Bile Salt/Apo A-I Interactions.....	35
C. Apo A-II Self Association.....	43

	PAGE
IV. DISCUSSION.....	47
A. Theoretical Analysis of Apo A-I Self Association.....	47
B. Effects of Solution Conditions on ΔG_D	60
C. Comparison with Literature Data.....	67
D. Self Association of Apo A-II.....	71
E. Interactions of Apo A-I and Bile Salts.....	74
F. Pathophysiological Correlations.....	76
G. Summary.....	78
REFERENCES.....	79

CHAPTER THREE: THE FORMATION OF MIXED MICELLES AND
VESICLES OF HUMAN APOLIPOPROTEINS A-I AND A-II, LECITHINS
AND THE BILE SALT TAUROCHOLATE: AN INVESTIGATION USING
QUASIELASTIC LIGHT SCATTERING

I. INTRODUCTION.....	83
II. EXPERIMENTAL.....	86
A. Materials.....	86
B. Methods.....	86
1. Solution Preparation.....	86
2. Quasielastic Light Scattering.....	88
3. Chemical Analysis of Phases.....	89
III. RESULTS.....	90
A. Thermodynamic Equilibration of Mixed Micelles and Vesicles.....	90
B. Apo A-I/DMPC Phase Equilibria.....	92
C. Phase Equilibria of Apo A-I/EYPC.....	97
D. Micelle to Vesicle Transition.....	99
E. Apo A-II/DMPC Phase Equilibria.....	110
IV. DISCUSSION.....	112
A. Apo A-I and Apo A-II/Lecithin Phase Equilibria.....	112
B. Apo A-I/EYPC Interactions.....	130
C. Kinetics of the Interaction of Apo A-I and Apo A-II with Lecithin.....	131
D. Pathophysiological Implications.....	132
E. Summary.....	135
REFERENCES.....	136

LIST OF FIGURES

	PAGE
CHAPTER TWO	
Figure 1. Concentration Dependence of Hydrodynamic Radius and Normalized Scattered Light Intensity of Apo A-I.....	30
Figure 2. Concentration Dependence of Hydrodynamic Radius of Apo A-I: Effects of Temperature...	32
Figure 3. Temperature Dependence of Hydrodynamic Radius of Apo A-I.....	33
Figure 4. Concentration Dependence of Hydrodynamic Radius of Apo A-I: Effects of NaCl Concentration.....	34
Figure 5. Concentration Dependence of Hydrodynamic Radius of Apo A-I: Effects of Guanidine HCl.	36
Figure 6. Dependence of Hydrodynamic Radius of Apo A-I on Guanidine HCl Concentration.....	37
Figure 7. Effect of Taurocholate Concentration on Equilibrium Binding to Apo A-I.....	38
Figure 8. Dependence of Hydrodynamic Radius of TC and TC-Apo A-I Solutions on TC Concentration.....	40
Figure 9. Dependence of Hydrodynamic Radius of Bile Salt-Apo A-I Solutions on Bile Salt Concentration.....	42
Figure 10. Concentration Dependence of Hydrodynamic Radius of Apo A-II.....	44
Figure 11. Self Association of Apo A-II: Temperature Dependence of Hydrodynamic Radius.....	45
Figure 12. Self Association of Apo A-II: Dependence of Hydrodynamic Radius on Guanidine HCl Concentration.....	46

	PAGE
Figure 13. Energy Ladder Diagram of Three Proposed Models of Apo A-I Self Association.....	48
Figure 14. Self Association of Apo A-I: Theoretical Dependence of Hydrodynamic Radius and Mean Aggregation Number on Apo A-I Concentration..	53
Figure 15. Dependence of $\Delta G_D/T$ on $1/T$	66
Figure 16. Self Association of Apo A-I: Concentration Dependence of Mean Aggregation Number.....	68
Figure 17. Self Association of Apo A-II: Concentration Dependence of Mean Aggregation Number.....	72
Figure 18. Self Association of Apo A-I: Dependence of Mean Aggregation Number on TC Concentration..	77

CHAPTER THREE

Figure 1. Dependence of Hydrodynamic Radius of Apo A-I/DMPC Micelles on DMPC Content: Effects of Concentration.....	93
Figure 2. Dependence of Hydrodynamic Radius of Apo A-I/DMPC Micelles on DMPC Content: Effects of Temperature.....	95
Figure 3. Dependence of Hydrodynamic Radius of Apo A-I/DMPC Micelles on DMPC Content: Effects of Guanidine HCl.....	96
Figure 4. Dependence of Hydrodynamic Radius of Apo A-I/EYPC/TC Micelles on % EYPC.....	98
Figure 5. Dependence of Hydrodynamic Radius of Apo A-I/EYPC/TC Micelles on % EYPC: Effects of Concentration.....	100
Figure 6. Micelle to Vesicle Transition of TC/EYPC: Effects of TC and Apo A-I in Diluent.....	101-6
Figure 7. Dependence of Hydrodynamic Radius of TC/EYPC/Apo A-I Vesicles on Apo A-I Concentration....	109

	PAGE
Figure 8. Dependence of Hydrodynamic Radius of Apo A-II/ DMPC Micelles on % DMPC: Effects of Concentration.....	111
Figure 9. Dependence of Hydrodynamic Radius of TC/EYPC Micelles on % EYPC: Effects of Total Solute Concentration.....	113
Figure 10. Determination of the IMC of Apo A-I and Apo A-II/Lecithin Mixed Micelles.....	117
Figure 11. Effect of Apo A-I in Diluent Buffer on Apo A-I/DMPC Mixed Micelles.....	120
Figure 12. Tests of Models of Apoprotein/DMPC Mixed Micelles.....	125
Figure 13. Dependence of Hydrodynamic Radius of Apolipoprotein/Lecithin Mixed Micelles on % Lecithin.....	128
Figure 14. Pathophysiological Correlation of Native and Recombinant HDL's with Apo A-I/DMPC Phase Diagram.....	134

LIST OF TABLES

	PAGE
CHAPTER TWO	
Table 1. Calculations of \bar{n} of Apo A-I/TC Mixed Micelles.	41
Table 2. Effect of Apo A-I Concentration on X_A	54
Table 3. Best Fit of F in Model III.....	59
Table 4. Values of ΔG_D at Various Temperatures and NaCl Concentrations.....	61
Table 5. Comparison of Experimental and Theoretical Values of ΔG_{e1}	63
Table 6. Variation of ΔG_D with Guanidine HCl Concentration.....	65
CHAPTER THREE	
Table 1. Comparison of \bar{R}_h of Apo A-I/DMPC Mixed Micelles Prepared by Different Pathways.....	91
Table 2. IMC Values of Apolipoprotein/Lecithin Mixed Micelles.....	118
Table 3. Data Used for Determination of L and α	124

CHAPTER ONE
INTRODUCTION

In the blood of man and other animals, high density lipoproteins (HDL) are important lipid-protein aggregates that may be considered to be pseudomicellar particles. HDL, together with other emulsion type lipoproteins (chylomicrons, very low density lipoproteins, and low density lipoproteins), transports otherwise insoluble lipids within the plasma compartment (Scanu et al., 1982, Tall and Small, 1980). The lipoprotein lipids are heterogeneous, being composed of both membrane lipids, e.g., cholesterol and phospholipids, and non-membrane lipids, e.g., cholesterol esters and triglycerides. The low aqueous solubilities of these compounds (approximately 10^{-20} M for triglycerides and cholesterol esters, 10^{-12} M for phospholipids, and 10^{-8} M for cholesterol) require that their solubilities be augmented by agents which either solubilize or emulsify them. In blood, the major apolipoproteins of HDL solubilize lipids to form complexes of HDL. The second major cholesterol transport system exists in bile, where bile salts form mixed micelles with large amounts of phospholipids and cholesterol. Thus, apolipoproteins in blood and bile salts in bile perform analogous functions of solubilizing cholesterol

and phospholipids. HDL is considered, in part, to transport cholesterol from peripheral tissues to the liver. Within the liver, HDL cholesterol is utilized for structural purposes in membranes, for synthesis of other lipoproteins, for conversion into bile salts and for direct secretion into bile. Therefore, these systems appear to share, albeit in different fluids, the fundamental physiological role of cholesterol movement within the organism and its secretion from one compartment of the organism to another.

It is now appreciated that each system is not isolated from the other: bile salts are present in micromolar concentrations in both systemic and portal circulations (Carey, 1982), and are bound, in part to HDL (Kramer et al., 1979). The major apolipoproteins of HDL, apolipoproteins A-I (apo A-I) and apolipoproteins A-II (apo A-II), have been shown to be present in bile (0.01 mg/ml) (Sewell et al., 1983). In contrast to blood, their physical state is not understood. In addition to associating with otherwise insoluble lipids, both bile salts and apolipoproteins self associate in dilute aqueous solution.

This dissertation will present investigations into the physical-chemical mechanisms of self association of the apolipoproteins and their hetero-association with various membrane lipids and with bile salts. It is hoped that these results will provide new insights into the size, shape, thermodynamics and interactions of these lipids in the native particles.

I. BACKGROUND

A. HDL. Several classes of lipid-protein complexes have been identified by ultracentrifugation of plasma. HDL is operationally defined as the class of serum proteins which are isolated between densities 1.063 and 1.21 g/ml. HDL can be divided into several subclasses on the basis of composition and density, although all classes of HDL have many features in common.

HDL is composed, by weight, of approximately 45% protein and 55% lipids (Morrisett et al., 1977). The two major subclasses of HDL are HDL₃ (mean particle weight 175,000, density 1.125 to 1.21 g/ml, 55% protein and 45% lipid, 40 to 70 Å in diameter by negative staining electron microscopy) and HDL₂ (mean particle weight 32,000, density 1.063 to 1.125 g/ml, 40 to 45% protein and 55 to 60% lipid, 70 to 100 Å in diameter). Two major apolipoproteins are associated with both classes of HDL: apo A-I, comprising 60% of total protein, and apo A-II, 25% of total protein. They are both structural proteins and act to solubilize the otherwise insoluble lipids of HDL. Apo A-I also activates the plasma enzyme lecithin:cholesterol acyl transferase. There are 2 to 5 molecules of apo A-I and 1 molecule of apo A-II in the average HDL complex. Minor constituents present in quantities less than one per HDL particle include apolipoproteins C-I (molecular weight (Mr) 6600, function unknown), C-II (Mr 8500, lipoprotein lipase cofactor), C-III (Mr 8200, lipoprotein lipase inhibitor), D (Mr 20,000, possibly cholesterol ester transfer protein), and E (Mr 35,000, which binds to chylomicron remnant receptors)

(Scanu et al., 1982). The minor apolipoproteins are thought to function as targetting "labels" to facilitate uptake by certain tissues, or as cofactors for enzymes in lipid metabolism. The lipid composition of mature circulating HDL is approximately 44% phospholipid, 6% cholesterol, 28% cholesterol ester, and 16% triglycerides (Tall and Small, 1980). The fatty acid acyl residues of these lipids are predominantly palmitic, oleic, and linoleic acids (Scanu et al., 1982). The apolipoproteins and polar lipids (phospholipids and cholesterol) are considered to cover the surface of the HDL particle, while the less polar (oily) lipids (cholesterol esters and triglycerides) form the interior. Cholesterol, cholesterol ester and triglycerides are thought to be in rapid equilibrium between surface pools and the less polar core (Hamilton and Small, 1981, Hamilton and Small, 1982).

It has been suggested that HDL is secreted in a nascent form (Tall and Small, 1980). Nascent HDL particles are relatively enriched in apolipoproteins and polar lipids, e.g., phospholipids and cholesterol. Their shape differs from that of the mature particle; a bilayer disc of membrane lipids is solubilized by apolipoproteins surrounding the hydrophobic edge composed of the fatty acid chains of the phospholipids. HDL is transformed from the nascent to the mature form by a plasma enzyme which is synthesized in the liver, lecithin: cholesterol acyl transferase. This enzyme is activated by apo A-I and catalyzes the transfer of a fatty acid from the sn-2 position of a surface phospholipid molecule to a surface

cholesterol molecule. This produces one molecule of cholesterol ester and a monoacylphospholipid, typically lysolecithin. Long chain cholesterol esters behave as apolar lipids and are transferred to the apolar core of the molecule by diffusion and dissolution. The lysolecithin dissociates from the particles, is bound to serum albumin, and is transported to the liver. Since the cholesterol esters accumulate between the lipid planes of the phospholipid and cholesterol bilayers, the nascent disc form of HDL is transformed into a quasi-spherical particle, i.e., mature HDL. This process is in constant dynamic flux: as cholesterol ester is formed, phospholipids and cholesterol are constantly being added to HDL particles from membranes and other lipoproteins. Cholesterol ester is also transferred from mature HDL to other lipoproteins by a plasma transfer protein.

B. Apo A-I. Apo A-I is a single chain polypeptide (Mr 28,200). The amino acid sequence has been determined (Baker et al., 1974, Brewer et al., 1978). Structural studies on the solution properties of apo A-I have shown that the secondary conformation is composed of 70% α -helix, 5 to 15% β -pleated sheet, and 15 to 20% random coil (Lux et al., 1982). Upon interaction with lecithin, the content of helical conformation increases at the expense of the random coils. The helix is considered to be an amphipathic (amphiphilic) helix, with one side composed of hydrophobic residues and the other composed of hydrophilic residues of the constituent amino acids. The hydrophobic surface binds HDL lipids, and the hydrophilic

surface interacts with the surrounding aqueous solution. The protein is easily denatured by low concentrations of guanidine HCl (transition midpoint, 1.1M) (Reynolds, 1976). Calorimetric studies have shown that the free energy change upon denaturation is -2.7 kcal/mol (Tall et al., 1976). This value is much smaller than that for soluble globular proteins, and is consistent with the hypothesis that many hydrophobic residues are exposed to the aqueous solution in the native state.

C. Apo A-II. Apo A-II is a single chain polypeptide dimer composed of two identical disulfide linked subunits (total Mr 17,400) (Scanu et al., 1982). It is present in HDL in smaller amounts than apo A-I, about one apo A-II molecule per average HDL complex. The secondary structure of apo A-II is composed of 35% α -helix, 13% β -pleated sheet, and 52% random coil (Lux et al., 1972). It is suggested that apo A-II is also an amphipathic (amphiphilic) helix. Circular dichroic studies show that denaturation of the helix to the random coil form occurs at a low concentration of guanidine HCl (transition midpoint, 0.6M) (Reynolds, 1976). This is similar to the solution behavior of apo A-I.

D. Bile salts. Bile salts are amphiphiles and are the most important class of soluble detergent-like steroid molecules (Carey, 1982). The hydroxylated alicyclic steroid nucleus of the molecules possesses a relatively flat hydrophilic side

and the fused ring system constitutes a convex hydrophobic side. The polar side chain also contributes to the hydrophilic part of the molecule. Self association of bile salts to form micelles has been well characterized (Mazer et al., 1979). Bile salt micelles have the capacity to solubilize membrane lipids, e.g., phospholipids and cholesterol in mixed micelles. The bile salt-lecithin-cholesterol system is a mixed micellar system with many analogies to HDL (Mazer et al., 1980). Bile salts and lecithin form disc shaped micelles, the core of the disc formed by a bilayer of lecithin molecules, as well as dimerized bile salts. The edges of the disc are covered by a bile salt bilayer juxtaposing their hydrophobic sides to the lipids and exposing their hydrophilic sides to the aqueous environment. These discs can solubilize up to about 10 moles cholesterol per 100 moles lipid at equilibrium. The cholesterol molecules are probably intercalated between the lecithin molecules, but may also be on the surfaces of these particles. Employing the technique of quasielastic light scattering (QLS), the size, shape and thermodynamic properties of these systems have been extensively investigated as functions of concentration, composition, ionic strength and temperature (Mazer et al., 1980, Mazer and Carey, 1983).

E. Quasielastic light scattering. We have employed QLS to investigate model systems of HDL. QLS takes advantage of the Brownian movement of particles to measure both the mean

hydrodynamic radius and the breadth of the distribution of particle sizes. QLS has the added advantage of allowing independent changes of many variables of physiological relevance without perturbing effects which are inherent in other techniques, e.g., analytical ultracentrifugation, electron microscopy, which have been widely employed to study these systems. QLS has been extensively used to investigate self associating systems such as classic detergents (Missel et al., 1980), bile salts (Mazer et al., 1979), and proteins (Cohen et al., 1976). QLS has also been used in a few limited studies of model and native lipoproteins (Eigner et al., 1979, Kunitake, et al., 1978, and Morrisett et al., 1974).

II. Summary. This dissertation presents an investigation of the physical chemical properties of HDL through a systematic approach using model systems of increasing complexity. We have begun with an investigation of apolipoprotein-apolipoprotein interactions and continued with the interactions of apolipoproteins with lecithin and bile salts. This is presented in two chapters: one covering the self association of apo A-I and apo A-II and their interactions with bile salts, and the second covering mixed micelle and vesicle formation by apo A-I and apo A-II with two distinct lecithins and the bile salt taurocholate.

REFERENCES

- Baker, H.N., T. Delahunty, A.M. Gotto, Jr., and R.L. Jackson, The Primary Structure of High Density Apolipoprotein Glutamine I, Proc. Natl. Acad. Sci., U.S.A. 71: 3631-3632 (1974).
- Brewer, H.B., Jr., T. Fairwell, A. LaRue, R. Ronan, A. Houser, and T.J. Bronzert, The Amino Acid Sequence of Human Apo A-I, an Apolipoprotein from High Density Lipoprotein, Biochem. Biophys. Res. Commun. 80: 623-630 (1978).
- Carey, M.C., The Enterohepatic Circulation, in The Liver: Biology and Pathobiology (I.M. Arias et al., ed.) 629-665 (1982).
- Cohen R.J., J.A. Jedziniak, and G.B. Benedek, The Functional Relationship Between Polymerization and Catalytic Activity of Beef Liver Glutamate Dehydrogenase. II. Experiment, J. Mol. Biol. 108: 179-199 (1966).
- Eigner, D., J. Schurz, G. Jurgers, and A. Holasek, Molecular Parameters of Lp(a)-lipoprotein by Light Scattering, FEBS Letters 106: 165-168 (1979).
- Hamilton, J.A., and D.M. Small, Solubilization and Localization of Cholesteryl Oleate in Egg Phosphatidylcholine Vesicles, J. Biol. Chem. 257: 7318-7321 (1982).
- Hamilton, J.A., and D.M. Small, Solubilization and Localization of Triglyceride Oleins in Phosphatidylcholine Bilayers: A ¹³C-N.M.R. Study, Proc. Natl. Acad. Sci., U.S.A. 78: 6878-6882 (1981).
- Kramer, W., H. Buscher, W. Gerok, and G. Kurz, Bile Salt Binding to Serum Components: Taurocholate Incorporation into HDLs Revealed by Photoaffinity Labeling, Eur. J. Biochem. 102: 1-9 (1979).
- Kunitake, S.T., E. Loh, V.N. Schumaker, S.K. Ma, C.M. Knobler, Molecular Weight Distributions of Polydisperse Systems: Application to Very Low Density Lipoproteins, Biochemistry 17: 1936-1942 (1978).
- Lux, S.E., R. Hirz, R.L. Shrager, and A.M. Gotto, The Influence of Lipid on the Conformation of Human Plasma High Density Apolipoproteins, J. Biol. Chem. 247: 2598-2606 (1972).
- Mazer, N.A., M.C. Carey, R.F. Kwasnick and G.B. Benedek, Quasielastic Light Scattering Studies of Aqueous Biliary Lipid Systems. Size, Shape and Thermodynamics of Bile Salt Micelles, Biochemistry 18: 3064-3075 (1979).

Mazer, N.A., G.B. Benedek, and M.C. Carey, Quasielastic Light Scattering Studies of Aqueous Biliary Lipid Systems: Mixed Micelle Formation in Bile Salt-Lecithin Solutions, *Biochemistry* 19: 601-615 (1980).

Mazer, N.A. and M.C. Carey, Quasielastic Light Scattering Studies of Aqueous Biliary Lipid Systems: Cholesterol Solubilization and Precipitation in Model Bile Solutions, *Biochemistry* 22: 426-442 (1983).

Missel, P.J., N.A. Mazer, G.B. Benedek, C.Y. Young, and M.C. Carey, Thermodynamic Analysis of the Growth of Sodium Dodecyl Sulfate Micelles, *J. Phys. Chem.* 84: 1044-1057 (1980).

Morrisett, J.D., J.G. Gallagher, K.C. Aune, and A.M. Gotto, Jr., Structure of the Major Complex Formed by Interaction of the Phosphatidylcholine Bilamellar Vesicles and Apolipoprotein-Alanine (Apo A-III), *Biochemistry* 13: 4765-4771 (1974).

Morrisett, J.D., R.L. Jackson and A.M. Gotto, Jr., Lipid Protein Interactions in the Plasma Lipoproteins, *Biochim. Biophys. Acta.* 472: 93-133 (1977).

Reynolds, J.A., Conformational Stability of the Polypeptide Components of Human High Density Serum Lipoprotein, *J. Biol. Chem.* 251: 6013-6015 (1976).

Scanu, A.M., C. Edelstein, and B.W. Shen, Lipid Protein Interactions in the Plasma Lipoproteins. Model: High Density Lipoproteins, in Lipid Protein Interactions (P.C. Jost and O.H. Griffith, eds.) 259-317 (1982).

Sewell, R.B., S.J.T. Mao, T. Kawamoto, and N.F. LaRusso, Apolipoproteins of High, Low, and Very Low Density Lipoproteins in Human Bile, *J. Lipid Res.* 24: 391-401 (1983).

Tall, A.R. and D.M. Small, Body Cholesterol Removal: Role of Plasma High Density Lipoproteins, *Adv. Lipid Res.* 17: 1-51 (1980).

Tall, A.R., G.G. Shipley, and D.M. Small, Conformational and Thermodynamic Properties of Apo A-I of Human Plasma High Density Lipoproteins, *J. Biol. Chem.* 251: 3749-3755 (1976).

CHAPTER TWO

THE SELF ASSOCIATION PATTERNS OF HUMAN APOLIPOPROTEINS

A-I AND A-II AND INTERACTIONS WITH BILE SALTS:

A QUANTITATIVE ANALYSIS BASED ON QUASIELASTIC LIGHT SCATTERING

I. INTRODUCTION

The bile salts are soluble amphiphilic lipids which form mixed micelles with otherwise insoluble hepatocyte membrane lipids, e.g., phospholipids and cholesterol, and thus promote their secretion into the gastrointestinal tract (Carey, 1982). In blood apolipoproteins A-I and A-II (apo A-I and apo A-II) perform analogous functions in solubilizing phospholipids and cholesterol in high density lipoproteins (HDL). These are pseudomicellar particles which are considered to transport cholesterol from peripheral tissues to the liver (Tall and Small, 1980). Bile salts are present in micromolar concentrations in systemic blood and in higher concentrations in portal blood (Carey, 1982) and apo A-I and apo A-II have been shown to be present at concentrations of approximately 0.010 mg/ml in human gallbladder bile (Sewell, et al., 1983). It therefore becomes important to understand the size, structure, thermodynamics and physical-chemical interactions between these

detergent-like molecules. Both apo A-I and apo A-II and bile salts self and hetero-associate in solution, and an extensive literature exists on self association of each molecular class employing a variety of physical-chemical techniques (Scanu et al., 1982, Carey, 1983). However, self association studies with apo A-I and apo A-II and their interactions with bile salts have been contradictory and limited by the inability to obtain direct information on self association above the monomer concentration (Scanu et al., 1982).

We have systematically studied the self association patterns of apo A-I and apo A-II in aqueous solution and investigated their interactions with the major lipid components (lecithin and cholesterol) of HDL, and with bile salts. We employed the the technique of quasielastic light scattering (QLS). This technique allows the non-invasive measurement of particle size as a function of variables of physiological interest (concentration, ionic strength, temperature, and guanidine HCl concentration) without perturbing the samples. Our aims were (1) to obtain direct information on the size and structure of the equilibrium self association products of apo A-I and apo A-II under varying physical-chemical conditions of pathophysiological importance and (2) to construct a basic molecular and thermodynamic framework for further studies of apo A-I and apo A-II/membrane lipid (lecithin and cholesterol) interactions which occur in nascent serum HDL particles and possibly in biliary mixed micelles and vesicles.

II. EXPERIMENTAL

A. Materials

1. Bile Salts. Bile salts (Calbiochem-Behring, LaJolla, CA), were purified (Norman, 1955, and Pope, 1967), and gave a single spot following a 200 μ g application on thin layer chromatography (Hofmann, 1962). Sodium ^{14}C -taurocholate (New England Nuclear, Boston, MA) had a specific activity of 50 mCi/mmole, and was greater than 98% radiochemically and chemically pure on TLC by plate scraping and scintillation counting.
2. Reagents. Urea (Bethesda Research Labs, Galthersburg, MD) was purified by passage of a 6M aqueous solution through an ion exchange column (Mixed Bed Resin, Biorad, Richmond, CA). NaCl (Mallenckrodt, Paris, KY) was roasted 3 hours at 500°C to oxidize and remove organic impurities. All other chemicals were reagent grade. Pyrex glassware was alkali washed overnight in EtOH-2M KOH (1:1, v:v), followed by 24 hour acid washing in 1M HNO₃, and rinsed thoroughly in filtered, deionized and glass distilled water.
3. Apo A-I and Apo A-II. HDL was isolated from fresh citrate-dextrose human plasma (American Red Cross, Boston, MA) by the phosphotungstate precipitation method (Burststein and Scholnick, 1973). The solution density was increased to 1.21 g/ml by the addition of solid KBr (Hatch and Lees, 1967). Two ultracentrifugal flotations (120,000 g, 20 hr, 18°C) yielded HDL which gave a single immunoprecipitation line against combined anti-human-apo A-I and anti-human-apo A-II antisera (Calbiochem-Behring,

LaJolla, CA) and no reaction with anti-human-LDL, anti-human-IgG (Miles Research Products, Elkhart, IN) or anti-human-albumin antisera (Calbiochem-Behring, LaJolla, CA). HDL was delipidated by extraction with diethyl ether and ethanol (3:2, v:v), at -10°C in a NaCl-ice-water bath (Scanu and Edelstein, 1971). Choline containing phospholipid contamination was less than 0.4% (by weight) when assayed by the choline oxidase method (Gurantz et al., 1981).

The holo apo-HDL was dried at 10 mtorr, dissolved in buffer (6M urea, 0.01M Tris, 0.001M NaN_3 , pH 8.6), and apo A-I and apo A-II were separated by gel chromatography using Sephacryl S-200 (Pharmacia Fine Chemicals, Piscataway, NJ). The separation was monitored by 0.1% SDS-polyacrylamide gel electrophoresis (Weber and Osborn, 1975). Apo A-I and apo A-II were rechromatographed (up to a total three times) until there was a single band present on 0.1% SDS-polyacrylamide gel electrophoresis (protein application of 100 μg). Both apo A-I and apo A-II gave specific immunoprecipitation patterns against either rabbit anti-human apo A-I or apo A-II antisera (courtesy of Dr. Angelo Scanu, Dept. of Biochemistry and Medicine, University of Chicago Medical School, Chicago, IL).

Following gel chromatography, the apo A-I and apo A-II were obtained by dialysis with four changes of buffer (0.15M NaCl, 0.01M Tris, 0.001M NaN_3 , pH 7.6) at 4°C , and stored at 4°C . All solutions in this study contained Tris- NaN_3 at the above concentration and pH. Protein concentrations were determined

spectrophotometrically using extinction coefficients of 32,350 L/mole/cm at 280 nm for apo A-I (Formisano et al., 1978) and 12,100 L/mole/cm for apo A-II (Stone and Reynolds, 1975). Apo A-I and apo A-II were also assayed by the method of Lowry et al. (1951) using bovine serum albumin (Sigma Chemical Co., St. Louis, MO) as a standard.

B. Methods

1. Solution Preparation. A series of aqueous apo A-I and apo A-II solutions (0.2 to 1.8 mg/ml) in guanidine HCl (0.25, 0.50, 1.0 and 2.0M) were prepared by mixing protein and 4.0M guanidine HCl solutions. Prior to use, the guanidine stock solution was filtered through a 0.22 μ filter (Millipore, Bedford, MA). Apo A-I solutions with various NaCl concentrations (0.15, 0.5, 1.0 and 2.0M) were prepared by mixing aqueous apo A-I and variable volumes of 4.0M NaCl solutions.

2. Sample Clarification. To remove dust for light scattering analysis, solutions were centrifuged in acid washed cylindrical scattering cells (6x50mm, Kimble, Toledo, OH) at 10,000g for 10 minutes to one hour. With dilute, weakly scattering samples, centrifugation for up to 15 hours was required. The centrifugal forces generated were insufficient to induce a protein concentration gradient within the scattering cells. This was verified by centrifugation for 30 hours which produced particle sizes which did not differ from those measured after 15 hours.

3. Quasielastic Light Scattering. The Brownian motion of particles results in temporal fluctuations in the intensity of

scattered laser light. The autocorrelation function, $\frac{R(\tau)}{R(0)}$, of the scattered light intensity is given by

$$\frac{R(\tau)}{R(0)} = \left(\sum_{n=1} G_n e^{-\Gamma_n \tau} \right)^2 \quad (1)$$

(Missel et al., 1980). The decay constant of the n th particle species, Γ_n , is equal to D_n/q^2 where q is the magnitude of the scattering vector and D_n is the diffusion coefficient of the n th particle species. For a monodisperse system, the decay constant, Γ , is proportional to $1/D$, where D is the diffusion coefficient. The autocorrelation function of each species, is weighted by the fraction of light scattered by each species:

$$G_n = \frac{C_n M_n}{\sum C_n M_n} \quad (2)$$

where C_n and M_n are the weight concentration and the molecular weight respectively of the n th species. The mean translational diffusion coefficient, \bar{D} , is calculated from the average decay constant: $\bar{D} = \bar{\Gamma}/q^2$, where $\bar{\Gamma}$ is defined as $\sum G_n \Gamma_n$. Using \bar{D} , the mean hydrodynamic radius, \bar{R}_h , is then calculated using the Stokes-Einstein relationship:

$$\bar{D} = \frac{k_B T}{6 \pi \eta \bar{R}_h} \quad (3)$$

where k_B is the Boltzman constant, T is the absolute temperature, and η is the viscosity of the solvent. Further details of the apparatus and the data analysis can be found elsewhere (Mazer and Carey, 1983). Values of the viscosity and refractive index for guanidine HCl solutions were obtained from Kawahara and Tanford (1966).

The polydispersity or variance of particle size, V , is given as a percentage. This value represents a measure of the width of a population distribution which is assumed to be unimodal. The variance function is weighted by the molecular weight of each species and its diffusion coefficient:

$$V = 100 \times \frac{(\overline{D^2} - \bar{D}^2)^{\frac{1}{2}}}{\bar{D}} \% \quad (4)$$

Each experimental result given is the average of \bar{R}_h values derived from analysis of three to five autocorrelation functions accumulated over a time period of ten seconds to five minutes. For some dilute solutions that scattered light weakly, only one or two autocorrelation functions were obtained. Temperature was thermostatically controlled within 0.5°C by a Peltier thermostatic device. \bar{R}_h values of the particles in various apo A-I and apo A-II solutions were measured at several temperatures over the range 10 to 50°C . Samples were allowed to equilibrate for 15 minutes at a given temperature. Longer equilibration times (up to 2 hours) did not change the measured \bar{R}_h values.

4. Mean Scattered Light Intensity. The relative intensity of the scattered light (90° angle) of apo A-I solutions (0.09 to 1.8 mg/ml) was also measured. The normalized mean intensity \bar{I} is defined as

$$\bar{I} = \frac{I_a - I_o}{I_o} \quad (5)$$

where I_a and I_o are the absolute intensities scattered from

solutions of apo A-I, and from the buffer alone, respectively. The intensity of the scattered light from a self associating solution depends on the mole fraction of each species, X_n , and the aggregation number of each species, n . Therefore, \bar{I} is proportional to $\sum n^2 X_n$. The weight average aggregation number, \bar{n} , is defined as

$$\bar{n} = \frac{\sum n^2 X_n}{\sum n X_n} \quad (6)$$

Because \bar{I} is proportional to $\sum n^2 X_n$, \bar{n} is proportional to $\bar{I}/\sum n X_n$. Since $\sum n X_n$ is the total molar concentration of monomers in any aggregation form, \bar{n} is also proportional to \bar{I}/C where C is the weight concentration of apo A-I.

5. Equilibrium Dialysis. Equilibrium dialysis of apo A-I (1 mg/ml) was carried out with taurocholate (TC) concentrations ranging from 0.15 to 70mM at 22°C. A 1 ml solution of apo A-I (1 mg/ml) in buffer was dialyzed against a 1 ml ^{14}C -TC solution in the same buffer. Equilibrium dialysis cells (1 ml) were separated by Spectrapor 2 dialysis membranes. To determine the time required for equilibration 0.05 ml aliquots from both cells were withdrawn at several intervals up to 72 hours and the TC concentration measured by scintillation counting. After 24 hours, 99% of the value at 72 hours was attained. Therefore for subsequent experiments, duplicate aliquots (0.100 ml) were withdrawn from each cell at 24 and 48 hours. Both \bar{R}_n and mean scattered intensity were measured at fixed apo A-I and various TC concentrations for the apo A-I/TC solution as well as the equilibrated TC solutions.

6. High Pressure Experiments. The \bar{R}_h of a 1 mg/ml apo A-I solution was measured at various pressures (1, 10, 20, 30, 40, 50, 75, 100, 200, and 500 atm) at 37°C in a high pressure cell which is described fully elsewhere (Fisch and Benedek, 1984). Following each change in pressure the apo A-I solution was equilibrated for 2 hours during which several measurements of \bar{R}_h were made. At 100 atm the sample was allowed to equilibrate for 15 hours. The hydrostatic pressure in the cell was measured with a manganin pressure gauge (Bridgman, 1931).

III. RESULTS

A. Self Association of Apo A-I

1. Concentration Dependence. Figure 1 shows the dependence of \bar{R}_h (\AA , left vertical axis) on total apo A-I concentration (mg/ml and μM , horizontal axes). Between apo A-I concentrations of 0.1 and 1.0 mg/ml, \bar{R}_h increases sharply as apo A-I concentration increases. At higher apo A-I concentrations, \bar{R}_h levels off and approaches an asymptotic value of approximately 68 \AA . The solid and dashed lines in Figure 1 are calculated from theories to be described later which assume step-wise self association of apo A-I from monomers to dimers and from dimers to limiting octamers with increasing concentration. Utilizing four separate plasma preparations of apo A-I (Figure 1), the data dispersion of \bar{R}_h values is approximately the same as the experimental error ($\pm 2\%$). At an apo A-I concentration of 1.8 mg/ml (in the plateau region), the polydispersity (V) of the micelles was approximately 25%, indicating a relatively monodisperse population. At lower apo A-I concentrations, V of the particles with smaller radii increased to 40 to 50%. This increase may be partly artifactual, due to a decrease in the signal to noise ratio.

In Figure 1, \bar{I}/C is also plotted on the right vertical axis against apo A-I concentration. As apo A-I concentration increases, there is a sharp increase in \bar{I}/C , reaching a plateau value at higher concentrations. Since \bar{n} is proportional to \bar{I}/C , \bar{n} , the weight average aggregation number, increases by a factor of 2.4 over the apo A-I concentration range 0.1 to 1.8 mg/ml.

CONCENTRATION DEPENDENCE OF HYDRODYNAMIC RADIUS AND NORMALIZED SCATTERED LIGHT INTENSITY OF APO A-I

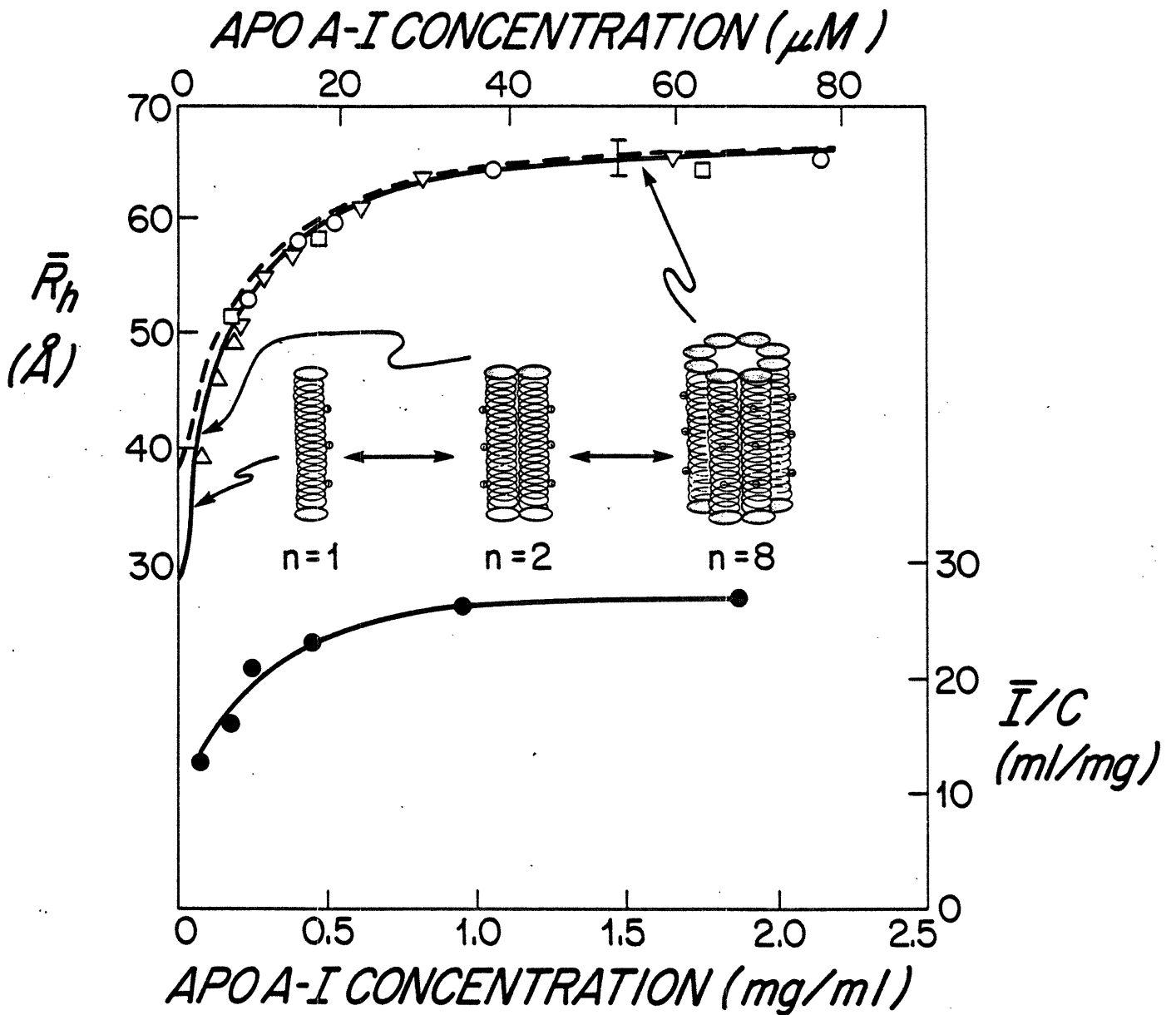


Figure 1. Concentration dependence of \bar{R}_h and normalized scattered light intensity (\bar{I}/C) of apo A-I (0.15M NaCl, 37°C, 1 atm). Measurements from four separate apo A-I preparations are shown (\circ ∇ \triangle \square). Error bar denotes experimental error in \bar{R}_h . Dashed and solid lines are based on theoretical models I and III for \bar{R}_h .

2. Temperature Dependence. In Figure 2, the dependence of \bar{R}_h (\AA) is plotted against apo A-I concentration (mg/ml) for several temperatures (10 to 50°C). At all temperatures there is a modest increase in \bar{R}_h with concentration, and the \bar{R}_h values level off at higher concentrations. However as temperature is increased, the increase in \bar{R}_h with concentration occurs at progressively higher concentrations. The solid curves are theoretically derived from a mathematical model to be described below. The temperature dependence (10 to 50°C) of \bar{R}_h is replotted in Figure 3 for three apo A-I concentrations (1.7, 0.85, and 0.42 mg/ml). \bar{R}_h changes little with increases in temperature up to 37°C and then decreases steeply up to 50°C . Between 10 and 50°C , with all increments or decrements in temperature, \bar{R}_h attained its new equilibrium value within 15 minutes. These changes were fully reversible.

At temperatures above 50°C , \bar{R}_h of apo A-I increased continuously over a period of several hours, to values of 100 to 200 \AA (not plotted). Upon lowering the temperature to 37°C , \bar{R}_h did not return to previous values. This suggests irreversible denaturation of apo A-I which has been documented to occur at 54°C by other methods (Tall et al., 1975).

3. Ionic Strength. Figure 4 demonstrates how the dependence of \bar{R}_h on apo A-I concentration (at 37°C) varies with increases in ionic strength. At all NaCl concentrations between 0.15 and 2.0M, \bar{R}_h increases strongly with apo A-I concentration, and asymptotically approaches a limiting value of 66 \AA .

CONCENTRATION DEPENDENCE OF HYDRODYNAMIC RADIUS OF APO A-I EFFECTS OF TEMPERATURE

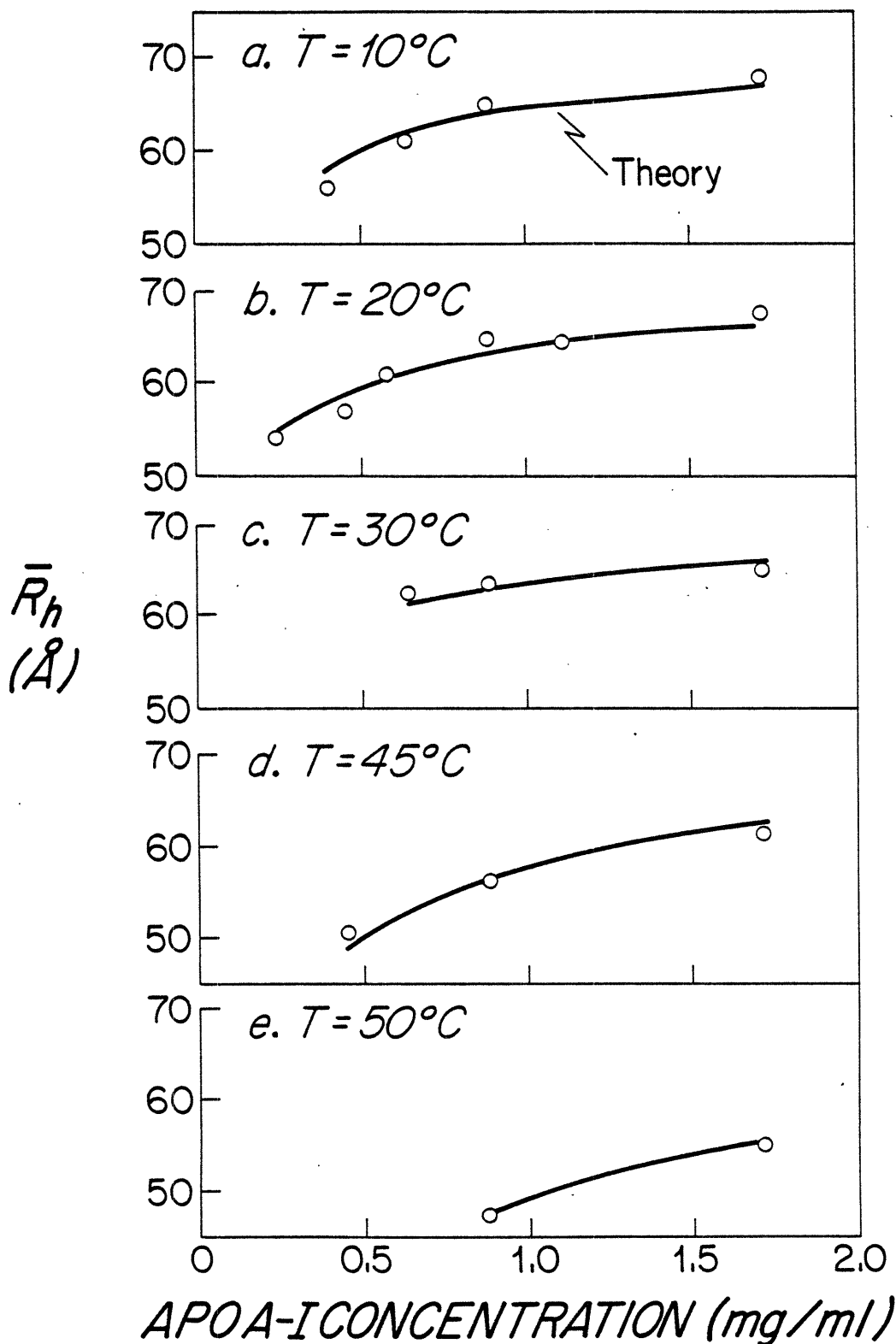


Figure 2. Concentration dependence of \bar{R}_h of apo A-I: effects of temperature (0.15M NaCl, 1 atm): a. 10°C ; b. 20°C ; c. 30°C ; d. 45°C ; e. 50°C .

TEMPERATURE DEPENDENCE OF HYDRODYNAMIC RADIUS OF APO A-I

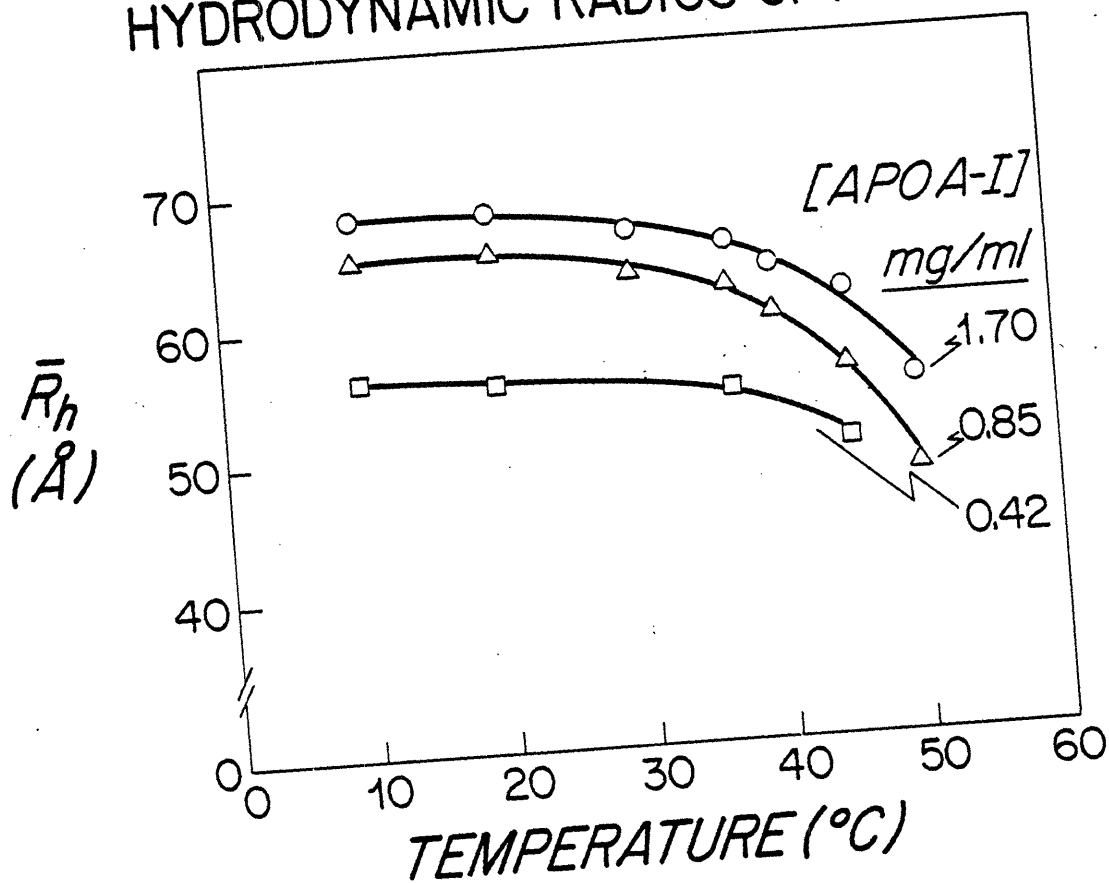


Figure 3. Dependence of \bar{R}_h on temperature at fixed apo A-I concentrations (0.15M NaCl, 1 atm): \circ 1.7 mg/ml; \triangle 0.85 mg/ml; \square 0.42 mg/ml.

CONCENTRATION DEPENDENCE
OF HYDRODYNAMIC RADIUS OF APO A-I
EFFECTS OF NaCl CONCENTRATION

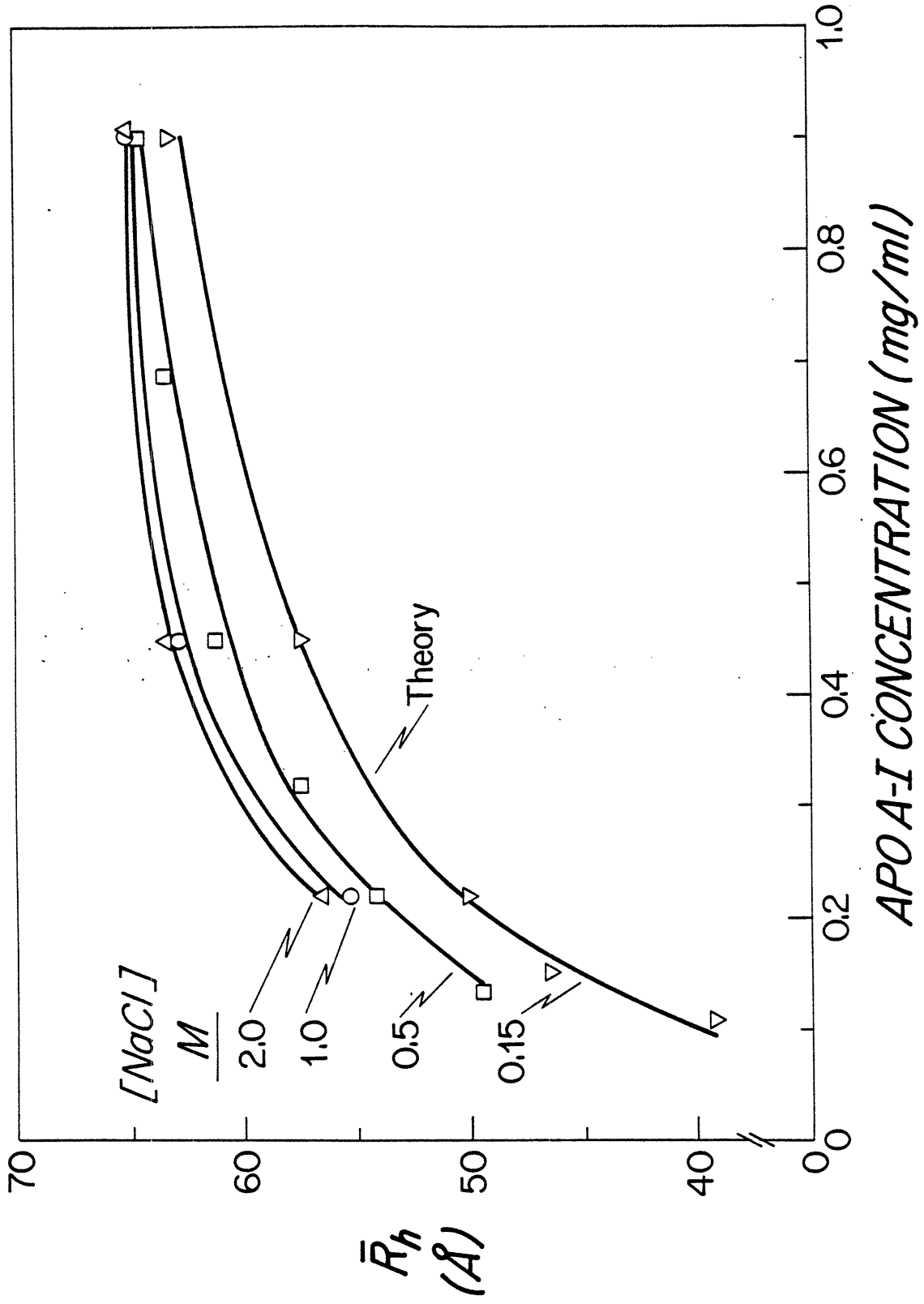


Figure 4. Concentration dependence of \bar{R}_h of apo A-I: effect of NaCl concentration (37°C, 1 atm): ∇ 0.15M NaCl; \square 0.5M NaCl; \circ 1.0M NaCl; \triangle 2.0M NaCl. Solid lines based on theoretical Model I described in text.

4. Effect of Guanidine HCl. Figure 5 demonstrates how the dependence of \bar{R}_h on apo A-I concentration (at 20°C) varies as guanidine HCl concentration increased from 0 to 2.0M. At the higher guanidine HCl concentrations, \bar{R}_h did not approach the limiting value of 68 Å observed in the absence of guanidine HCl. At 2.0M guanidine HCl, \bar{R}_h (28 Å) did not change with apo A-I concentration. In Figure 6, we replot these data to demonstrate the dependence of \bar{R}_h on guanidine concentration at fixed apo A-I concentrations (1.8, 0.9 and 0.45 mg/ml). It is apparent that \bar{R}_h approaches a limiting value of approximately 28 Å irrespective of the initial apo A-I concentration.

5. Pressure Effects. At pressures which ranged from 1 to 500 atmospheres, the \bar{R}_h of a 1 mg/ml apo A-I solution remained constant at 63 ± 2 Å (not plotted). This value did not vary when the equilibration time was extended to 15 hours at 100 atm. After exposure to the highest pressures, the concentration dependence of the sample was measured at 1 atm pressure and found to be identical to earlier data at 1 atm. These results exclude the possibility that high pressures may irreversibly denature apo A-I.

B. Bile Salt-Apo A-I Interactions. Figure 7 depicts the equilibrium binding curve (solid line) of TC and apo A-I (1 mg/ml) plotted as moles TC bound per mole apo A-I against TC concentration (mM). At concentrations well below the CMC of TC (approximately 3 mM) (Carey and Small, 1969), less than

CONCENTRATION DEPENDENCE OF HYDRODYNAMIC RADIUS OF APO A-I EFFECTS OF GUANIDINE HCl

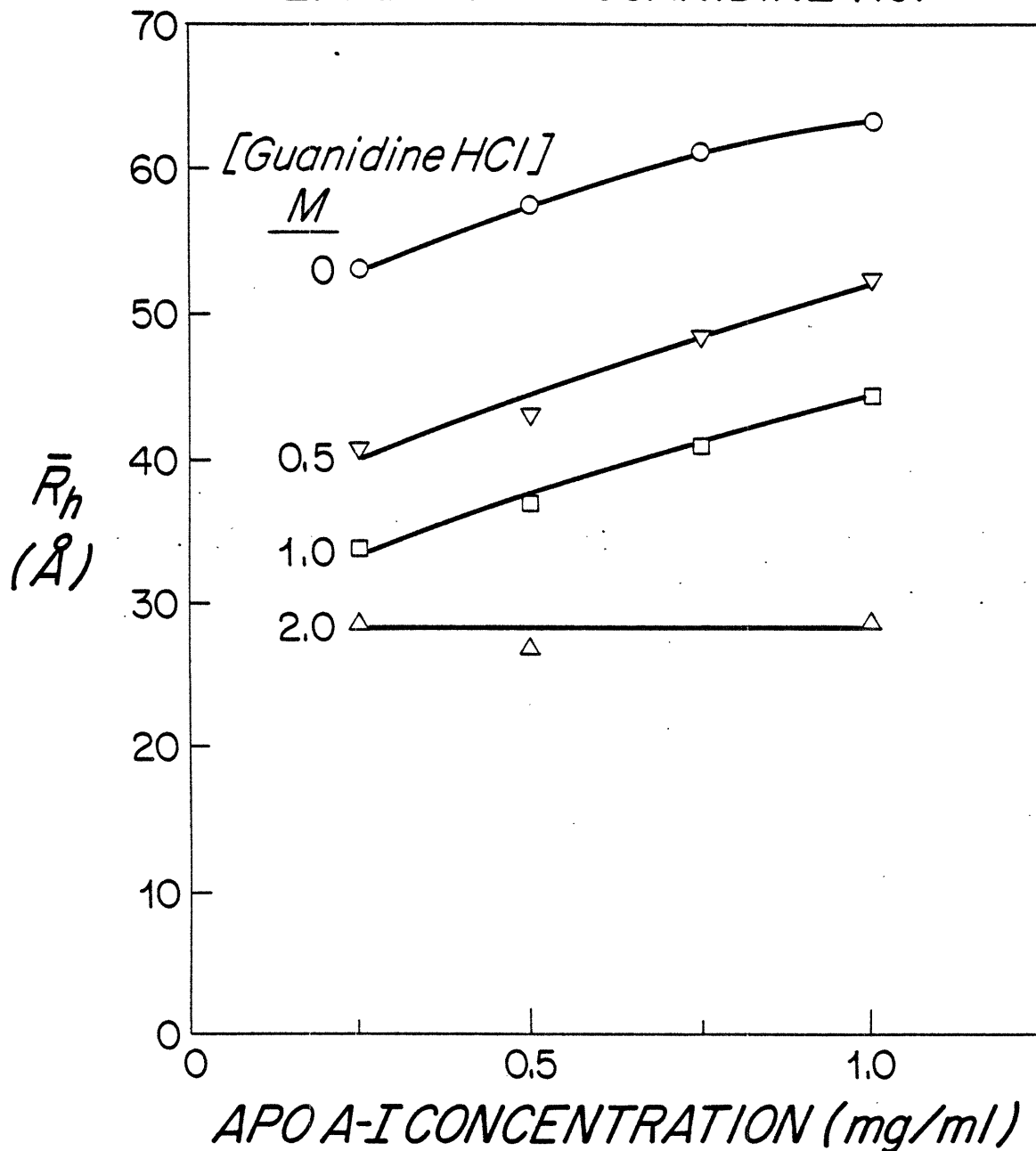


Figure 5. Dependence of \bar{R}_h on apo A-I concentration at various guanidinium HCl concentrations (0.15M NaCl, 37°C, 1 atm): ○ 0.0M; ▽ 0.5M; □ 1.0M; △ 2.0M.

DEPENDENCE OF HYDRODYNAMIC RADIUS OF APO A-I ON GUANIDINE HCl CONCENTRATION

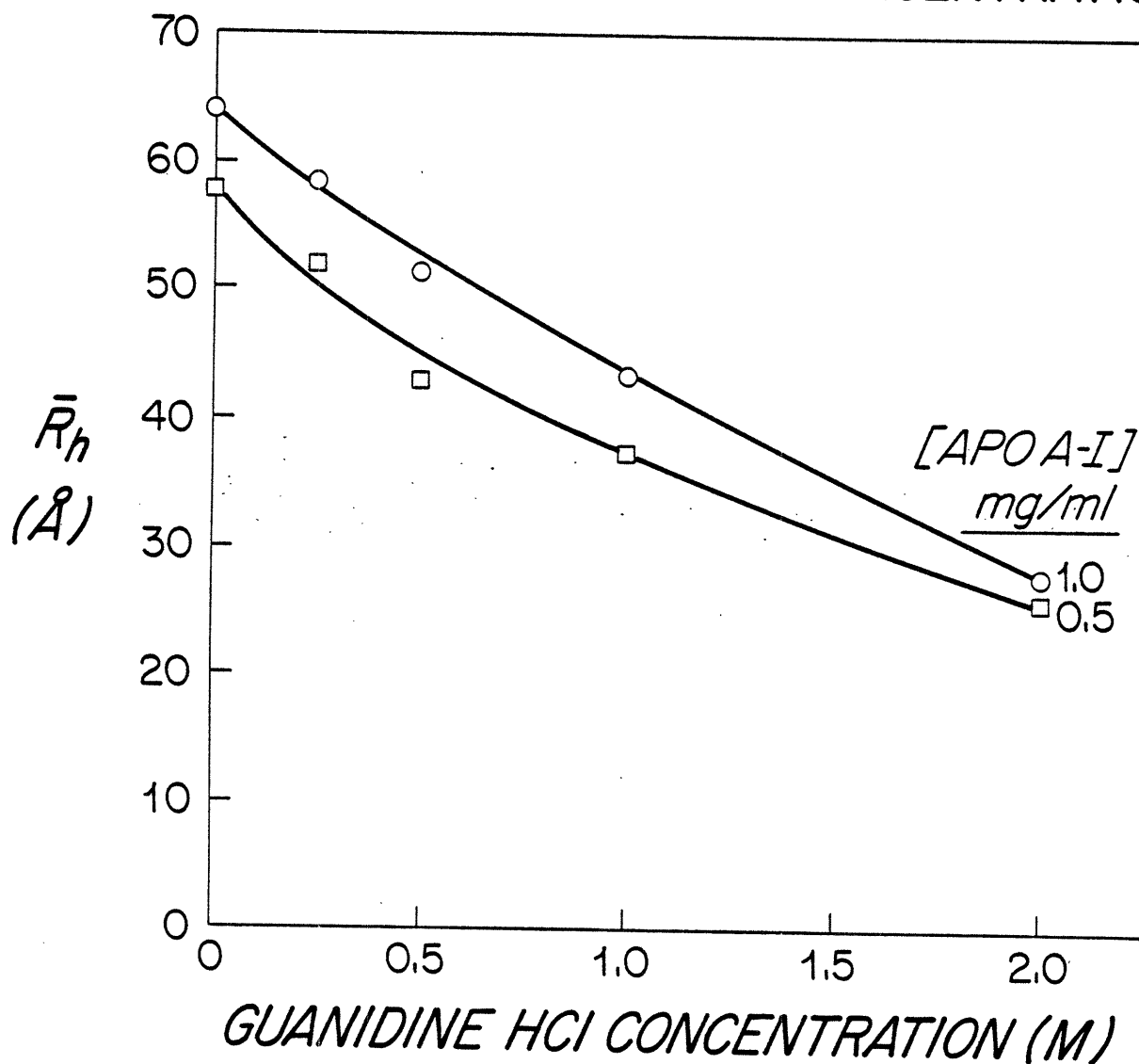


Figure 6. Dependence of \bar{R}_h of apo A-I on guanidine HCl concentration (0.15M NaCl, 37°C, 1 atm): \circ 1.0 mg/ml apo A-I; \square 0.5 mg/ml apo A-I.

EFFECT OF TAUROCHOLATE (TC) CONCENTRATION ON EQUILIBRIUM BINDING TO APO A-I

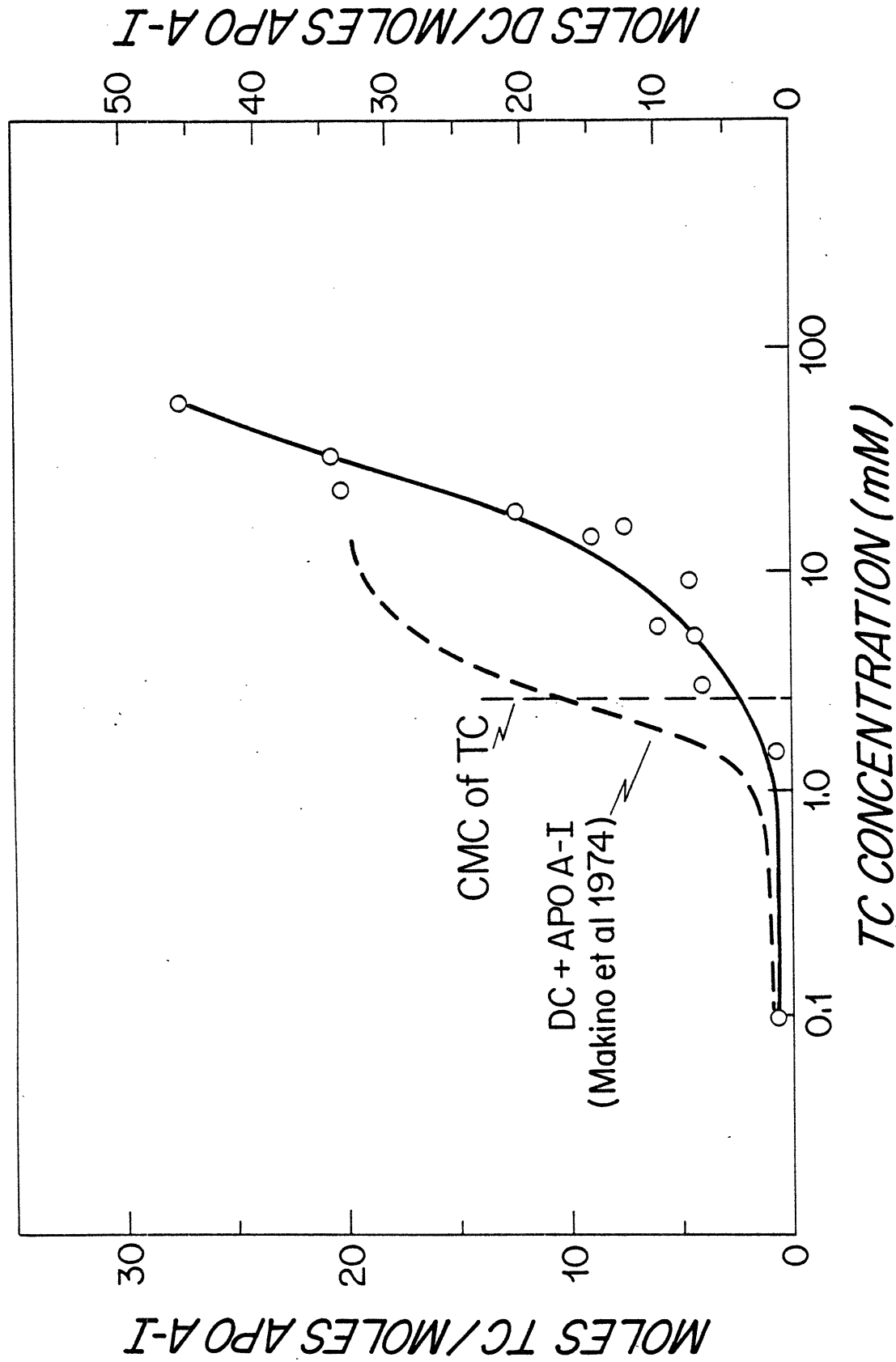


Figure 7. Effect of TC concentration on equilibrium binding of TC to apo A-I. (1 mg/ml apo A-I, 22°C, 1 atm, 0.15M NaCl). Dashed curve is from Makino et al. (1974) for deoxycholate (DC) binding to apo A-I.

1 mole TC/mole apo A-I is bound. Above the CMC of TC, there is a gradual increase in binding to about 25 moles TC/mole apo A-I. TC binding does not reach a limiting value at the highest TC concentrations studied (70 mM).

Figure 8 displays \bar{R}_h as a function of TC concentration for solutions with and without apo A-I (1 mg/ml) at 20 and 40°C. At both temperatures, \bar{R}_h remains constant below 1 mM TC. At higher TC concentrations, \bar{R}_h falls steeply to approach the \bar{R}_h of smaller simple TC micelles, 11 Å. To determine whether these \bar{R}_h values represent mixed micelles or a weighted average of apo A-I and TC simple micelles, the intensities of the apo A-I/TC solution, the equilibrated TC solution, and the buffer were measured (Table 1). This information will be used below in conjunction with a mathematical model of apo A-I self association to demonstrate the presence of apo A-I/TC mixed micelles, and not a weighted average of apo A-I and TC micelles.

The physical interactions of apo A-I and two other bile salts, one more hydrophobic than TC, taurodeoxycholate (TDC), and one more hydrophilic than TC, tauroursodeoxycholate (TUDC), were also investigated using QLS. Figure 9 demonstrates \bar{R}_h values of these 1 mg/ml apo A-I/bile salt solutions plotted against bile salt concentration. Bile salt concentrations at which \bar{R}_h begins to decrease correspond to the order of the aqueous CMC's: TDC < TUDC < TC.

DEPENDENCE OF HYDRODYNAMIC RADIUS OF TC
AND TC-APO A-I SOLUTIONS ON TC CONCENTRATION

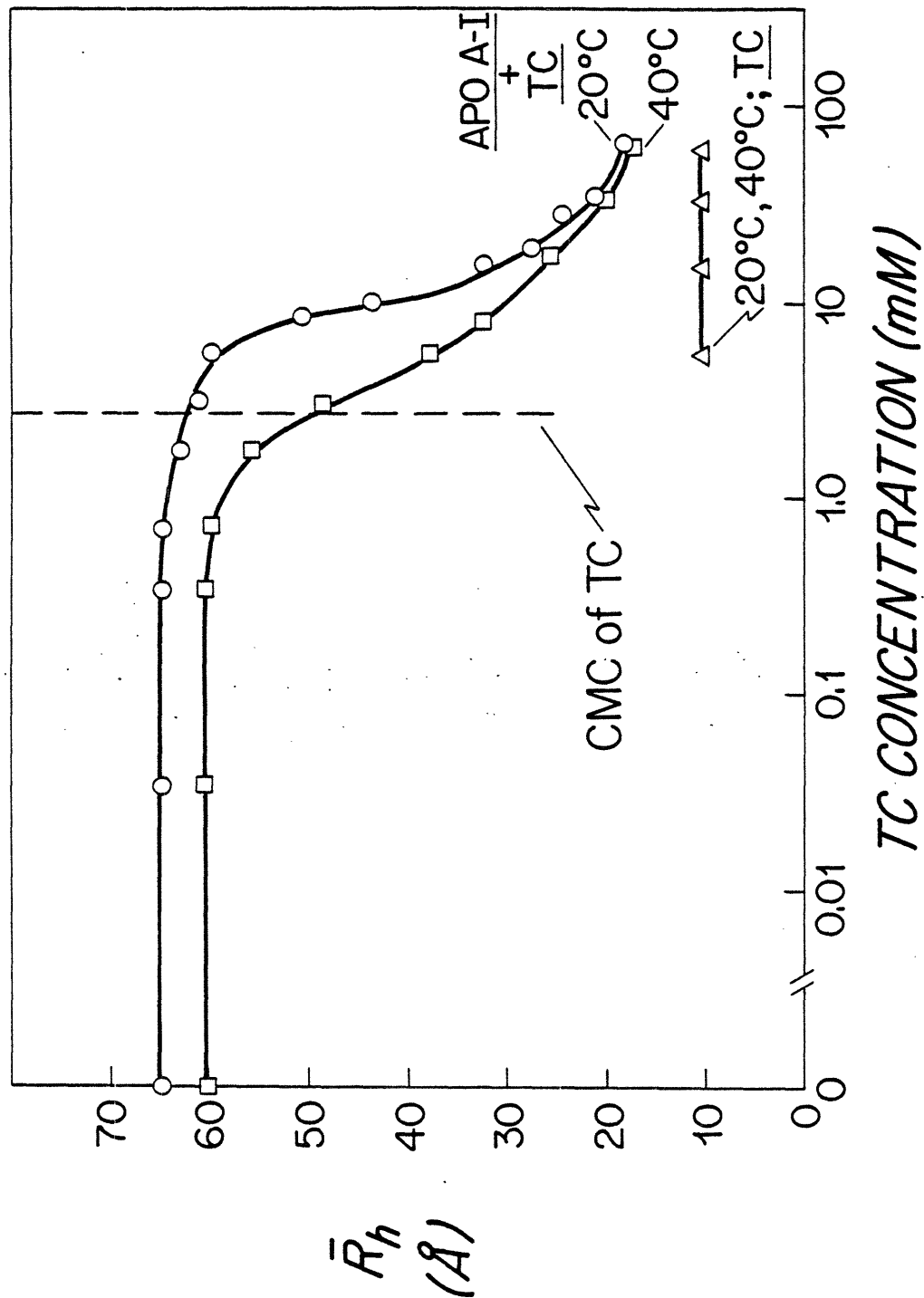


Figure 8. Dependence of \bar{R}_h of TC and TC/apo A-I solutions on TC concentration (0.15M NaCl, 1 atm): O 20°C, 1 mg/ml apo A-I; □ 40°C, 1 mg/ml apo A-I; Δ 20 and 40°C, 0 mg/ml apo A-I.

TABLE 1
CALCULATIONS OF \bar{n} OF APO A-I/TC MIXED MICELLES

TC Concentration (mM)	\bar{R}_h (\AA)	\bar{n}
0.036	64.5	6.6
0.36	64.5	6.6
1.8	63.0	6.1
3.6	62.0	5.7
5.6	60.0	5.2
9.0	51.0	3.5

TC Concentration (mM)	\bar{R}_h (\AA)	I_{TC}	$I_{apo\ A-I + TC}$	\bar{n}
9.0	51.0	0.9	15.5	4.1
11.0	43.5	2.2	29.7	3.7
17.2	37.0	2.5	17.8	2.8
18.0	33.0	0.9	20.9	2.3
24.0	27.0	3.9	15.6	1.8
31.5	24.5	7.0	29.2	2.2
35.5	21.5	4.9	17.5	2.0
66.0	18.0	10.5	20.5	1.3

DEPENDENCE OF HYDRODYNAMIC RADIUS OF
BILE SALT-APO A-I SOLUTIONS
ON BILE SALT CONCENTRATION

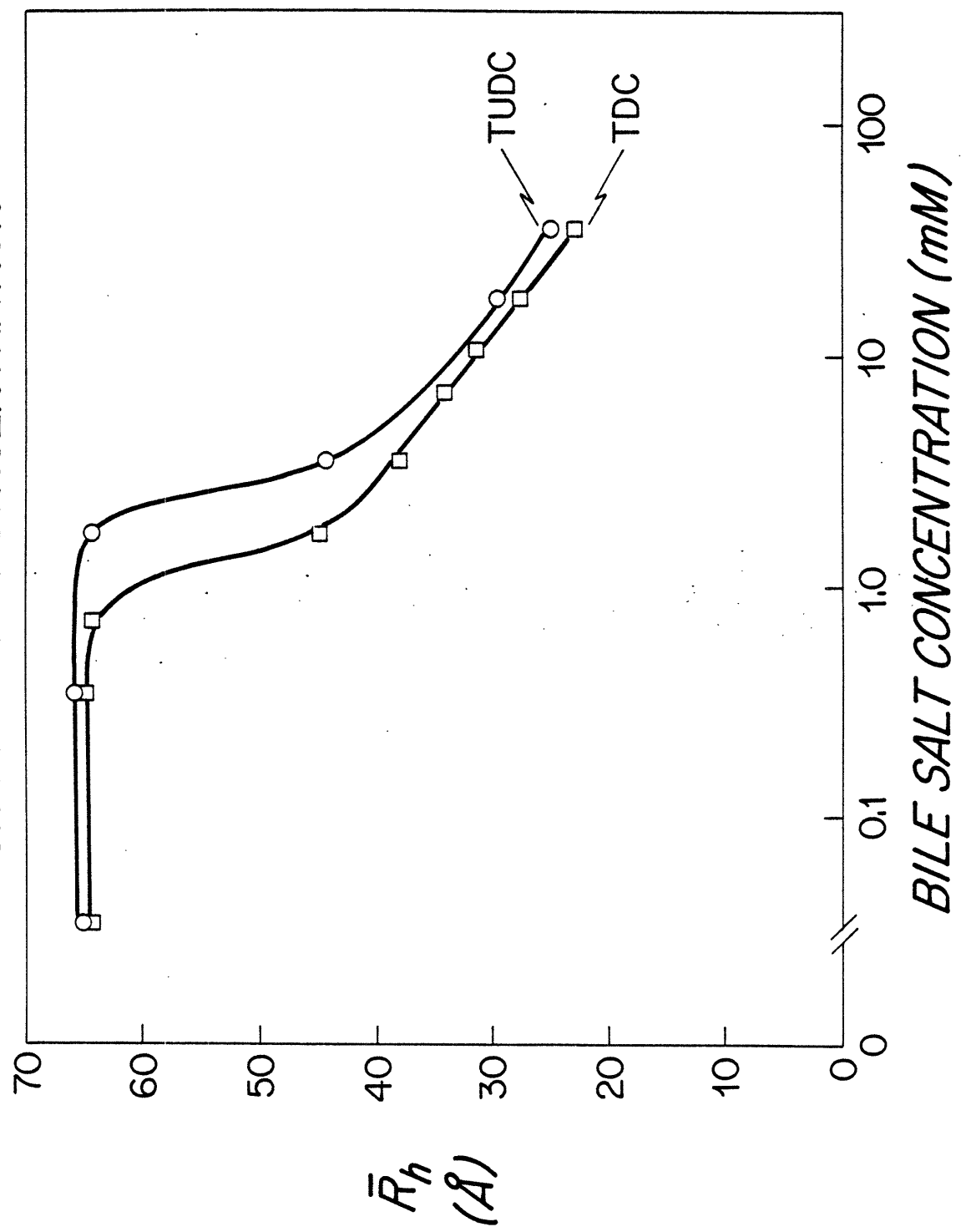


Figure 9. Dependence of \bar{R}_h of bile salt/apo A-I solutions on bile salt concentration (1 mg/ml apo A-I, 0.15M NaCl, 20°C, 1 atm): O TUDC; □ TDC.

C. Apo A-II Self Association. Data on the self association of apo A-II solutions as functions of concentration, temperature, and guanidine HCl concentration were more difficult to collect due to the difficulty of isolating apo A-II, and the low intensity of light scattered from the smaller micelles of apo A-II. Figure 10 depicts the dependence of \bar{R}_h on apo A-II concentration at 37°C. \bar{R}_h increases from 21.5 Å at 0.22 mg/ml to 34 Å at 1.8 mg/ml, leveling off at the highest apo A-II concentrations. In Figure 11, the dependence of \bar{R}_h on temperature is shown. At the four apo A-II concentrations studied (1.8, 0.9, 0.45 and 0.22 mg/ml), there was no variation of \bar{R}_h over the range 10 to 37°C. Figure 12 shows the \bar{R}_h of two apo A-II solutions (0.45 and 0.9 mg/ml) in 0, 0.5 and 1.0 guanidine HCl (37°C). As guanidine HCl concentration increases, \bar{R}_h approaches a minimum value of approximately 20.5 Å at both apo A-II concentrations.

CONCENTRATION DEPENDENCE OF HYDRODYNAMIC RADIUS OF APO A-II

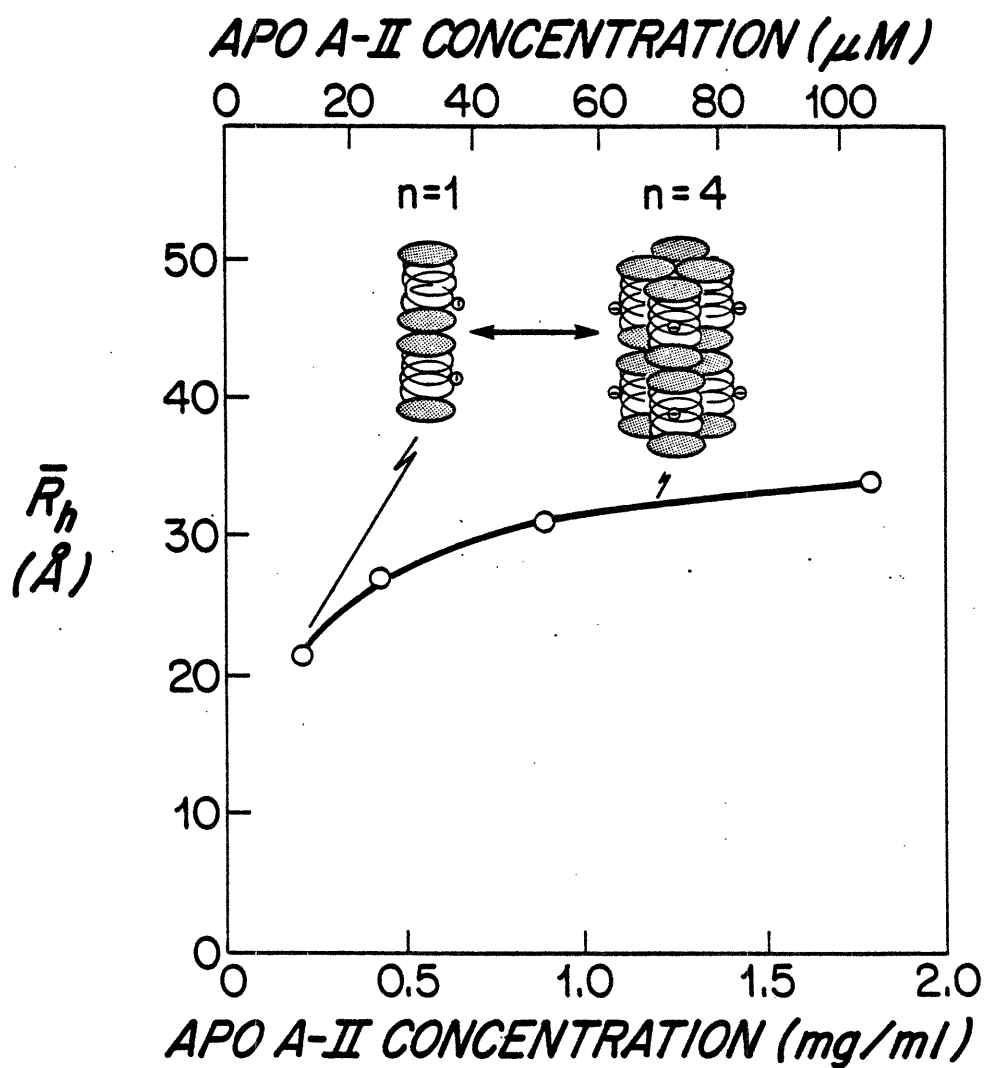


Figure 10. Concentration dependence of \bar{R}_h of apo A-II.
(0.15M NaCl, 37°C, 1 atm).

SELF ASSOCIATION OF APOA-II
TEMPERATURE DEPENDENCE OF \bar{R}_h

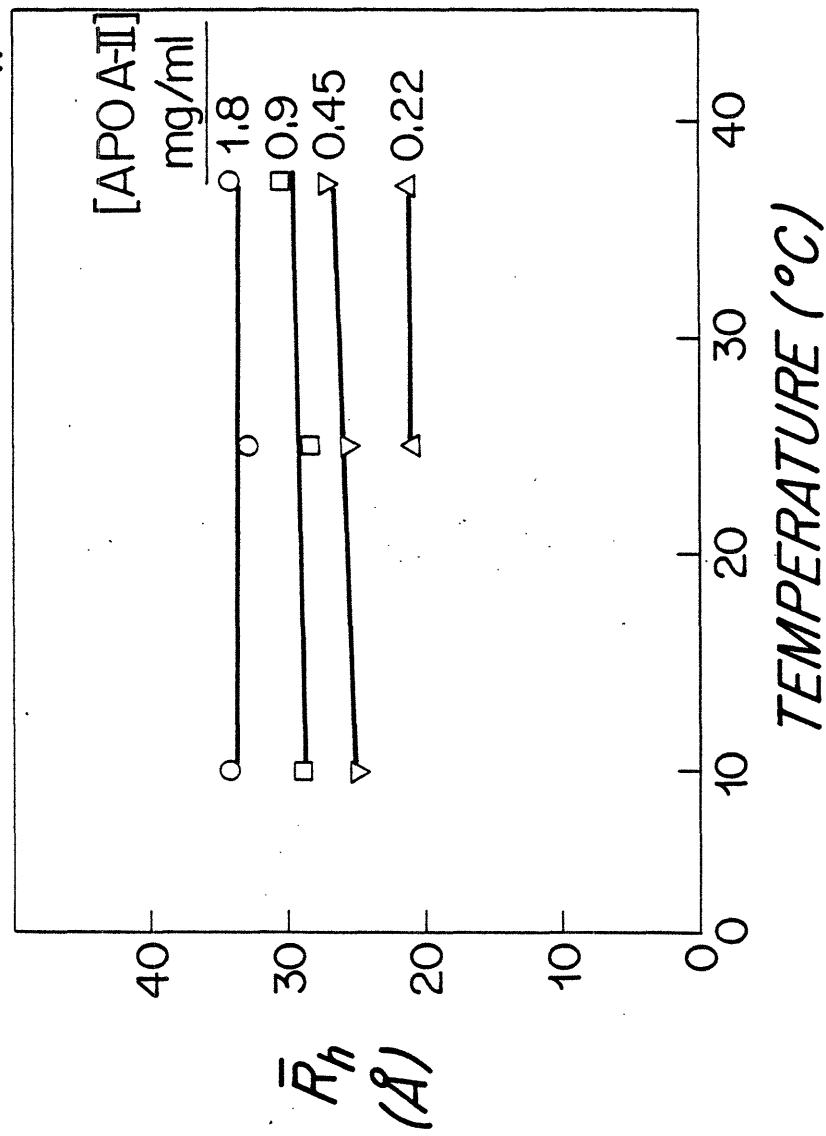


Figure 11. Temperature dependence of \bar{R}_h of apo A-II at various concentrations (0.15M NaCl, 1 atm): \circ 1.8 mg/ml; \square 0.9 mg/ml; ∇ 0.45 mg/ml; \triangle 0.22 mg/ml.

SELF ASSOCIATION OF APO A-II
 DEPENDENCE OF \bar{R}_h
 ON GUANIDINE HCl CONCENTRATION

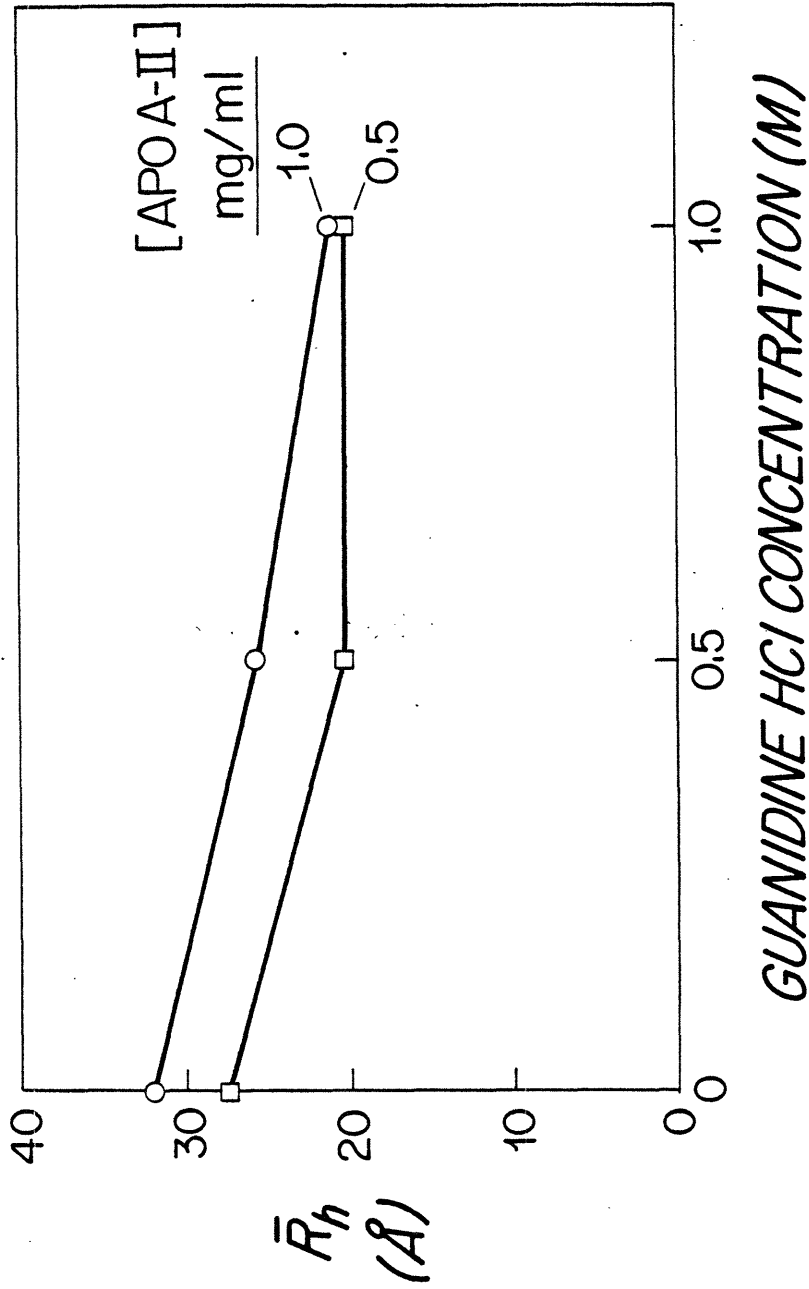


Figure 12. Dependence of \bar{R}_h of apo A-II on guanidine HCl concentration (0.15M NaCl, 37°C, 1 atm): \circ 1.0 mg/ml; \square 0.5 mg/ml.

IV. DISCUSSION

A. Theoretical Analysis of Apo A-I Self Association. The concentration dependence of \bar{R}_h has similar features under all experimental conditions, such as variations in NaCl concentration, temperature, and guanidine HCl concentration, which are examined in this work: as apo A-I concentration increased, \bar{R}_h increased to gradually reach a limiting value. We will now describe and test three possible apo A-I self association models, each with an increasing degree of complexity (shown schematically in Figure 13). In Model I, we examine an equilibria of four dimers to form an octamer, ignoring the existence of monomers. In model II, we examine the case of multiple equilibria between dimers, tetramers, hexamers and octamers. In model III, we extend Model I to allow equilibria between monomers, dimers, and octamers. We will show below that our experimental data is most consistent with Model III.

Both mean intensity (\bar{I}) and \bar{R}_h data suggest that apo A-I self associates to a discrete limit (Figure 1), not exceeded under any physical chemical conditions studied here. At 37°C, the smallest \bar{R}_h measured (39 Å) is approximately the size of the dimer as determined by gel filtration (39 Å) (Morrisett et al., 1977). Over an apo A-I concentration range of 0.1 to 0.9 mg/ml, \bar{I}/C increases by a factor of 2.4. Over the same range, \bar{R}_h increases from the dimeric size (39 Å) to 59 Å. Since \bar{I}/C is proportional to \bar{n} , this implies that \bar{n} increases from approximately two monomers (0.1 mg/ml) to five monomers

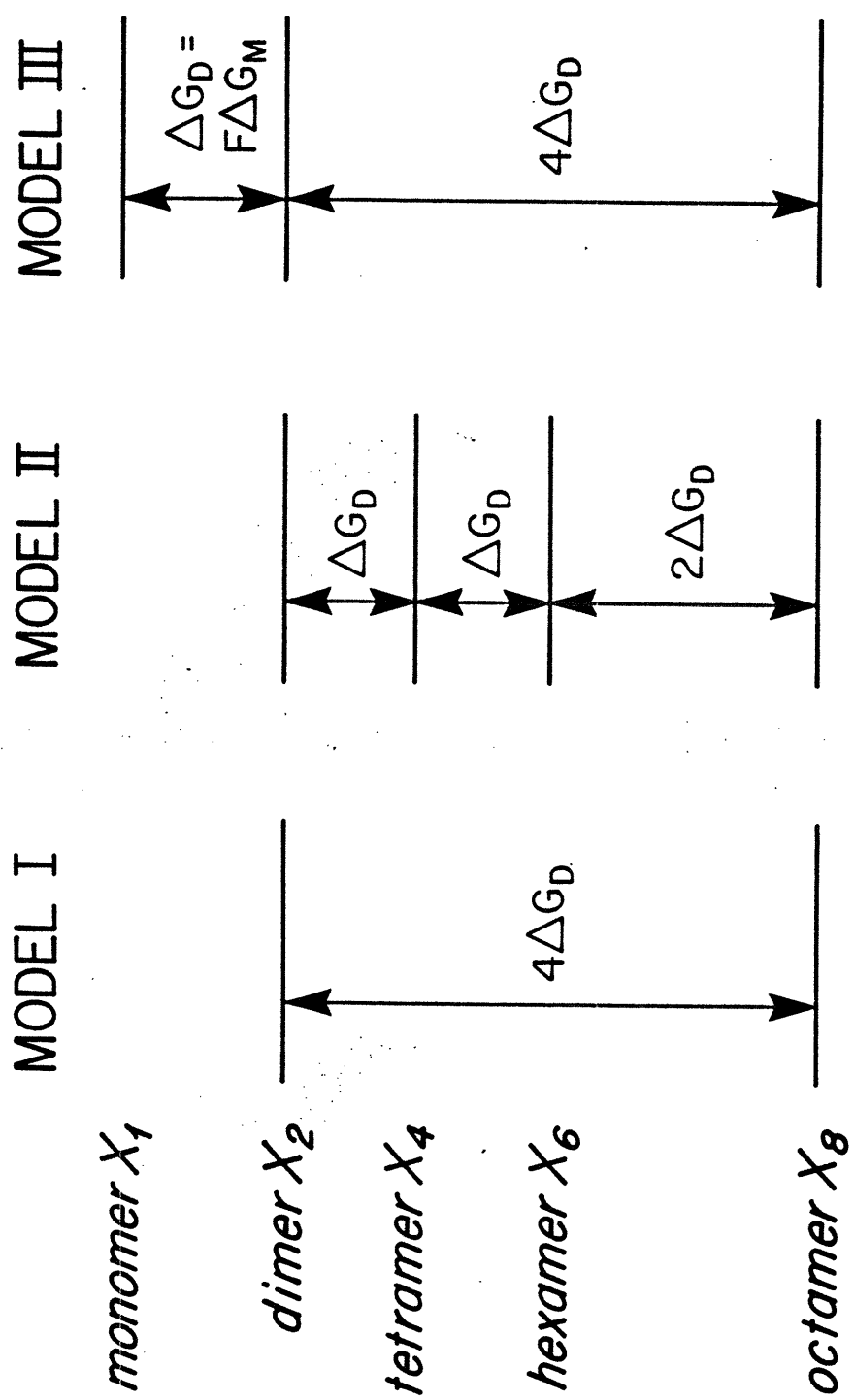


Figure 13. Energy ladder diagram of three proposed models of apo A-I self association. Horizontal lines indicate possible aggregation states in each model, and vertical arrows depict the free energy change between each aggregation state.

(0.9 mg/ml). At 0.9 mg/ml, \bar{R}_h is less than the asymptotic value (68 Å). Therefore, five is a minimum estimate for the limiting value of \bar{n} .

Because apo A-I self association reaches a limit, the model that we propose must provide for a closed structure in which further association of apo A-I is disadvantageous. To calculate values of \bar{R}_h for various models, we require an estimate of \bar{R}_h of aggregates of varying molecular weight and shape. We shall first demonstrate how \bar{R}_h allows us to estimate the shape of a particle, and we will then use this method to make an informed estimate on the shape of apo A-I self aggregates.

If the apo A-I monomer is spherical, then its \bar{R}_h can be estimated as follows: the total volume of the molecule is the sum of the volume of the protein (V_p) and the added volume due to hydration (V_h). The former can be calculated from the partial specific volume of apo A-I (\bar{V}) (0.74 ml/g) estimated from the amino acid content and the molecular weight, M_r (28,200) (Scanu et al., 1982):

$$V_p = \frac{\bar{V} M_r}{N_o} \quad (7)$$

where N_o is Avogadro's number. Since typical values of protein hydration are 0.3 to 0.4 g H₂O/ g protein (Cantor and Schimmel, 1980), and the specific volume of water (\bar{V}_w) is 1.0 ml/g, we have

$$V_h = \frac{M_r}{N_o} (0.35) V_p \quad (8)$$

By solving this equation, we obtain an approximate total volume of the apo A-I monomer, V , of $33,900 \text{ \AA}^3$. On this basis, the hydrodynamic radius, R_h , is obtained:

$$R_h = \left(\frac{3V}{4\pi} \right)^{1/3} \quad (9)$$

and is found to be approximately 22 \AA . From the limiting value of the sedimentation coefficient at low apo A-I concentrations, we calculate R_h of the apo A-I monomer to be approximately 28 \AA (Vitello and Scanu, 1976a). The calculated R_h value assumes a spherical particle, and we denote it as $(R_h)_s$. The ratio of $R_h/(R_h)_s$ can then be defined as the friction factor, f . Values of f have been calculated for prolate and oblate ellipsoids of varying axial ratio (Cantor and Schimmer, 1980). In this way the shape of the monomer has been estimated from R_h derived from sedimentation coefficients and the specific volume to be a prolate ellipsoid, with semi-major axis of 150 \AA and semi-minor axis of 25 \AA (Barbeau and Scanu, 1979). Similarly, for a dimer with an experimental R_h of 38 \AA (Morrisett et al., 1977) and the same \bar{V} , we calculate that a prolate ellipsoid would have semi-major axis of 190 \AA and semi-minor axis of 30 \AA .

The building blocks of monomers and dimers could self associate in a number of ways, but our derivation is constrained by the fact that the limiting aggregate has an R_h of 68 \AA . If dimers associated end to end, the R_h of a hexamer can be estimated from the molecular weight and f to be approximately 65 to 75 \AA . This result fits well with the limiting size of 68 \AA obtained by QLS in this work. However, forces which favor

aggregation should tend to promote indefinite aggregation. The R_h of an octamer composed of dimers which self associate end to end is estimated to be 80 to 90 Å. This is 15 Å larger than the observed \bar{R}_h value in this study. If dimers associate side to side to form a "donut shaped" aggregate, R_h can be estimated using values of f for toroids (Allison et al., 1980) to be about 60 to 70 Å. A schematic depiction of this octamer is shown in Figure 1. This structure has the advantage that there is an intrinsic limit on n , and no further apo A-I molecules could be added easily.

To model mathematically apo A-I self association, we now make use of these values for R_h . In Figure 13, we show an energy ladder representation of Model I (Missel et al., 1980). The horizontal lines represent possible aggregation states, and distances between these lines represent the free energy change upon interaction of monomer or oligomers of various n . The mole fraction of each possible aggregate of n monomers (X_n) is defined:

$$X_n = \frac{C_n}{N_0 \text{Mr } M} \quad (10)$$

where C_n is the concentration of n -mers in mg/ml, Mr is the molecular weight of the monomer, and M is the molarity of water. To form an octamer from four dimers, the free energy change is defined as $4\Delta G_D$, where ΔG_D is the free energy change for the interaction of two dimers. The relative mole fraction of X_2 and X_8 can then be expressed by the equilibrium condition

$$K_{eq} = \frac{X_8}{X_2^4} \quad (11)$$

From the definition of equilibrium constants,

$$K_{eq} = \exp\left(\frac{-4\Delta G_D}{RT}\right) \quad (12)$$

We define a mole fraction of monomers

$$X_A = \exp\left(\frac{4\Delta G_D}{3RT}\right) \quad (13)$$

Substituting equation 13 into equations 11 and 12, and eliminating K_{eq} , X_8 can be expressed as a function of X_2 :

$$\frac{X_8}{X_A} = \left(\frac{X_2}{X_A}\right)^4 \quad (14)$$

We then define:

$$\frac{X_8}{X_A} = X_8', \quad \frac{X_2}{X_A} = X_2', \quad \frac{X_n}{X_A} = X_n' \quad (15)$$

By conservation of matter, we can also express the total concentration of monomers (X) present as either dimers or octamers as a function of X_2 and X_A :

$$X = 2X_2 + 8X_8 \quad \text{or} \quad X' = 2X_2' + 8(X_2')^4 \quad (16)$$

Using values of R_h of the dimer ($R_{h-dimer} = 38 \text{ \AA}$) and R_h of the octamer ($R_{h-octamer} = 68 \text{ \AA}$) together with the definitions of \bar{R}_h and \bar{n} , we can then express \bar{R}_h and \bar{n} solely as functions of X_2/X_A :

$$\frac{1}{\bar{R}_h} = \frac{\sum R_{h-n-mer}}{\sum n^2 X_n} = \frac{R_{h-dimer}}{4X_2'} + \frac{R_{h-octamer}}{64(X_2')^4} \quad (17)$$

$$\bar{n} = \frac{4X_2' + 64(X_2')^4}{2X_2' + 8(X_2')^4} \quad (18)$$

where $R_{h-n-mer}$ is the R_h of an n -mer ($R_{h-dimer} = 38 \text{ \AA}$ and $R_{h-octamer} = 68 \text{ \AA}$). By choosing a value for X_2' , we can calculate X' , \bar{n} , and \bar{R}_h . In Figure 14, we show the dependence of \bar{R}_h and \bar{n} on total apo A-I concentration. Each value of \bar{R}_h and \bar{n} corresponds to a single value of total apo A-I concentration. This dependence of \bar{R}_h on concentration has the same characteristics of our experimental curve (Figure 1). Using this theoretical curve, for any measured value of \bar{R}_h , we can read off the corresponding value of X' and the mean aggregation number, \bar{n} . Since the total mole fraction of monomers, X , is known, we can calculate X_A for each measured value of \bar{R}_h . At a fixed temperature and ionic strength, X_A should not vary with concentration, allowing us to calculate a single value of X_A for a series of concentrations (see Table 2). It is apparent that there is random scatter of the values about a mean X_A of 1.35×10^{-7} . With this X_A value, and the relationship between \bar{R}_h and X/X_A in Figure 14, we can compare the predicted dependency of \bar{R}_h on apo A-I concentration with our experimental results. The dashed curve in Figure 1 is derived in this way, and shows excellent agreement between model I and our data; however, there is some deviation of \bar{R}_h at

SELF ASSOCIATION OF APO A-I
THEORETICAL DEPENDENCE OF \bar{R}_h AND \bar{n}
ON APO A-I CONCENTRATION

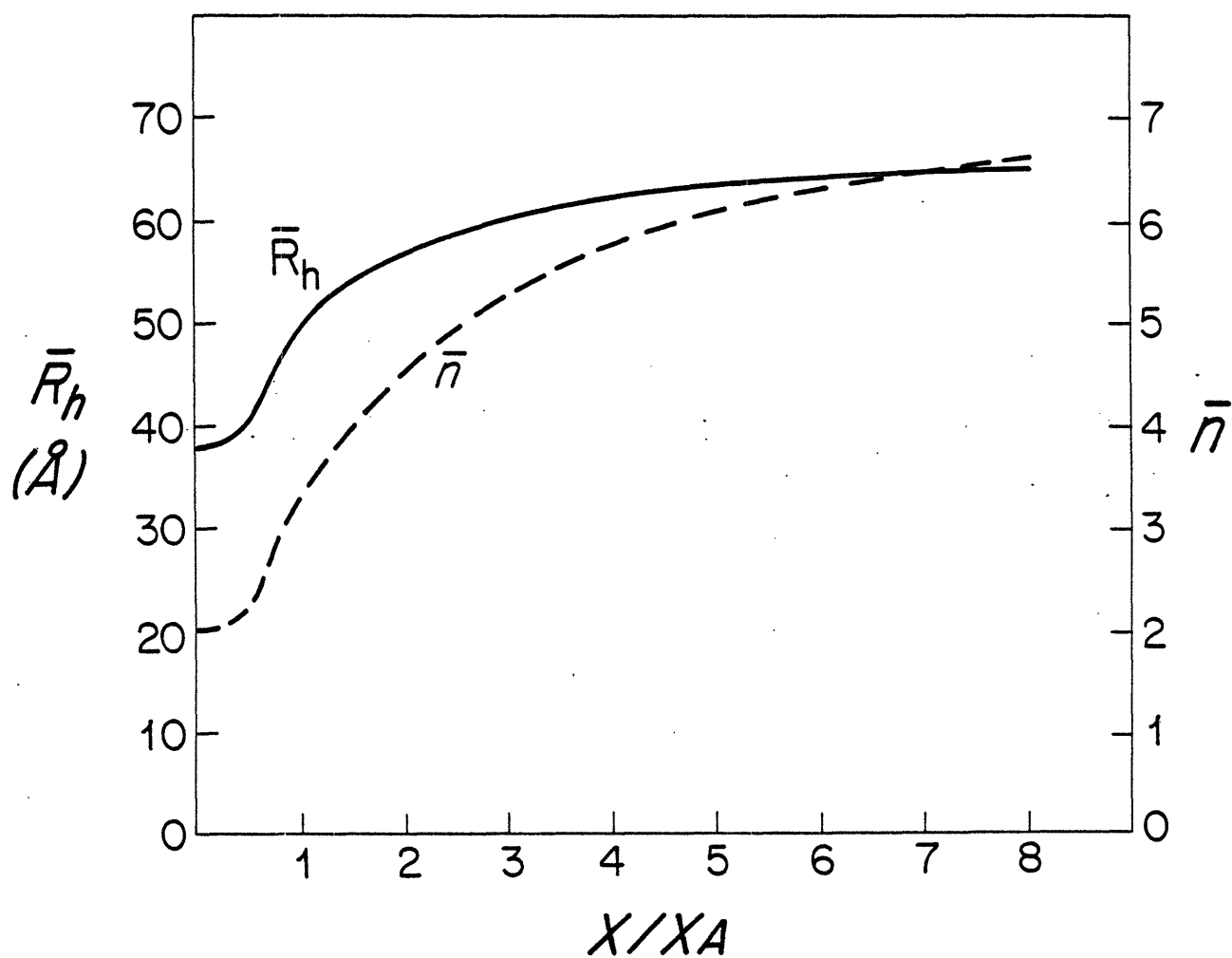


Figure 14. Theoretical curve of model I showing dependence of \bar{R}_h (solid curve) and \bar{n} (dotted curve) on X/X_A .

TABLE 2
EFFECT OF APO A-I CONCENTRATION ON X_A

Apo A-I Concentration (mg/ml)	X_A
0.10	1.82×10^{-7}
0.15	1.19×10^{-7}
0.20	1.21×10^{-7}
0.25	1.23×10^{-7}
0.44	1.37×10^{-7}
0.66	1.37×10^{-7}
1.00	1.22×10^{-7}
1.80	1.39×10^{-7}
mean	1.35×10^{-7}

apo A-I concentrations below 0.2 mg/ml.

In Model I, by taking into account dimers and octamers only, we have an excellent fit of the predicted \bar{R}_h values at apo A-I concentrations above 0.2 mg/ml. We will demonstrate later that this model provides an excellent fit for our data at various temperatures and NaCl concentrations. However, intermediate forms probably exist between dimers and octamers, and in Model II we shall investigate whether this affects the fit between theory and experiment.

In Model II we assume that (1) the energy advantage for the association of two dimers to form a tetramer is ΔG_D ; this value is the same as for a tetramer associating with a dimer to form a hexamer; and (2) the energy advantage for a dimer associating with a hexamer to form an octamer is $2\Delta G_D$, since in the "donut" model two dimer-dimer interactions occur as the ring is closed. The energy level diagram of Model II is shown schematically in Figure 11. We can express X_4 , X_6 , and X_8 as functions of X_2 by:

$$X_4 = X_2^2 \exp\left(-\frac{\Delta G_D}{RT}\right) \quad (19a)$$

$$X_6 = X_2^3 \exp\left(-\frac{2\Delta G_D}{RT}\right) \quad (19b)$$

$$X_8 = X_2^4 \exp\left(-\frac{4\Delta G_D}{RT}\right)$$

If we define a mole fraction of monomers:

$$X_B = \exp\left(\frac{\Delta G_D}{RT}\right) \quad (20)$$

and

$$X_n' = \frac{X_n}{X_B} \quad (21)$$

we can express the mole fraction of n-mers as:

$$X_4 = \frac{X_2^2}{X_B} \quad X_6 = \frac{X_2^3}{X_B^2} \quad X_8 = \left(\frac{X_2}{X_B}\right)^4 \quad (22)$$

or

$$X_4' = (X_2')^2 \quad X_6' = (X_2')^3 \quad X_8' = \frac{(X_2')^4}{X_B} \quad (23)$$

We can again express X' , \bar{R}_h , and \bar{n} as functions of X_2' and X_B , with estimates of the values for $R_{h-tetramer}$ ($R_{h-tetramer} = 48 \text{ \AA}$) and hexamer ($R_{h-hexamer} = 55 \text{ \AA}$):

$$X' = 2X_2' + 4(X_2')^2 + 6(X_2')^3 + 8 \frac{(X_2')^4}{X_B} \quad (24)$$

$$\frac{1}{\bar{R}_h} = \frac{\frac{4(X_2')}{R_{h-dimer}} + \frac{16(X_2')^2}{R_{h-tetramer}} + \frac{36(X_2')^3}{R_{h-hexamer}} + \frac{64(X_2')^4}{R_{h-octamer}} \frac{1}{X_B}}{4X_2' + 16(X_2')^2 + 36(X_2')^3 + \frac{64(X_2')^4}{X_B}} \quad (25)$$

In contrast to Model I, \bar{R}_h is a function of X' as well as the absolute value of X_B . To compare Models I and II we have used the value of X_B obtained from Model I corresponding to ΔG_D at 37°C , 0.15M NaCl . For this value of X_B we can determine the dependence of \bar{R}_h on X' . This curve is entirely superimposable on the theoretical curve for Model I shown in Figure 14.

Therefore since models I and II predict the same dependence of \bar{R}_h on apo A-I concentration, methods which measure \bar{R}_h and \bar{n} such as QLS and sedimentation equilibrium would be unable to distinguish between Models I and II.*

Whereas in Models I and II the existence of monomers has been ignored, Model III (Figure 11) includes monomers. There are two free energies, ΔG_D and ΔG_M , the free energy change of two monomers dimerizing. Since both ΔG_D and ΔG_M can be expected to be similarly affected by changes in solution properties (NaCl concentration, temperature, guanidine HCl concentration), we have assumed that ΔG_M is related to ΔG_D by a constant factor F:

$$\Delta G_M = F \Delta G_D \quad (26)$$

Since we have demonstrated that the presence of tetramers and hexamers do not significantly alter our results, we investigate in Model III the case of a monomer-dimer-octamer equilibrium. We can express mole fractions of the n-mers as follows:

$$X_2 = X_1^2 \exp\left(-\frac{F \Delta G_D}{RT}\right) \quad \text{or} \quad X_1 = X_2^{\frac{1}{2}} \exp\left(-\frac{F \Delta G_D}{2RT}\right) \quad (27a)$$

$$X_8 = X_2^4 \exp\left(-\frac{4 \Delta G_D}{RT}\right)$$

To assess how well Model III fits the experimental data, values of X_A (defined as in equation 13) and F were obtained as

* Because of the large free energy change of $2\Delta G_D$ between the hexamer and octamer, equilibria strongly favors octamer formation. The absolute amount of monomer present as tetramers and hexamers is negligible. Therefore the weighted averages \bar{R}_h and \bar{n} are unaffected by the presence of these intermediates.

follows. Using the definitions of \bar{R}_h and \bar{n} , theoretical curves of \bar{R}_h against X/X_A for several values of F were calculated as described for previous models. For each value of F the average value of X_A at 37°C , 0.15M NaCl was determined. The sums of the squares of the relative deviations of \bar{R}_h from this theoretical curve are shown in Table 3. It is evident that the minimum corresponds to a value of approximately 5.3 for F ; ΔG_M is approximately -38 kcal/mol. Since our data is limited in the low concentration regime where monomers contribute significantly to \bar{R}_h , ΔG_M cannot be determined with precision. However, we can conclude from the relative values of ΔG_M and ΔG_D that the free energy change for the association of monomers to form dimers is much stronger than that for the association of dimers to form octamers.

The solid curve in Figure 1 is the best theoretical fit for Model III. Models I (the dotted curve in Figure 1) and III differ very little at values of \bar{R}_h above 45 \AA . At higher concentrations the monomers contribute little to \bar{R}_h and \bar{n} which are weighted toward larger molecular weight species. At lower concentrations the curves of Model I and III approach different limiting values for R_h of the dimer (38 \AA) and monomer (28 \AA) respectively. The experimental point at 0.09 mg/ml fits Model III in a more satisfactory manner.

Values of \bar{R}_h for most of our experimental data show that apo A-I is extensively self associated, where Models I and II are virtually identical. Since values of X_A are considerably

TABLE 3
BEST FIT OF F IN MODEL III

F	$\Sigma \left(\frac{\Delta \bar{R}_h}{\bar{R}_h} \right)^2$
1.33	0.131
2.67	0.138
4.00	0.079
5.33	0.090
6.65	0.088
8.0	0.125
10.6	0.211
∞	0.312

easier to compute for Model I than for Model III, we have used Model I to determine values of ΔG_D under various experimental conditions.

B. Effect of Solution Conditions on ΔG_D . With Model I of apo A-I self association we can analyze the effects of temperature, ionic strength and guanidine HCl concentration on apo A-I self association. Table 4 lists values of X_A and ΔG_D determined for each temperature and ionic strength studied. As demonstrated by the solid curves in Figures 2 and 4 which were derived from these values, there is excellent agreement between theory and experiment.

The relative magnitude of the hydrophobic and electrostatic components of ΔG_D can be estimated from the effect of ionic strength on ΔG_D . The electrostatic component of ΔG_D , ΔG_{el} , is the difference between ΔG_D at a given NaCl concentration and ΔG_D with complete shielding of charges. ΔG_{el} was estimated using the Verwey-Overbeek theory of electrical interaction between two spherical double layers (Mazer, 1978).* The net charge at pH 7.6 per dimer was taken as +8 from measurements of the surface charge of apo A-I (Heuck et al., 1983) and the radius of the dimers was taken as the hydrodynamic radius (38 Å). In Table 5 we show ΔG_{el} estimated for each of the four NaCl concentrations studied. Since two positively charged dimers

*This is only an approximation since the apo A-I dimers are neither spheres nor have a symmetrical charge distribution.

TABLE 4

VALUES OF ΔG_D AT VARIOUS TEMPERATURES AND NaCl CONCENTRATIONS

T ($^{\circ}\text{C}$)	NaCl concentration (M)	X_A	ΔG_D (kcal/mol)
10	0.15	1.08×10^{-7}	-6.78
20	0.15	1.10×10^{-7}	-7.00
30	0.15	1.14×10^{-7}	-7.21
37	0.15	1.39×10^{-7}	-7.31
45	0.15	3.19×10^{-7}	-7.09
50	0.15	6.14×10^{-7}	-6.89

37	0.50	0.96×10^{-7}	-7.47
37	1.00	0.77×10^{-7}	-7.56
37	2.00	0.74×10^{-7}	-7.58

repel one another as they associate, ΔG_{e1} is a positive value. At 0.15M NaCl, the estimated repulsive force of ΔG_{e1} is only 0.34 kcal/mol, compared with a net attractive force of ΔG_D of -7.31 kcal/mol. At 2.0M NaCl, ΔG_{e1} decreases to only 0.01 kcal/mol. In the last column of Table 5 we show the difference between the value of ΔG_D at a given NaCl concentration and ΔG_D at 2.0M NaCl ($\Delta G_D - \Delta G_{D(2.0M\ NaCl)}$). Since ΔG_{e1} at 2.0M NaCl is very small, $\Delta G_D - \Delta G_{D(2.0M\ NaCl)}$ is approximately ΔG_{e1} , and agrees well with our theoretical predictions of ΔG_{e1} . These changes in ΔG_D with variations in ionic strength are proportionally small; however, the resultant changes in \bar{R}_h are easily observed experimentally.

Since ΔG_{e1} makes only a small contribution to ΔG_D , the driving force for self association is predominantly hydrophobic. Reynolds et al. (1974) have estimated that the free energy change in creating a hydrocarbon-aqueous interface is about 20 cal/Å². The surface area of apo A-I removed from aqueous contact (Δ_{area}) can be calculated from the experimental values of ΔG_D and ΔG_M :

$$\Delta_{area} = \frac{\Delta G_D}{20\ \text{cal}/\text{Å}^2} \quad \text{or} \quad \frac{\Delta G_M}{20\ \text{cal}/\text{Å}^2} \quad (27)$$

We calculate from equation 27 that when two monomers interact a total cavity surface area of 1600 Å² is removed from aqueous contact, which is equivalent to 800 Å² per monomer. When two dimers interact, a total cavity surface area of 370 Å² is removed from aqueous contact, equivalent to 90 Å² per monomer. The area for the monomer-monomer interaction is substantially

TABLE 5

COMPARISON OF EXPERIMENTAL AND THEORETICAL VALUES OF ΔG_{e1}

NaCl concentration (M)	ΔG_D (kcal/mol)	ΔG_{e1} (kcal/mol)	$\Delta G_D - \Delta G_D(2.0M \text{ NaCl})$ (kcal/mol)
0.15	-7.31	0.34	0.27
0.50	-7.47	0.08	0.11
1.00	-7.56	0.03	0.02
2.00	-7.58	0.01	0.00

less than the area per apo A-I at an air-water interface, approximately 2500 \AA^2 (Shen and Scanu, 1980). There are several possibilities to explain this discrepancy. The surface area of an air-water interface is likely to be overestimated since proteins (including apo A-I) undergo changes in secondary structure. Also since the hydrophobic portions which interact in self association are not as hydrophobic as a pure hydrocarbon, the free energy change in creating an apo A-I aqueous interface will be somewhat less than 20 cal/\AA^2 .

Since guanidine HCl is known to decrease hydrophobic interactions and unfold proteins, the hydrophobic component of ΔG_D should decrease with increasing amounts of guanidine HCl. Since experimental values of \bar{R}_h fall in the range of monomers and dimers, we have used Model III to determine ΔG_D . In Table 6 we show values of ΔG_D for a 1.0 mg/ml apo A-I solution at 0.15M NaCl.

From the variation of ΔG_D with temperature, the thermodynamic quantities ΔH and ΔS can theoretically be determined from the relation

$$\frac{\Delta G_D}{T} = \frac{\Delta H}{T} - \Delta S \quad (28)$$

In Figure 15, $\Delta G/T$ is shown on the vertical axis and $1/T$ is shown on the horizontal axis. From 10 to 30°C , the dependence of $\Delta G/T$ on $1/T$ is linear and ΔH and ΔS were deduced as -0.7 kcal/mol and $21.5 \text{ cal/mol}^\circ\text{K}$ respectively. Therefore at low temperatures the major driving force for association is

TABLE 6

VARIATION OF ΔG_D WITH GUANIDINE HCl CONCENTRATION

Guanidine HCl concentration (M)	ΔG_D (kcal/mol)
0.0	-7.31
0.5	-6.71
1.0	-6.39

DEPENDENCE OF $\Delta G_D/T$ ON $1/T$

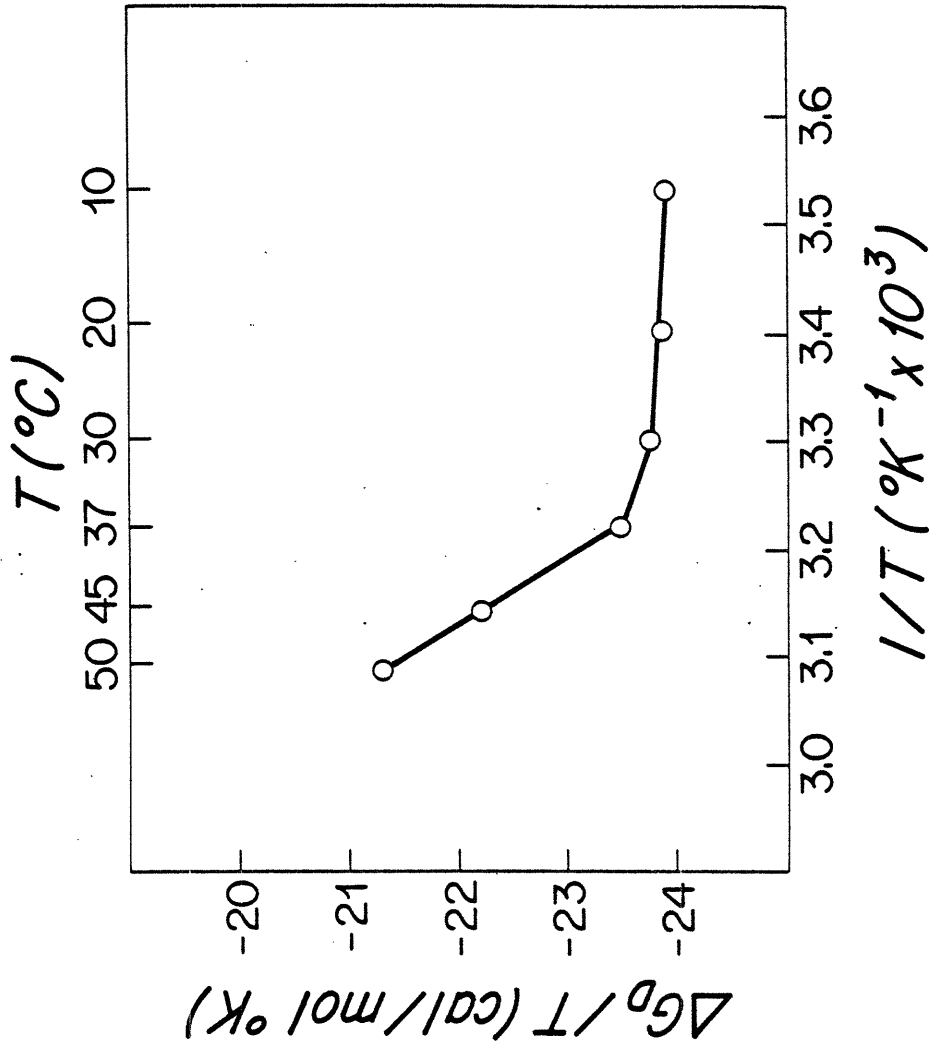


Figure 15. Dependence of $\Delta G_D/T$ on $1/T$.

entropic. This is also the case for the self association of bile salts (Mazer et al., 1979). The marked change in the dependence of $\Delta G/T$ on $1/T$ at temperatures above 37°C suggests that other factors such as conformational changes become important in apo A-I self association.

C. Comparison with Literature Data. There are substantial discrepancies in the literature concerning the concentration dependence of apo A-I self association. Sedimentation equilibrium studies have been reported to be consistent with a maximum aggregation number of dimers (Gwynne et al., 1974) tetramers (Stone and Reynolds, 1975) and octamers (Vitello and Scanu, 1976a). In Figure 16 we show the dependence of \bar{n} (vertical axis) on concentration (horizontal axis) from these studies, as well as from sedimentation equilibria studies of Swaney and O'Brien (1978). There are wide differences in \bar{n} deduced from these studies. Formisano et al. (1978) attempted to resolve these differences by considering the hypothesis that hydrostatic pressures generated by the ultracentrifuge affected self association. Equilibrium constants over a range of rotor speeds were extrapolated to zero acceleration, and this predicted a concentration dependence of \bar{n} as shown in Figure 16. They found that the acceleration promotes dissociation, i.e., decreases \bar{n} , and concluded that hydrostatic pressure generated in the ultracentrifuge (up to 100 atm) favored dissociation.

For comparison, Figure 16 shows the theoretical concentration dependence of \bar{n} at 20°C predicted from the present work.

SELF ASSOCIATION OF APO A-I CONCENTRATION DEPENDENCE OF \bar{n}

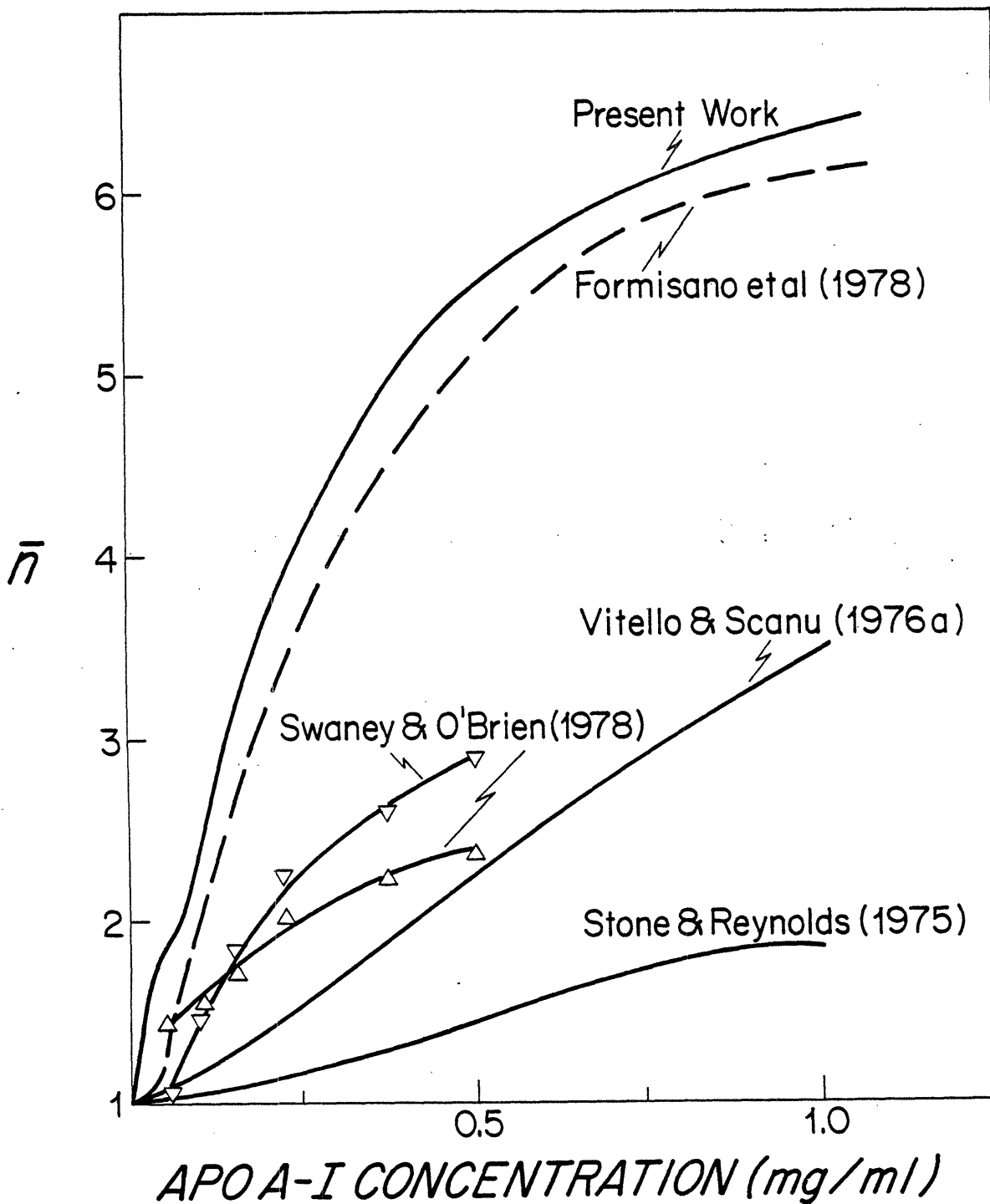


Figure 16. Dependence of \bar{n} on apo A-I concentration, literature values: ∇ Swaney (1978) $\mu=0.245$, 20°C ; Δ Swaney (1978) $\mu=0.045$, 20°C ; Vitello (1976a) $\mu=0.02$, 20°C ; Stone (1975) $\mu=0.045$, 20°C ; Formisane (1978) $\mu=0.11$, 20°C , extrapolation to zero rotor speed; present work, $\mu=0.16$, 20°C .

There is excellent agreement with the extrapolation to zero acceleration obtained by Formisano, and poor agreement with results from other ultracentrifugal studies. In the present study we have directly measured \bar{R}_h at pressures within and above the range generated in the ultracentrifuge (up to 100 atm), at comparable concentrations and did not observe any effect on \bar{R}_h . Our results confirm the empirical observation of the effect of rotor speed, but we are unable to support the hypothesis that there is a direct pressure effect on apo A-I particle size. These differences may be attributable to other perturbations inherent in the sedimentation equilibrium technique, most notably the effect of differing sedimentation rates of counterions and self associating apo A-I molecules.

The viscometry studies of Barbeau et al. (1979) suggested an indefinite association model with pairs of dimers associating end to end, a model our studies do not confirm. Swaney and O'Brien (1978), using crosslinking with diethylsuberimide, studied the dependence of self association on concentration, ionic strength, guanidine HCl concentration and temperature. The maximum aggregation number observed by this method was only five, with half maximal aggregation at an apo A-I concentration of 0.4 mg/ml. The discrepancy between Swaney and O'Brien's maximum aggregation number and our maximum aggregation number of eight may be due to steric factors which may hinder complete crosslinking. Their data compare well with our prediction of half maximal aggregation ($\bar{n} = 4.5$) at 0.3 mg/ml.

The temperature dependence of apo A-I self association has been less well studied. Swaney and O'Brien found apo A-I was most extensively self associated from 5 to 25°C and gradually dissociated at higher temperatures, results similar to ours. Calorimetric studies (Tall et al., 1975) demonstrated that apo A-I undergoes a conformational change at approximately 54°C. The irreversible aggregation above 50°C observed in the present work indicates a change in self association properties, consistent with irreversible or slowly reversible denaturation above 54°C.

Both Formisano et al. (1978) and Swaney and O'Brien (1978) found that the self association of apo A-I increased as ionic strength increased, up to an ionic strength of 0.51. These results are consistent with our finding that \bar{R}_h and \bar{n} increase with increasing NaCl concentration. Swaney and O'Brien (1978) and Massey et al. (1981) demonstrated dissociation of apo A-I below 1.0M guanidine HCl. Edelstein et al. (1980) measured mean residue ellipticity at 3 mg/ml apo A-I and found two transitions with midpoints at 0.25 and 1.08M guanidine HCl, and found by sedimentation equilibrium that apo A-I was highly dissociated in 0.4M guanidine HCl, with $\bar{n} = 1.3$ at 1 mg/ml apo A-I. Gel permeation studies showed that apo A-I was present as the dimer in 0.4M guanidine HCl and as the monomer in 2.0 or 6.0M guanidine HCl. These effects of guanidine HCl are consistent with ours, except the sedimentation equilibrium data shows \bar{n} values substantially lower than our results. This discrepancy may reflect several of the physical chemical factors discussed above.

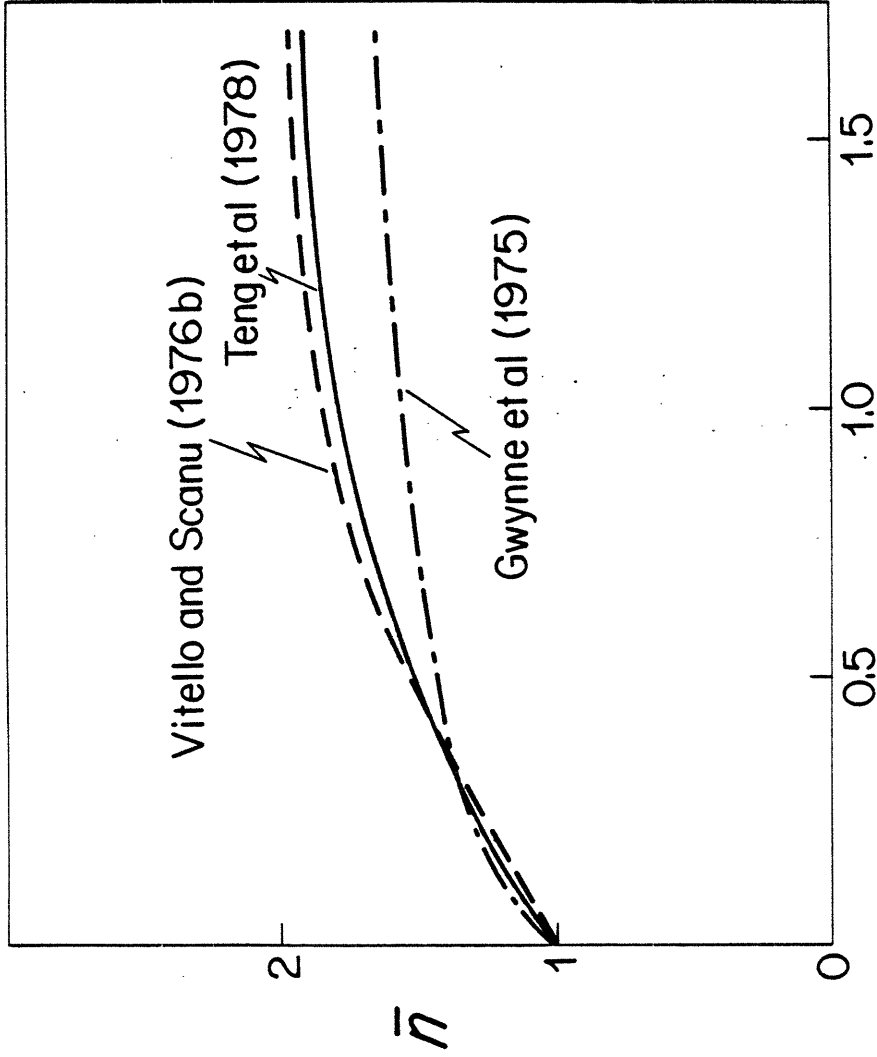
D. Self Association of Apo A-II. Since the \bar{R}_h of apo A-II micelles does not reach an asymptote in the concentration range studied, we cannot propose an exact model as we have done with apo A-I. The size of the apo A-II monomer can be estimated from \bar{V} , the specific volume (0.74 ml/g) (Gwynne, et al., 1975) assuming a typical hydration δ of 0.35 g H₂O/g protein:

$$(\bar{R}_h)_s = \left[\frac{3}{4\pi} \bar{V} \left(1 + \frac{\delta}{V_p} \right) \right]^{1/3} \quad (29)$$

where ρ is the solution density. \bar{R}_h obtained by this method is 19.3 Å. The minimum value of \bar{R}_h observed in our studies in 0M guanidine HCl was 21.5 Å, and about 21 Å at higher guanidine HCl concentration. Therefore, the friction factor f is about 1.1 for apo A-II (Cantor and Schimmel, 1980). For a prolate ellipsoid, this corresponds to an axial ratio of about 3, with a semi-major axis of 72 Å, and a semi-minor axis of 22 Å. Therefore apo A-II is likely to be a smaller version of apo A-I (axes 150 and 25 Å).

Based on sedimentation equilibrium data, there are also discrepancies in the literature regarding the self association of apo A-II. Stone and Reynolds (1975) concluded that apo A-II was a dimer over all concentrations studied. Vitello and Scanu's data (1976b) were consistent with a monomer-dimer-trimer or indefinite association scheme. Teng et al. (1978), from the same laboratory, concluded that a monomer-dimer-trimer association fit the data best, but schemes with tetramers could not be definitely excluded. They also found that self association

SELF ASSOCIATION OF APO A-II
CONCENTRATION DEPENDENCE OF \bar{n}



APO A-II CONCENTRATION (mg/ml)

Figure 17. Dependence of \bar{n} on apo A-II concentration, literature values: Teng (1978) $\mu = 0.02$, 20°C; Vitello (1976b) $\mu = 0.02$, 20°C; Gwynne (1975) $\mu = 0.01$, 22°C.

did not vary with temperature (5 to 30°C). Swaney and O'Brien (1978), after crosslinking with diethylsuberimide and SDS-PAGE, found dimers to be the largest species at concentrations of 2.5 mg/ml apo A-II. In Figure 17 we show various literature estimates for \bar{n} as a function of concentration. In the concentration range we have studied, literature values suggest that apo A-II is no larger than a dimer. However, we obtain \bar{R}_h values consistent with \bar{n} of 3 to 4, which suggests apo A-II is more highly aggregated.

Using the same line of reasoning employed for apo A-I, we can estimate the R_h of an apo A-II trimer or tetramer as 31 or 34 Å respectively. The largest value of \bar{R}_h observed was 34 Å. We find that there is no variation in \bar{R}_h with increases in temperature from 10 to 37°C, which is consistent with the findings of Teng et al. (1978). The discrepancy between our \bar{R}_h values and literature reports of \bar{n} may be due to the same factors affecting apo A-I self association as inferred from ultracentrifugal results.

E. Interactions of Apo A-I and Bile Salts. The interactions of apo A-I and bile salts can be interpreted using Model I of apo A-I self association. Since the mean intensity of scattered light (\bar{I}) from a solution is proportional to the molecular weight of the species and the weight concentration, we can employ \bar{I} to establish the presence or absence of apo A-I/TC mixed micelles.

I_{TC} , the intensity of light scattered from a solution containing TC and buffer, is proportional to $C_{TC}M_{TC}^N$, where C_{TC} is the weight concentration of TC, M_{TC} is the molecular weight of TC (538), and N is the aggregation number of TC micelles (5) (Mazer et al., 1979, Small, 1971). $I_{apo A-I}$, the intensity of light scattered from a solution containing TC and apo A-I, contains two components: TC micelles and apo A-I/TC mixed micelles, and can be expressed as the sum:

$$C_{TC}M_{TC}^N + C_{apo A-I}M_{apo A-I}^{\bar{n}}(1 + C_B) = I_{apo A-I} \quad (30)$$

where $C_{apo A-I}$ is the apo A-I concentration (1 mg/ml), $M_{apo A-I}$ is the monomer molecular weight (28,200), and C_B is the weight ratio of bound TC to apo A-I (from Figure 8). We can then calculate \bar{n} , the aggregation number of apo A-I in the mixed micelles:

$$\frac{I_{TC}}{I_{apo A-I}} = \frac{C_{TC}M_{TC}^N}{C_{TC}M_{TC}^N + C_{apo A-I}M_{apo A-I}^{\bar{n}}(1 + C_B)} \quad (31)$$

In Table 1 we show \bar{n} obtained by this equation and the relative intensity of the light scattered from these solutions. As the TC concentration approaches the CMC, I_{TC} becomes very small and the relative error is large. Therefore for TC concentrations below 6 mM we have calculated \bar{n} from the measured value of \bar{R}_h since the contribution of TC micelles to the measured \bar{R}_h is less than 3% at these TC concentrations. In the theoretical curve in Figure 14, a single value of \bar{n} corresponds to each value of \bar{R}_h . These values of \bar{n} are also shown in Table 1.

All values of \bar{n} are plotted on the vertical axis against TC concentration on the horizontal axis in Figure 18. Below 1mM, TC has no effect on the \bar{n} of apo A-I micelles. Above this concentration \bar{n} decreases smoothly to approach one, the apo A-I monomer. Makino (1974) demonstrated deoxycholate (DC) binding to apo A-I as also shown in Figure 7 (pH 9.2, 0.33M NaCl). DC, a more hydrophobic bile salt (Armstrong and Carey, 1982) is more strongly associated with apo A-I at any given bile salt concentration.

F. Pathophysiological correlations. We have shown that in the absence of other lipids, apo A-I and apo A-II are self associated at physiological serum concentrations (1 and 0.3 mg/ml respectively). However, most serum apo A-I and apo A-II are associated with membrane lipids (phospholipids, cholesterol, etc.); therefore, these hetero-associations must be more favorable than self association. The knowledge of apoprotein self association we have gained here is crucial for understanding HDL lipid-protein interactions in the next phase of our study.

In contrast to proteins such as serum albumin, apo A-I at serum concentrations binds very little bile salt at concentrations substantially below the CMC of the bile salt, in the physiological range. The preferential binding of serum bile salts to HDL over other lipoproteins must therefore be due to other components of HDL. This lipoprotein is organized by apo A-I and apo A-II, but these apolipoproteins are not the principle bile salt binders, as was demonstrated by Kramer et

SELF ASSOCIATION OF APO A-I
DEPENDENCE OF \bar{n} ON TC CONCENTRATION

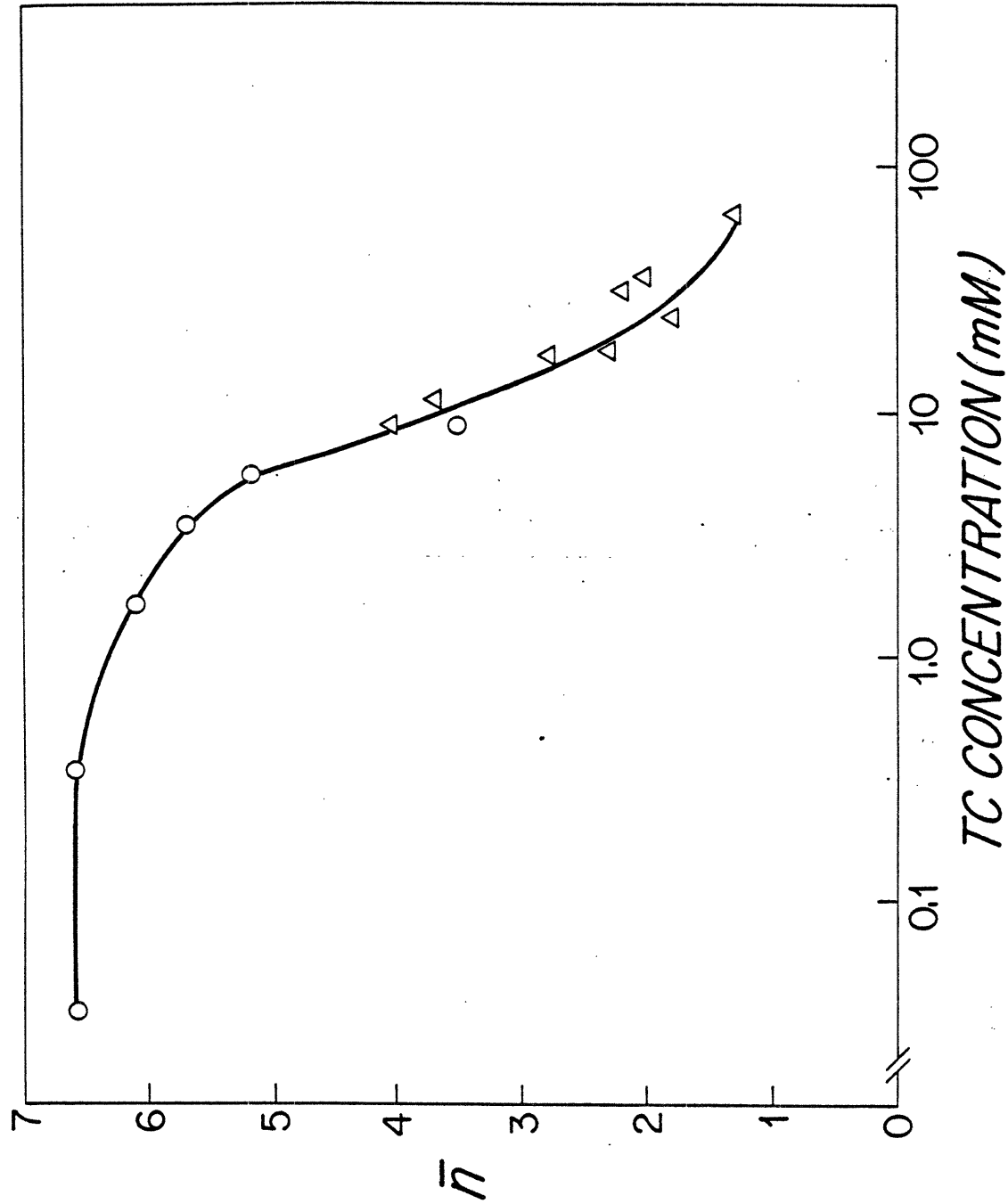


Figure 18. Estimated dependence of \bar{n} on TC concentration (1 mg/ml apo A-I, 0.15M NaCl, 37°C, 1 atm). Values (O) below 7 mM were estimated from R_h ; values (Δ) above 7 mM were estimated using intensity measurements as described in the text.

al. (1979). The major effect of bile salts on serum HDL are mediated through the affinities of bile salts for phospholipid and cholesterol within these particles.

In bile, where apo A-I is present at a concentration of approximately 0.02 mg/ml (2% of serum concentration), and bile salts are present at 100 to 200mM, apo A-I would not be associated (see Figure 1). It is interesting to note the similarities of association patterns of these two physiological detergents. Both associate first into primary micelles - bile salts with aggregation numbers of 3 to 4, apo A-I into dimers. These primary micelles then further associate, indefinitely for bile salts, and up to octamers for apo A-I. The driving force for association for both is primarily hydrophobic, with minimal repulsive electrostatic forces.

G. Conclusions. In summary, using the non-perturbing technique of QLS, we have established (1) apo A-I and apo A-II self associate to form octamers and trimer/tetramers respectively at concentrations up to 2 mg/ml. (2) This behavior is well described by a monomer-dimer-octamer self association model for apo A-I. In this model, the equilibrium constants are shown to vary with temperature, ionic strength and guanidine HCl concentration, and the free energy of association is shown to be due almost entirely to hydrophobic forces; and (3) Bile salts have little effect on apo A-I self association below their CMC; in contrast, bile salts above the CMC dissociate apo A-I octamers.

REFERENCES

- Allison, S.A., R.A. Easterly, and D.C. Teller, The Translational Friction of Toroids, *Biopolymers* 19: 1475-1480 (1980).
- Armstrong, M.J., M.C. Carey, The Hydrophobic-Hydrophilic Balance of Bile Salts: Inverse Correlation between Reverse Phase High Performance Liquid Chromatography Mobilities and Micellar Cholesterol Solubilizing Capacities, *J. Lipid Res.* 23: 70 (1982).
- Burstein, M. and H.R. Scholnick, Lipoprotein-Polyanion-Metal Interactions, *Adv. Lipid Res.* 11: 68-108 (1973).
- Barbeau, D.L., A. Jonas, T. Teng, and A.M. Scanu, Asymmetry of Apolipoprotein A-I in Solution as Assessed from Ultracentrifugal, Viscometric and Fluorescence Polarization Studies, *Biochemistry* 18: 362-369 (1979).
- Bridgman, P.W., The Physics of High Pressure, Dover, New York (1931).
- Cantor, C.R., and P.R. Schimmel, Biophysical Chemistry: Techniques for the Study of Biological Structure and Function, W. H. Freeman & Co., San Francisco, CA (1980).
- Carey, M.C., The Enterohepatic Circulation, in The Liver: Biology and Pathobiology, (I.M. Arias et al, eds), Raven Press, New York (1982).
- Carey, M.C., Measurement of the Physical Chemical Properties of Bile Salt Solutions, in Bile Acids in Gastroenterology (L. Barbara, R.H. Dowling, A.F. Hofmann, and E. Roda, eds.), MTP Press, Boston (1983).
- Edelstein, C. and A.M. Scanu, Effect of Guanidine Hydrochloride on the Hydrodynamic and Thermodynamic Properties of Human Apolipoprotein A-I in Solution, *J. Biol. Chem.* 255: 5747-5754 (1980).
- Fisch, M. and G.B. Benedek, manuscript in preparation (1984).
- Formisano, S., H.B. Brewer, Jr., and J.C. Osbourne, Jr., Effect of Pressure and Ionic Strength on the Self Association of Apo A-I from the Human High Density Lipoprotein Complex, *J. Biol. Chem.* 253: 354-360 (1978).
- Gurantz, D., M.F. Laker, A.F. Hofmann, Enzymatic Measurement of Choline Containing Phospholipids in Bile, *J. Lipid Res.* 33: 373-376 (1981).

Gwynne, J., H.B. Brewer, Jr., H. Edelhoch, The Molecular Properties of Apo A-I from Human High Density Lipoprotein, *J. Biol. Chem.* 249: 2411-2416 (1974).

Gwynne, J., G. Palumbo, J.C. Osbourne, H.B. Brewer, and H. Edelhoch, The Self Association of Apo A-II, an Apoprotein of the Human High Density Lipoprotein Complex, *Archives of Biochem. and Biophys.* 170: 204-212 (1975).

Hatch, F.T. and R.S. Lees, Practical Methods for Lipoprotein Analysis, *Adv. Lipid Res.* 6: 1-68 (1968).

Heuck, C.C., W. Daerr, W. Haberbosch, D. Horn and E. Luddecke, The Surface Charge of Apolipoproteins, Phospholipid Liposomes and Human Very Low Density Lipoproteins, *J. Biol. Chem.* 258: 8317-8322 (1983).

Hofmann, A.F., Thin Layer Adsorption Chromatography of Free and Conjugated Bile Acids on Silicic Acid, *J. Lipid Res.* 3: 127-129 (1962).

Kawahara, K. C. Tanford, Viscosity and Density of Aqueous Solutions of Urea and Guanidine Hydrochloride, *J. Biol. Chem.* 241: 3228-3232 (1966).

Kramer, W., H. Buschers, W. Gerok and G. Kurz, Taurocholate Incorporation into High Density Lipoprotein Revealed by Photoaffinity Labeling, *Eur. J. Biochem.* 102: 1-9 (1979).

Lowry, O.H., N.J. Rosebrough, A.L. Farr, and R.J. Randall, Protein Measurement with the Folin Phenol Reagent, *J. Biol. Chem.* 193: 265-275 (1951).

Makino, S., C. Tanford, and J.A. Reynolds, The Interactions of Polypeptide Components of Human High Density Serum Lipoprotein with Detergents, *J. Biol. Chem.* 249: 7379-7382 (1974).

Massey, J.B., A.M. Gotto, H.J. Pownall, Human Plasma High Density Apolipoprotein A-I: Effect of Protein-Protein Interactions on the Spontaneous Formation of a Lipid Protein Recombinant, *Biochem. Biophys. Res. Commun.* 99: 466-474 (1981).

Mazer, N.A., Quasielastic Light Scattering Studies of Micelle Formation, Solubilization and Precipitation in Aqueous Biliary Lipid Systems, Ph.D. Thesis, M.I.T. (1978).

Mazer, N.A. M.C. Carey, R.F. Kwasnick, G.B. Benedek, Quasi-elastic Light Scattering Studies of Aqueous Biliary Lipid Systems: Size, Shape, and Thermodynamics of Bile Salt Micelles, *Biochemistry* 18: 3064-3075 (1979).

Mazer, N.A. and M.C. Carey, Quasielastic Light Scattering Studies of Aqueous Biliary Lipid Systems: Cholesterol Solubilization and Precipitation in Model Bile Solutions, *Biochemistry* 22: 426-442 (1983).

Missel, P.J., N.A. Mazer, G.B. Benedek, C.Y. Young, and M.C. Carey, Thermodynamic Analysis of the Growth of Sodium Dodecyl Sulfate Micelles, *J. Phys. Chem.* 84: 1044-1057 (1980).

Morrisett, J.D., R.L. Jackson, A.M. Gotto, Jr., Lipid-Protein Interactions in the Plasma Lipoproteins, *Biochim. Biophys. Acta.* 472: 93-133 (1977).

Norman, A., Preparation of Conjugated Bile Acids Using Mixed Carboxylic Acid Anhydride, *Arkiv. Kemi.* 8: 331-342 (1955).

Pope, J.L., Crystallization of Sodium Taurocholate, *J. Lipid Res.* 8: 146-147 (1967).

Reynolds, J.A., D.B. Gilbert, and C. Tanford, Empirical Correlation between Hydrophobic Free Energy and Aqueous Cavity Surface Area, *Proc. Natl. Acad. Sci., U.S.A.* 71: 2925-2927 (1974).

Scanu, A.M., C. Edelstein, Solubility in Aqueous Ethanol of the Small Molecular Weight Peptides of the Serum Very Low Density and High Density Lipoproteins, *Anal. Biochem.* 44: 576-588 (1971).

Scanu, A.M., C. Edelstein, and B.W. Shen, Lipid Protein Interactions in the Plasma Lipoproteins. Model: High Density Lipoproteins, in Lipid Protein Interactions (P.C. Jost and O.H. Griffith, eds.), Wiley & Sons, New York, 259-371 (1982).

Shen, B.W. and A.M. Scanu, Properties of Human Apolipoprotein A-I at the Air Water Interface, *Biochemistry* 19: 3643-3650.

Sewell, R.B., S.J.T. Mao, T. Kawamoto, and N.F. LaRusso, Apolipoproteins of High, Low and Very Low Density Lipoproteins in Human Bile, *J. Lipid Res.* 24: 391-401 (1983).

Small, D.M., The Physical Chemistry of Cholanic Acids, in The Bile Acids: Chemistry, Physiology and Metabolism (P.P. Nair, D. Kritchevsky, eds.) Plenum Publishing, New York (1971).

Stone, W.L. and J.A. Reynolds, The Self Association of the Apo-Gln-I and Apo-Gln-II Polypeptides of the Human High Density Serum Lipoproteins, *J. Biol. Chem.* 250: 8045-8048 (1975).

Swaney, J.B. and K. O'Brien, Crosslinking Studies of the Self Association Properties of Apo A-I and Apo A-II from Human High Density Lipoprotein, *J. Biol. Chem.* 253: 7069-7077 (1978).

Tall, A.R. and D.M. Small, Body Cholesterol Removal: Role of Plasma High Density Lipoproteins, *Adv. Lipid Res.* 17: 1-50 (1980).

Teng, T., D.L. Barbeau, A.M. Scanu, Sedimentation Behavior of Native and Reduced Apolipoprotein A-II from Human High Density Lipoproteins, *Biochemistry* 17: 17-21 (1978).

Vitello, L.B., A.M. Scanu, Studies on Human Serum High Density Lipoproteins: Self Association of Apolipoprotein A-I in Aqueous Solution, *J. Biol. Chem.* 252: 1131-1136 (1976a).

Vitello, L.B., A.M. Scanu, Studies on Human Serum High Density Lipoproteins: Self Association of Human Serum Apolipoprotein A-II in Aqueous Solution, *Biochemistry* 15: 1161-1165 (1976b).

Weber, R., M. Osborn, Proteins and Sodium Dodecyl Sulfate: Molecular Weight Determination on Polyacrylamide Gels and Related Procedures, in *The Proteins* (H. Neurath, R.L. Hill, eds.), Academic Press, New York, 180-224 (1975).

CHAPTER THREE

FORMATION OF MIXED MICELLES AND VESICLES OF
HUMAN APOLIPOPROTEINS A-I AND A-II, LECITHINS
AND THE BILE SALT TAUROCHOLATE:
AN INVESTIGATION USING QUASIELASTIC LIGHT SCATTERING

I. INTRODUCTION

In man, high density lipoproteins (HDL) play a central role in cholesterol transport in blood (Tall and Small, 1980). The unique properties of this class of lipoproteins are, in part, determined by their major apolipoproteins, namely apolipoprotein A-I (apo A-I) and apolipoprotein A-II (apo A-II). HDL precursors (nascent HDL) are synthesized in the liver and intestine and from the surface coat of chylomicrons and very low density lipoproteins during their metabolism in the circulation. Nascent HDL are phospholipid-cholesterol bilayers encapsulated by the principal apolipoproteins. These disc shaped mixed micelles are transformed into spherical (mature) HDL by the action of the plasma enzyme lecithin:cholesterol acyl transferase. This enzyme catalyzes the transfer of a fatty acyl chain from the sn-2 position of phosphatidylcholine to cholesterol. This results in the production of a cholesterol ester molecule and a lysolecithin molecule. Mature HDL appears to act primarily to transport cholesterol from peripheral tissues to the liver.

Some of the cholesterol is secreted into bile as phospholipid-cholesterol bilayers solubilized by bile salts (mixed micelles). Thus apolipoproteins and bile salts perform analogous functions of solubilizing cholesterol, each predominating in one of the body's two major cholesterol transport systems, serum lipoproteins and biliary lipid micelles, respectively.

Bile salts are present physiologically in low concentrations at the sites of nascent HDL synthesis, in the hepatocyte and enterocyte as well as in plasma. In fact, mature HDL is one of the major plasma carriers (in addition to albumin) of bile salts. Moreover, apo A-I and apo A-II have been shown to be present in gallbladder bile (Sewell et al., 1983). Therefore, we have extended our previous studies of the interactions of apo A-I and apo A-II with bile salts to study the size and thermodynamic properties of mixed micelles and liquid crystalline vesicles, composed of apo A-I and apo A-II, lecithin and the bile salt, taurocholate (TC). We have employed the technique of quasielastic light scattering (QLS) which allows us to change variables of physiological relevance without perturbing effects inherent in other techniques (e.g., sedimentation equilibrium which produces increased hydrostatic pressure, gel filtration which results in dilution, etc.). We have systematically derived and studied the phase equilibria of apo A-I and apo A-II, lecithin and TC. We have established the equilibrium phase diagram of apo A-I and apo A-II with the synthetic lecithin dimyristoyl phosphatidylcholine (DMPC).

We have also determined that bile salts may be important in the formation of mixed micelles containing apo A-I and the natural lecithin, egg yolk phosphatidylcholine (EYPC), with which apo A-I does not otherwise interact. Moreover, at concentrations comparable to those found in native bile, apo A-I alters the size and stability of the mixed micelles and vesicles formed by the model biliary lipid system of TC/EYPC. These results suggest that these two detergent-like molecules, apo A-I and bile salts, may act cooperatively to solubilize lipids physiologically, particularly in bile.

II. EXPERIMENTAL

A. Materials. Taurocholate (TC) and other chemicals were obtained as described in the previous chapter. Dimyristoyl phosphatidylcholine (DMPC) (Calbiochem-Behring, LaJolla, CA), a synthetic lecithin with two 16 carbon acyl chains, and egg yolk phosphatidylcholine (EYPC) (Lipid Products, South Nutfield, UK), a natural lecithin with a mixture of acyl chains (average 17.5 carbons), were >99% pure by thin layer chromatography (200 μg sample application, $\text{CHCl}_3:\text{MeOH}:\text{H}_2\text{O}$, 65:30:5, v:v:v). Apo A-I and apo A-II were prepared and purified as described in the previous chapter.

B. Methods.

1. Preparation of Solutions. Solutions with various concentrations of apo A-I or apo A-II, lecithin, and TC were prepared by drying appropriate amounts of lipid (lecithin and/or TC) in $\text{CHCl}_3:\text{MeOH}$ (3:1, v:v) first under N_2 and then under reduced pressure (10 mtorr) for 12 hours. After preincubation at the final incubation temperature, the buffer (0.15M NaCl, 0.01M Tris, 0.001M NaN_3 , pH 7.6) with or without apo A-I or apo A-II was added and vortexed mixed for a total of 2 to 3 minutes. Samples were sealed with teflon tape and incubated at temperatures for intervals described below. Final protein and lecithin concentrations were determined by the method of Lowry et al. (1951) and by the choline oxidase method (Gurantz et al., 1981) respectively. When solutions with final lecithin concentrations

less than 1 mg/ml were prepared, small amounts of lecithin (<10%) were apparently surface adsorbed, and the final lecithin concentrations were slightly lower than expected. Therefore the compositions reported here are actual compositions determined by analysis rather than the expected compositions. All solutions were a single phase unless otherwise noted.

The phase equilibria of apo A-I or apo A-II and DMPC or EYPC were studied at various total concentrations of lipid plus protein (0.25, 0.50 and 1.0 mg/ml). A series of solutions ranging from 0 to 90% lecithin by weight was prepared as above and incubated for up to 96 hours at 25°C (samples containing DMPC) or 37°C (samples containing EYPC) (method A). Two other paths were also employed to reach the same final apo A-I and DMPC concentrations. In method B, two stock solutions with 0 and 80% DMPC (1 mg/ml total concentration) were mixed in varying proportions and incubated for 48 hours at 25°C to give a range of solutions with compositions which varied from 0 to 80%DMPC. In method C, several apo A-I/DMPC solutions (1 mg/ml) were diluted four fold with aqueous solutions containing a range of apo A-I concentrations (0 to 0.1 mg/ml) and incubated at 25°C for up to 72 hours to produce solutions with final apo A-I and DMPC concentrations as in previous series. The phase equilibria of apo A-I/DMPC were studied at 37°C by preparing solutions with 0.25 to 1.0 mg/ml total concentration, from 0 to 90% DMPC. These solutions were first incubated at 25°C for 48 hours, and then at 37°C for 48 hours. In order to

examine whether this process was reversible, the samples were studied after reincubation at 25°C for 48 hours.

Solutions containing apo A-I, EYPC and TC were composed by three separate paths: (A) EYPC/TC lipid films were incubated at 37°C for up to 96 hours with aqueous apo A-I solutions (final lipid and protein concentration 1.0 mg/ml, TC/EYPC weight ratio 1.0); (B) Stock solutions of TC/EYPC (weight ratios 4.0, 2.3, 1.5, and 1.0, 10 mg/ml total lipid) were diluted with an aqueous apo A-I solution and incubated for 48 hours at 37°C. Four series of solutions were thus obtained in which the total protein and lecithin concentrations were held constant at 1.0 mg/ml; and (C) A stock solution of TC/EYPC (weight ratio 4.0, 10 mg/ml) was diluted with aqueous solutions of varying apo A-I concentrations (0 to 0.5 mg/ml). Within each series the TC/EYPC ratio and the final apo A-I concentration were held constant, and the total lipid concentration varied from 0.5 to 4.5 mg/ml.

2. Quasielastic Light Scattering. Equipment, sample clarification, and measurements of \bar{R}_h were identical to those described in the previous chapter. In order to determine whether equilibrium of protein/lipid solutions had occurred, \bar{R}_h was measured at intervals up to 96 hours. If \bar{R}_h was unchanged over a 24 hour interval, we assumed that micellar solutions had reached equilibrium, and that vesicular solutions were in a metastable state.

3. Chemical Analysis of Phases. Both phases of a two phase solution (total composition 90% DMPC, 10% apo A-I, 1 mg/ml total concentration) were separately analyzed. Centrifugation (10,000 g, 30 minutes) yielded a pellet and a clear supernatant phase. The measured \bar{R}_h of the supernatant did not change upon further centrifugation for up to 2 hours. The pellet was dissolved in 5% TC, and protein and lecithin concentrations were determined as described above.

III. RESULTS

A. Thermodynamic Equilibration of Mixed Micelles and Vesicles.

The solution state of lecithin in apo A-I/lecithin or apo A-II/lecithin solutions greatly influenced the time required to reach equilibrium. Solutions prepared with DMPC by any of the methods described above were found to have the same final \bar{R}_h values, although the time required to reach equilibrium varied from 24 to 72 hours. The measured \bar{R}_h of apo A-I/DMPC or apo A-II/DMPC solutions prepared by addition of aqueous apolipoprotein to dry DMPC (method A) reached a stable value after 48 hours. When two apo A-I/DMPC micellar solutions (0 and 80% DMPC, 1 mg/ml total concentration) were mixed (method B), after 24 hours \bar{R}_h reached stable values, and these were identical to those obtained by method A. When apo A-I/DMPC solutions (68 and 80% DMPC) were diluted from 1.0 to 0.25 mg/ml (method C), \bar{R}_h did not reach a stable value until 72 hours. Table 1 shows \bar{R}_h values of mixed micellar solutions obtained by method C, and estimates of \bar{R}_h values for the same solutions produced by method A. There is excellent agreement between the two methods.

In contrast, the measured \bar{R}_h of apo A-I/EYPC/TC solutions depended critically on the method of preparing the solutions. When an aqueous apo A-I solution was mixed with dried EYPC/TC containing TC concentrations below the CMC (method A), the solutions remained turbid. The \bar{R}_h values of the supernatant phase ranged from 200 to 1000 Å. Therefore apo A-I was unable to form mixed micelles with EYPC/TC vesicles. Solutions of identical composition were also prepared by mixing appropriate

TABLE I
COMPARISON OF \bar{R}_h OF APO A-I/DMPG MIXED MICELLES PREPARED BY DIFFERENT PATHWAYS

Initial Concentrations (mg/ml) Apo A-I	Initial Concentrations (mg/ml) DMPG	Final Concentrations (mg/ml) Apo A-I	Final Concentrations (mg/ml) DMPG	Final % DMPG	Initial \bar{R}_h (Å)	Method C Final \bar{R}_h (Å)	Method A Final \bar{R}_h (Å) (estimated)
0.20	0.80	0.125	0.20	62	135	69	67
		0.087	0.20	70	135	87	94
		0.069	0.20	74	135	205	150
		0.050	0.20	80	135	267	150
0.32	0.68	0.155	0.17	52	64	58	56
		0.117	0.17	59	64	62	61
		0.099	0.17	63	64	67	69
		0.080	0.17	68	64	79	74

amounts of a micellar EYPC/TC solution ($\bar{R}_h = 30 \text{ \AA}$) with an aqueous apo A-I solution ($\bar{R}_h = 67 \text{ \AA}$) (method B). These solutions remained optically clear, with \bar{R}_h values less than 200 \AA . These mixed micellar solutions reached fixed \bar{R}_h values after 24 hours; in contrast, \bar{R}_h values of vesicular solutions made by method A changed slowly over several days of observation.

B. Apo A-I/DMPC Phase Equilibria. Figure 1 shows the phase diagram of apo A-I/DMPC at three total lipid plus protein concentration (0.25, 0.50 and 1.0 mg/ml) plotted as \bar{R}_h on the vertical axis and the weight % DMPC on the horizontal axis. At low DMPC contents (up to about 50% DMPC), \bar{R}_h remains relatively constant at the size of simple apo A-I micelles (data points at 0% DMPC). These simple micelles increase in size as apo A-I concentration is increased. A similar increase in \bar{R}_h with apo A-I plus DMPC concentration occurs for all solutions below 50% DMPC. We will later propose a model describing the coexistence of simple apo A-I micelles and mixed apo A-I/DMPC micelles in this region of the phase diagram. At higher DMPC contents (>50% DMPC), \bar{R}_h increases and diverges. This divergence leads to a macroscopic phase limit (shown at the bottom of Figure 1) above which solutions became visible cloudy. Beyond this phase limit, \bar{R}_h continues to increase, reaching values of several hundred \AA . In our model, we will propose that only mixed micelles are present in this divergence region, and liquid crystalline vesicles are present beyond the phase limit. When

DEPENDENCE OF HYDRODYNAMIC RADIUS OF APO A-I/DMPC MICELLES ON DMPC CONTENT: EFFECTS OF CONCENTRATION

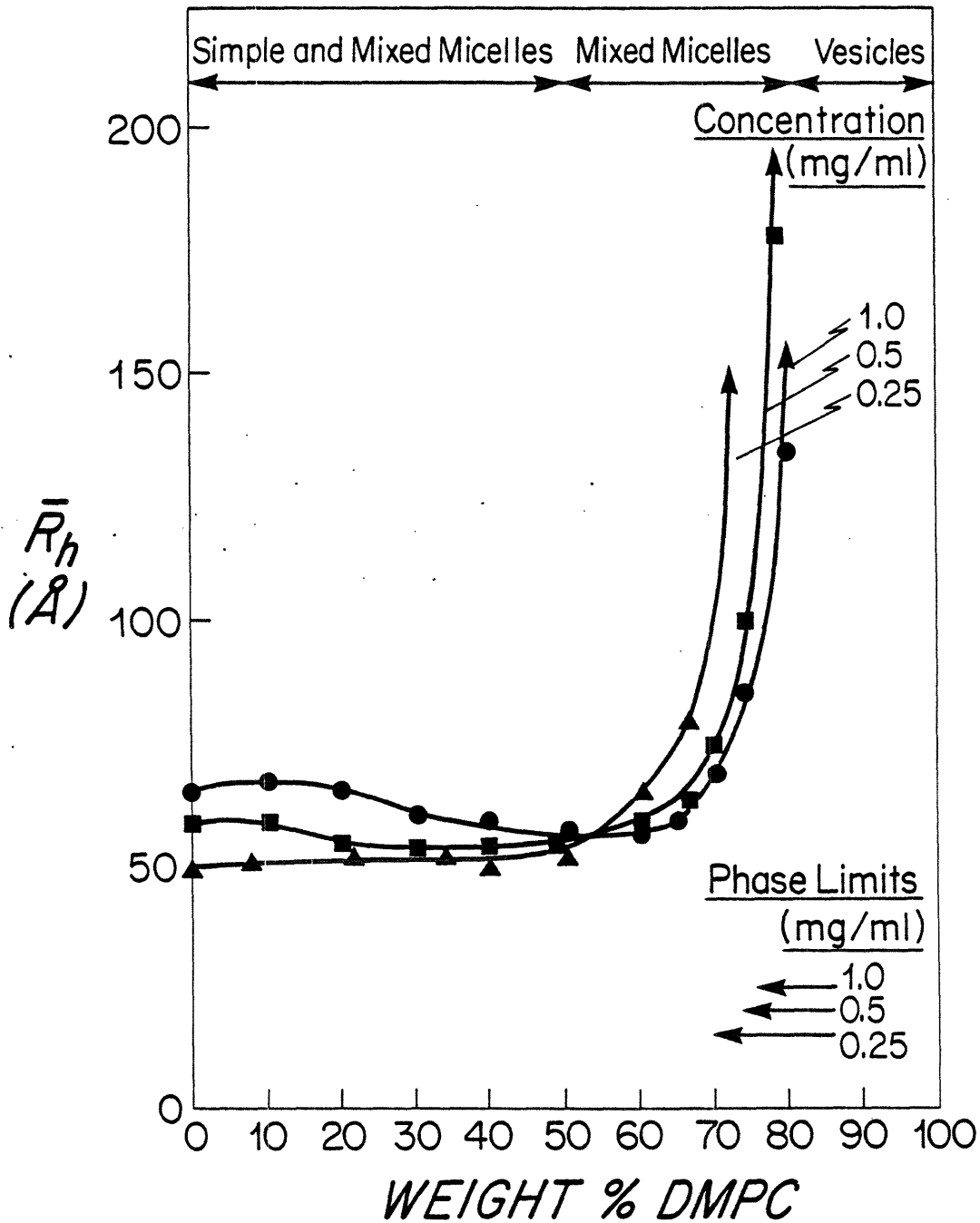


Figure 1. Dependence of \bar{R}_h of apo A-I/DMPC micelles on % DMPC at various total solute concentrations (0.15M NaCl, 25°C): ● 1.0 mg/ml; ■ 0.5 mg/ml; ▲ 0.25 mg/ml. The macroscopic phase limits are also shown.

the total solute concentration is decreased within the mixed micellar region, \bar{R}_h increases and diverges, and a liquid crystalline phase appears at lower DMPC contents. Chemical analysis of this precipitant phase (present above 80% DMPC) showed that it contained 88% DMPC, and 12% apo A-I.

Figure 2 shows the \bar{R}_h values as a function of % DMPC (from 60 to 80%) for three total apo A-I and DMPC concentrations (0.25, 0.50, and 1.0 mg/ml) at two temperatures (25 and 37°C). Below 60% DMPC (1 mg/ml apo A-I plus DMPC concentration) \bar{R}_h was not dependent on temperature (data not shown). Above 60% DMPC, \bar{R}_h increased as temperature increased from 25 to 37°C, and diverged at a lower DMPC contents.

The possibility that simple and mixed micelles coexisted from 0 to 50% DMPC was examined by measuring \bar{R}_h under conditions where simple apo A-I micelles became dissociated, whereas mixed micelles remained largely unaffected. To this end guanidine HCl, a well known disruptor of hydrophobic forces was employed. As previously demonstrated (Chapter 2) 2M guanidine HCl dissociated apo A-I micelles from \bar{R}_h of 65 Å to \bar{R}_h of 32 Å (1 mg/ml). To investigate the effect of guanidine HCl on apo A-I/DMPC mixed micelles, apo A-I and DMPC were allowed to interact in the presence of 2M guanidine HCl (25°C, 1 mg/ml apo A-I plus DMPC concentration, 48 hours incubation). The variation of \bar{R}_h with % DMPC in 0 and 2M guanidine HCl is shown in Figure 3. At 0 % DMPC, \bar{R}_h is only 32 Å in 2M guanidine HCl, reflecting dissociation of simple apo A-I micelles ($\bar{R}_h = 65$ Å). As the relative % DMPC increases

DEPENDENCE OF HYDRODYNAMIC RADIUS OF APO A-I/DMPC MICELLES ON DMPC CONTENT EFFECTS OF TEMPERATURE

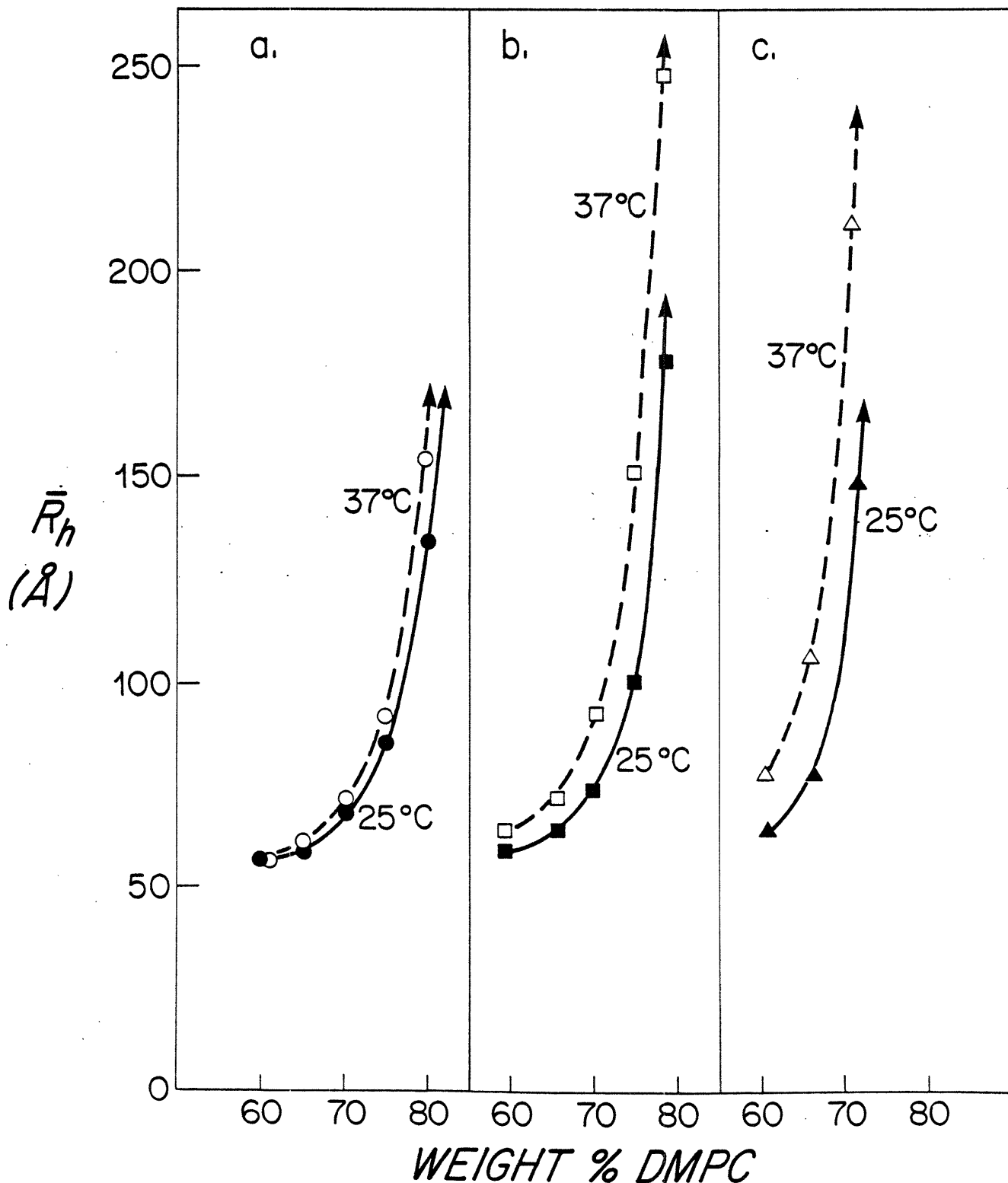


Figure 2. Dependence of \bar{R}_h of apo A-I/DMPC micelles on DMPC content (0.15M NaCl): a. ●○ 1.0 mg/ml; b. ■□ 0.5 mg/ml; c. ▲△ 0.25 mg/ml.

DEPENDENCE OF HYDRODYNAMIC RADIUS
OF APO A-I/DMPC MICELLES ON DMPC
CONTENT: EFFECTS OF GUANIDINE HCl

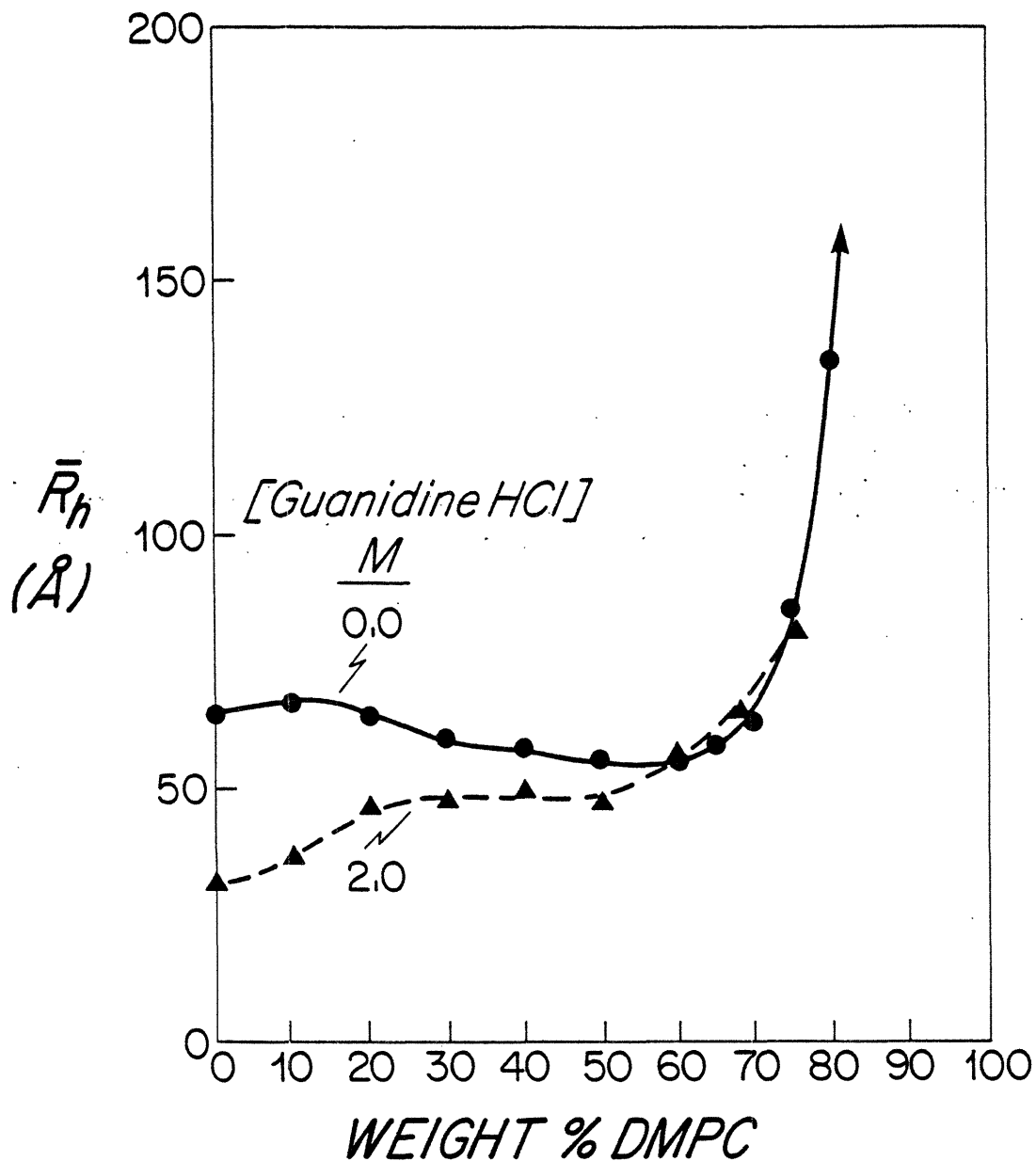


Figure 3. Dependence of \bar{R}_h of apo A-I/DMPC micelles on % DMPC in the presence of 2.0M guanidine (\blacktriangle), and without guanidine HCl (\bullet) (25°C, 1 mg/ml total solute concentration).

from 20 to 50 %, \bar{R}_h increases to a plateau of approximately 48 Å, and with higher % DMPC increases markedly to 80 Å at 76% DMPC. Between 60 and 76% DMPC, the variation of \bar{R}_h with relative DMPC content is approximately the same in the presence or absence of guanidine HCl.

C. Phase Equilibria of Apo A-I/EYPC. As appreciated in other studies, aqueous solutions of apo A-I did not interact with EYPC to form mixed micelles at incubation times up to 96 hours (method A). We therefore attempted to reach equilibrium by employing an alternative path. Preformed EYPC/TC mixed micelles at constant EYPC/TC ratio were prepared with varying % EYPC (defined as $\{\text{EYPC}\} / \{\text{EYPC}\} + \{\text{apo A-I}\}$) with total apo A-I plus EYPC held constant (method B). By comparing solutions with the same % EYPC but different TC concentrations, we extrapolated to zero TC concentration to obtain the phase diagram of apo A-I/EYPC. Figure 4 shows the phase diagram from 0 to 100% EYPC of apo A-I/EYPC/TC solutions at a constant protein plus lecithin concentration (1 mg/ml). Data at 4 different EYPC/TC ratios are shown (initial weight ratios 4.0, 2.3, 1.5, and 1.0). The final TC concentration is below the CMC for all data points shown except four data points which are enclosed by the dotted line. The dependence of \bar{R}_h on % EYPC is similar to that observed with apo A-I/DMPC (shown in Figure 1). However, in solutions with TC concentrations below the CMC, \bar{R}_h values are smaller than values observed in solutions with similar % EYPC and TC concentrations below the

DEPENDENCE OF HYDRODYNAMIC RADIUS OF APO A-I/EYPC/TC MICELLES ON % EYPC

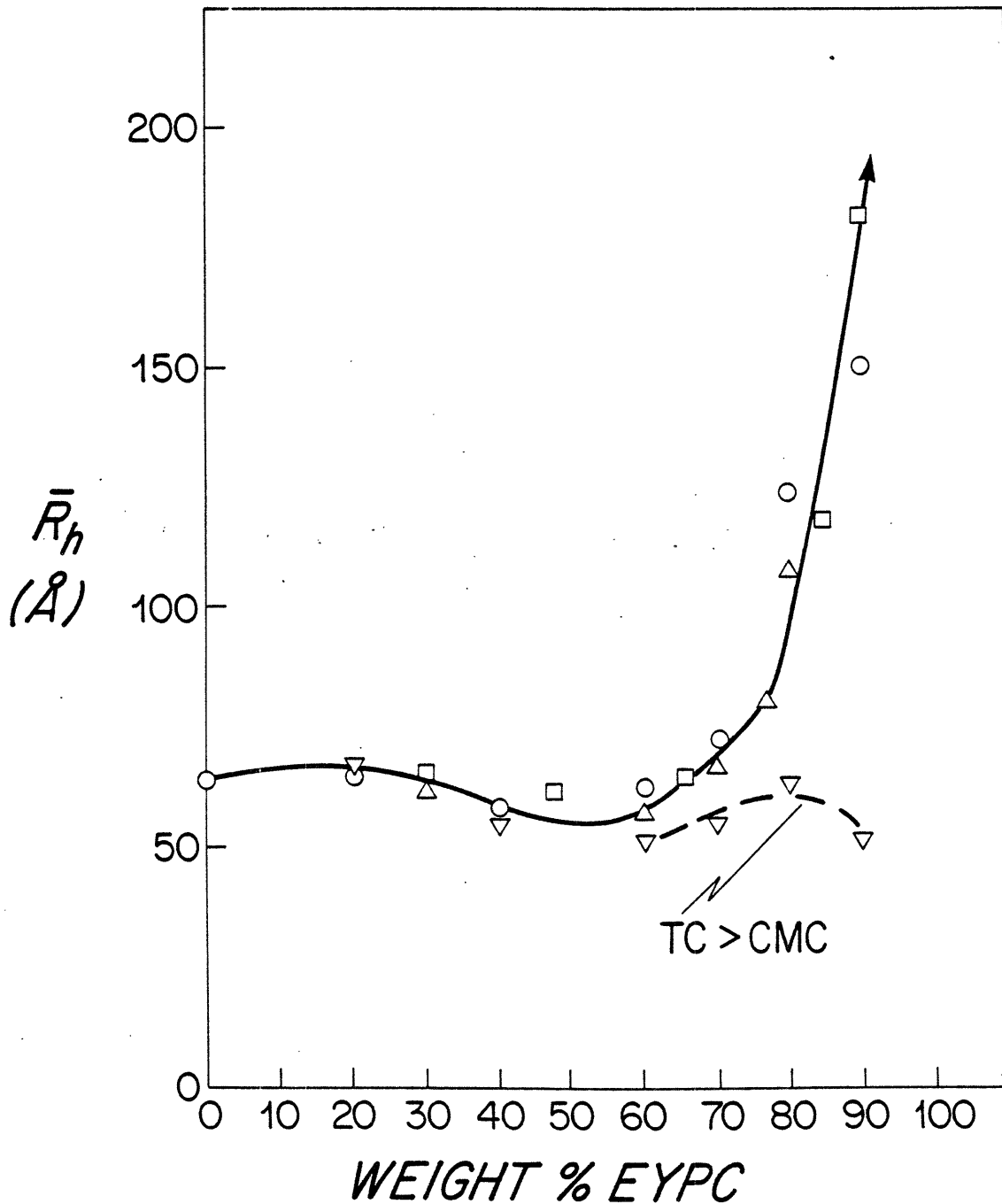


Figure 4. Dependence of \bar{R}_h of apo A-I/EYPC/TC micelles on % EYPC at various TC/EYPC ratios (37°C, apo A-I plus EYPC concentration 1 mg/ml): ○ TC/EYPC = 1.0; □ TC/EYPC = 1.5; △ TC/EYPC = 2.3; ▽ TC/EYPC = 4.0. The final TC concentration of the four indicated points is above the CMC of TC.

CMC. Above the CMC of TC, \bar{R}_h does not diverge as the % EYPC increases, but actually decreases.

Figure 5 shows the dependence of \bar{R}_h on % EYPC for two total protein and lecithin concentrations (0.25 and 1.0 mg/ml) at a EYPC/TC ratio of 1.0 (below the CMC of TC, method B). At the lower total solute concentration, \bar{R}_h diverged at a lower % EYPC. Similar behavior was also observed in the apo A-I/DMPC phase diagram (Figure 1).

To test the hypothesis that submicellar concentrations of bile salts might catalyze the formation of apo A-I/EYPC mixed micelles, solutions were prepared by adding aqueous apo A-I to dried EYPC/TC (method A). Final concentrations were identical to the series with EYPC/TC weight ratio of 1.0 in Figure 4. All solutions remained turbid after 96 hours, and \bar{R}_h of the supernatant phase was in the range 200 to 500 Å, suggesting the presence of vesicles (data not plotted).

D. Micelle to Vesicle Transition. The phase limit of bile salt/lecithin solutions is concentration dependent (Mazer et al., 1980). Therefore, as a mixed micellar solution is diluted, the phase limit is exceeded and the mixed micelles are transformed into unilamellar vesicles (Mazer and Carey, 1983, Schurtenberger et al., 1983). This is demonstrated in Figure 6a, where \bar{R}_h is plotted as a function of the total lipid concentration (top axis) as a EYPC/TC solution (weight ratio 2.7, total concentration 4.5 mg/ml) is diluted. On the lower axis, the

DEPENDENCE OF HYDRODYNAMIC RADIUS
 OF APO A-I/EYPC/TC MICELLES
 ON % DMPC: EFFECTS OF CONCENTRATION

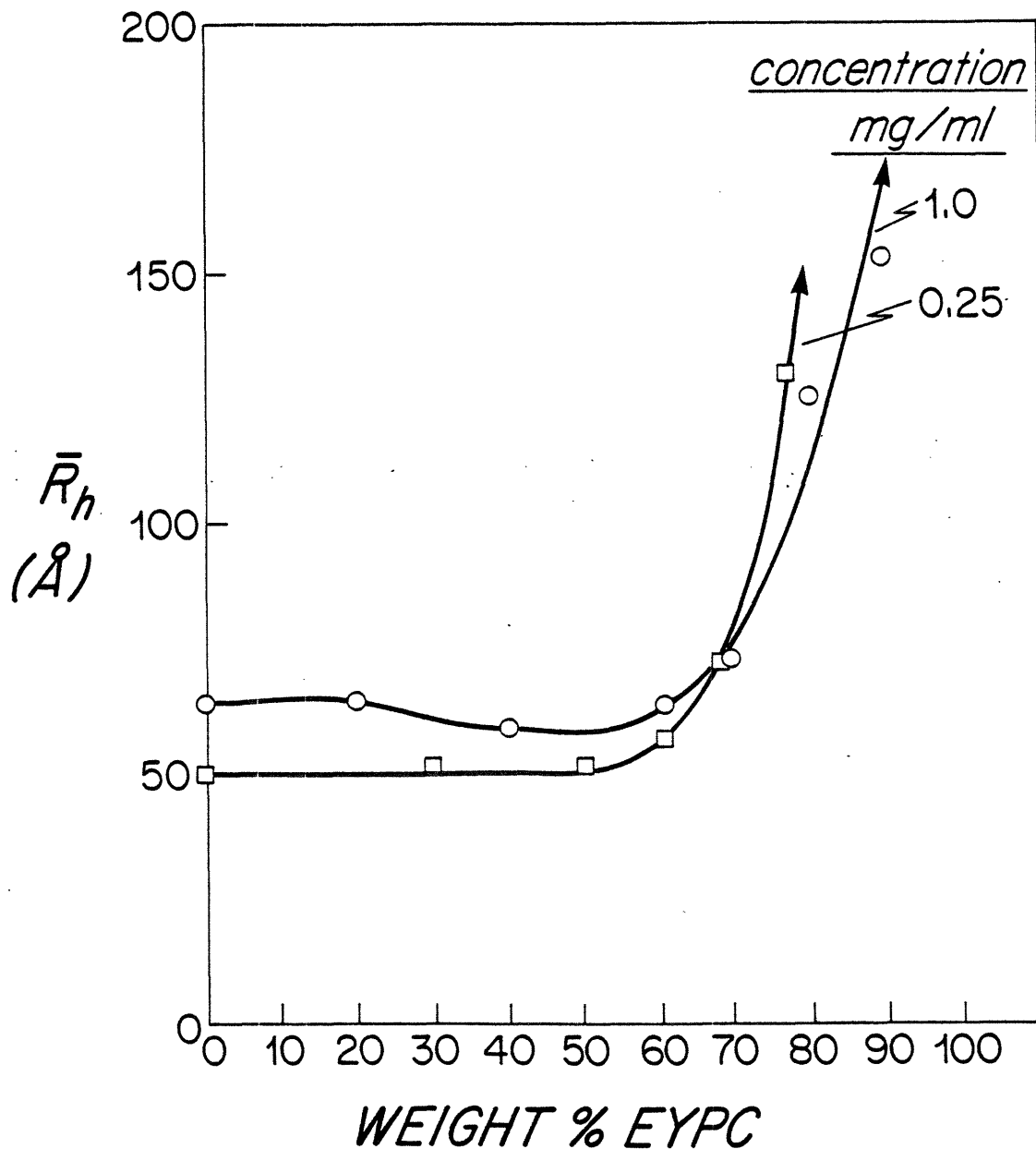


Figure 5. Dependence of \bar{R}_h of apo A-I/EYPC/TC micelles on % EYPC at various total apo A-I plus EYPC concentrations (0.15M NaCl, 37°C): ○ 1.0 mg/ml; □ 0.25 mg/ml.

MICELLE TO VESICLE TRANSITION OF TC/EYPC
EFFECTS OF TC AND APO A-I IN DILUENT

TOTAL TC PLUS EYPC CONCENTRATION (mg/ml)

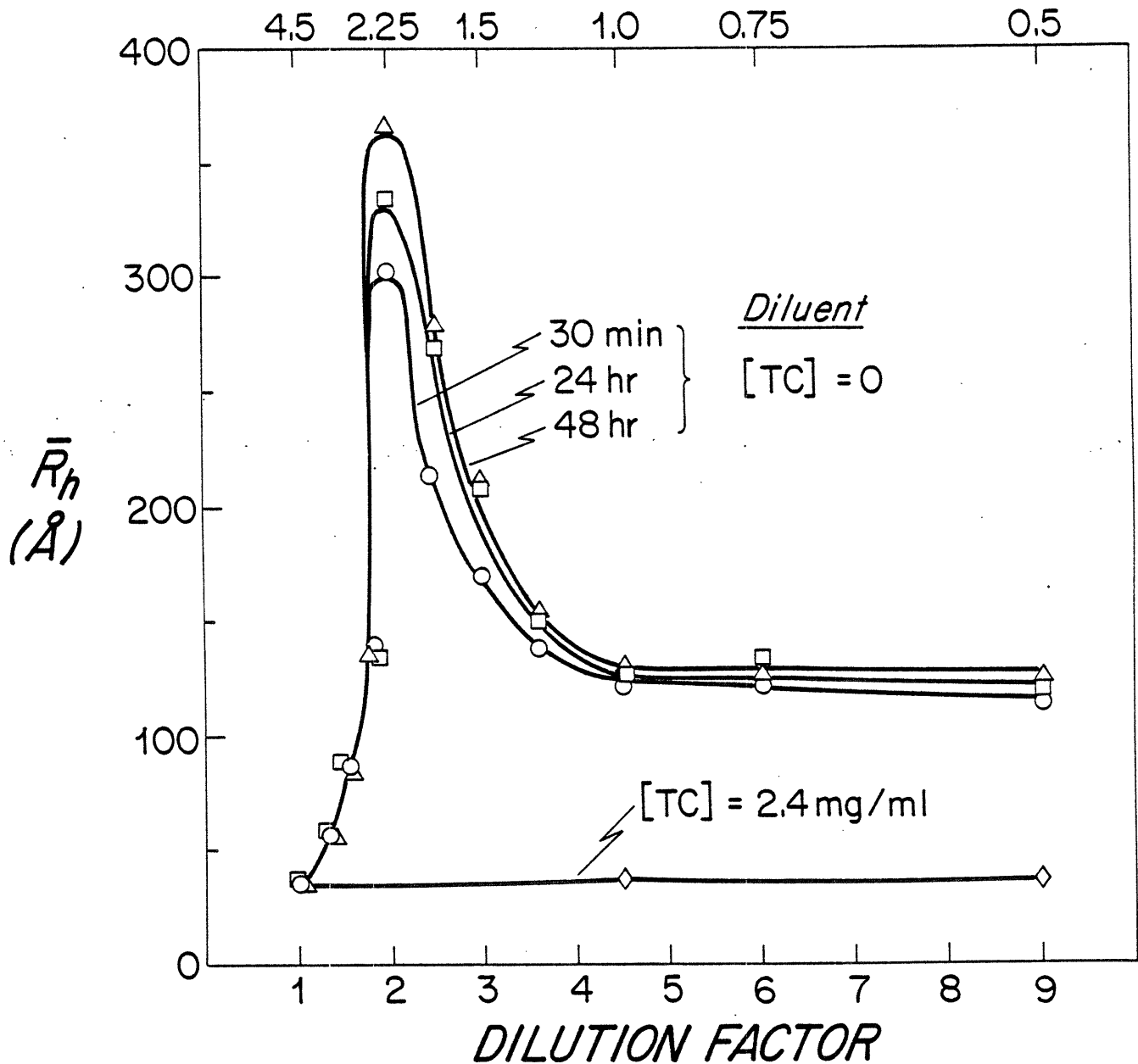


Figure 6(a-f). Effect of TC or apo A-I in the diluent buffer on the micelle to vesicle transition of TC/EYPC (initial weight ratio 2.4, 4.5 mg/ml total lipid concentration, 37°C). \bar{R}_g values are shown at times: ○ 30 minutes; □ 24 hours; △ 48 hours. a. Diluent buffer contains no TC or apo A-I, or 2.4 mg/ml TC as indicated.

MICELLE TO VESICLE TRANSITION OF TC/EYPC EFFECTS OF TC AND APO A-I IN DILUENT

TOTAL TC PLUS EYPC CONCENTRATION (mg/ml)

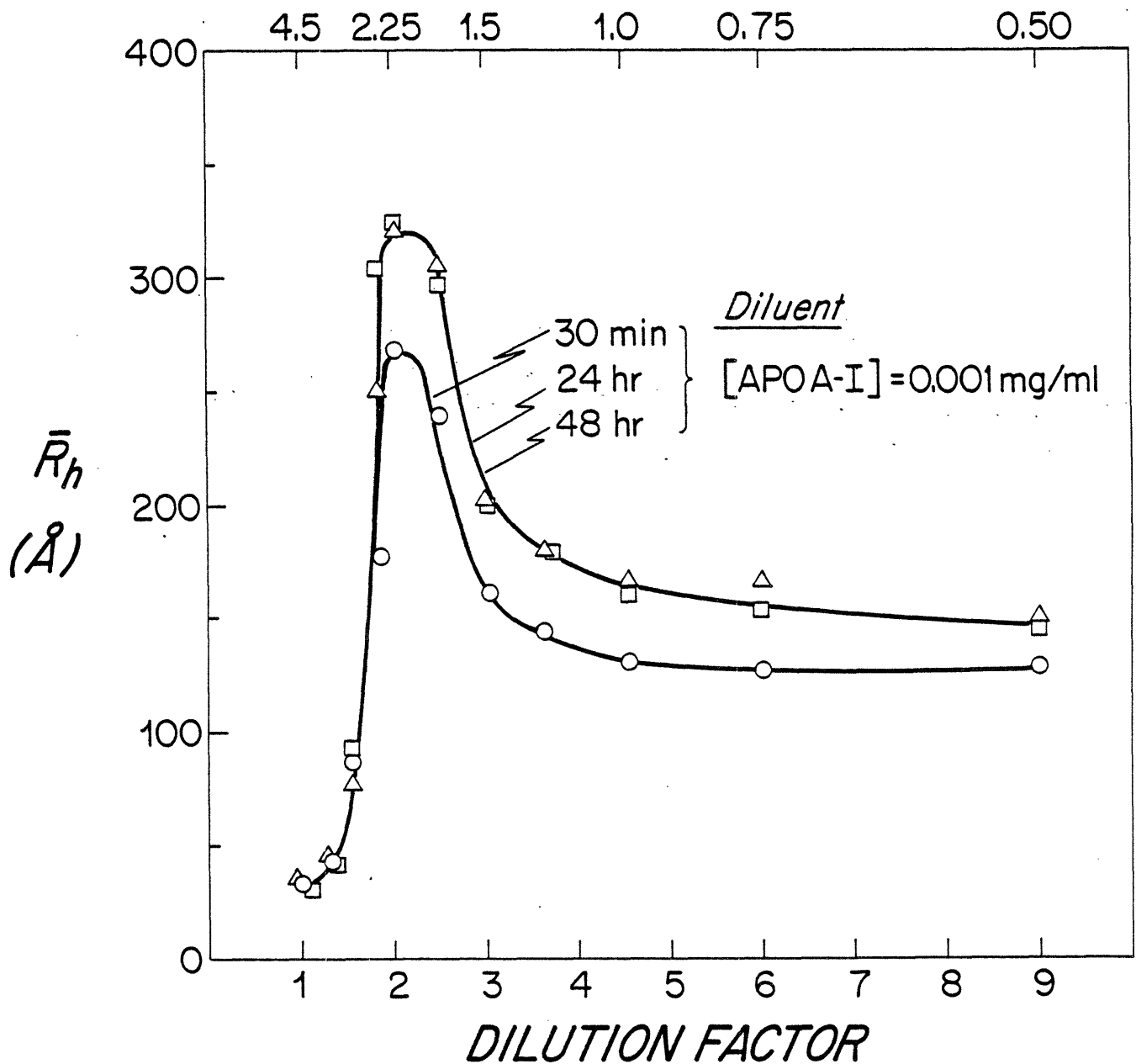


Figure 6b. Diluent contains 0.001 mg/ml apo A-I.

MICELLE TO VESICLE TRANSITION OF TC/EYPC
EFFECTS OF TC AND APO A-I IN DILUENT

TOTAL TC PLUS EYPC CONCENTRATION (mg/ml)

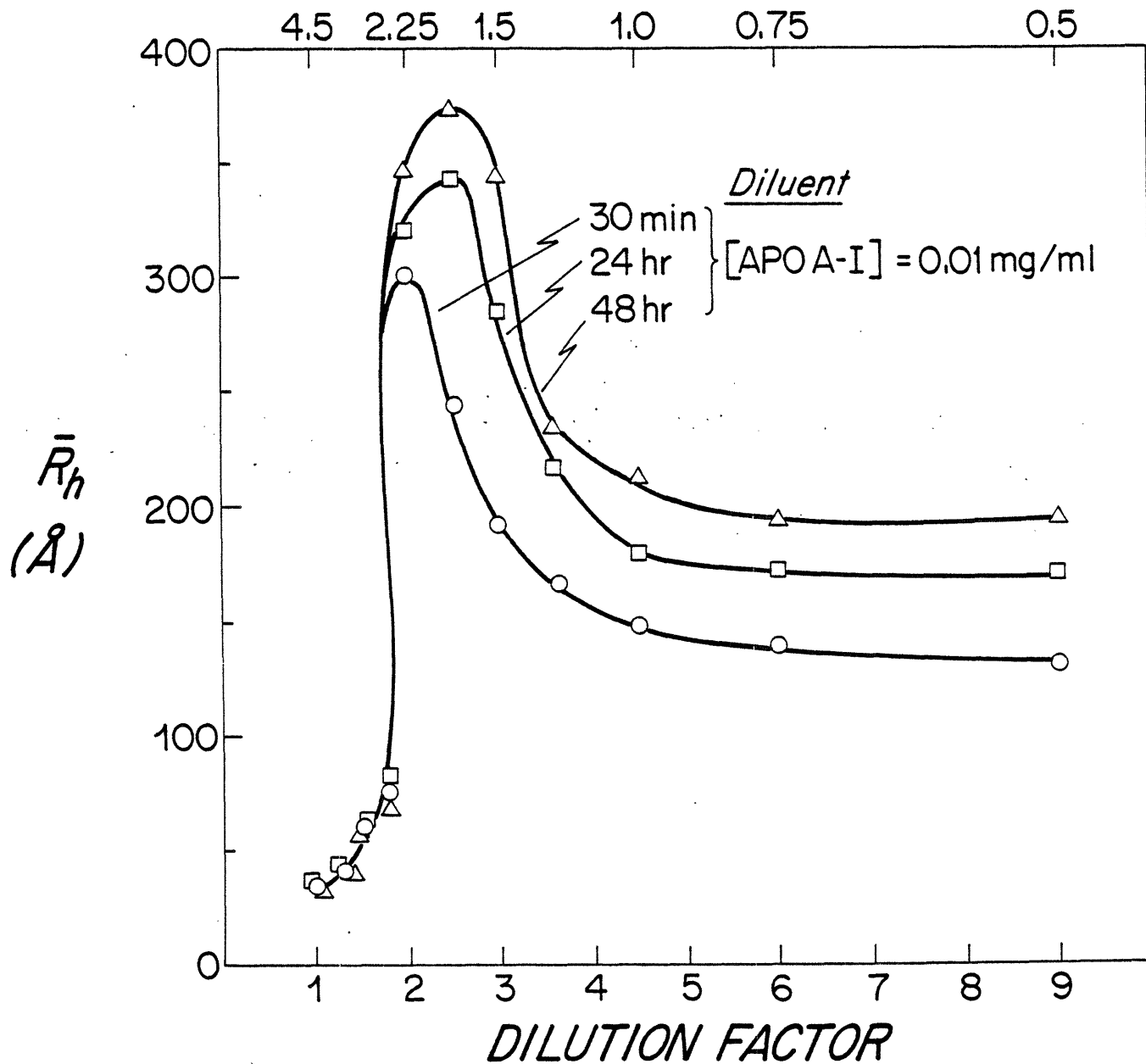


Figure 6c. Diluent contains 0.01 mg/ml apo A-I.

MICELLE TO VESICLE TRANSITION OF TC/EYPC
EFFECTS OF TC AND APO A-I IN DILUENT

TOTAL TC PLUS EYPC CONCENTRATION (mg/ml)

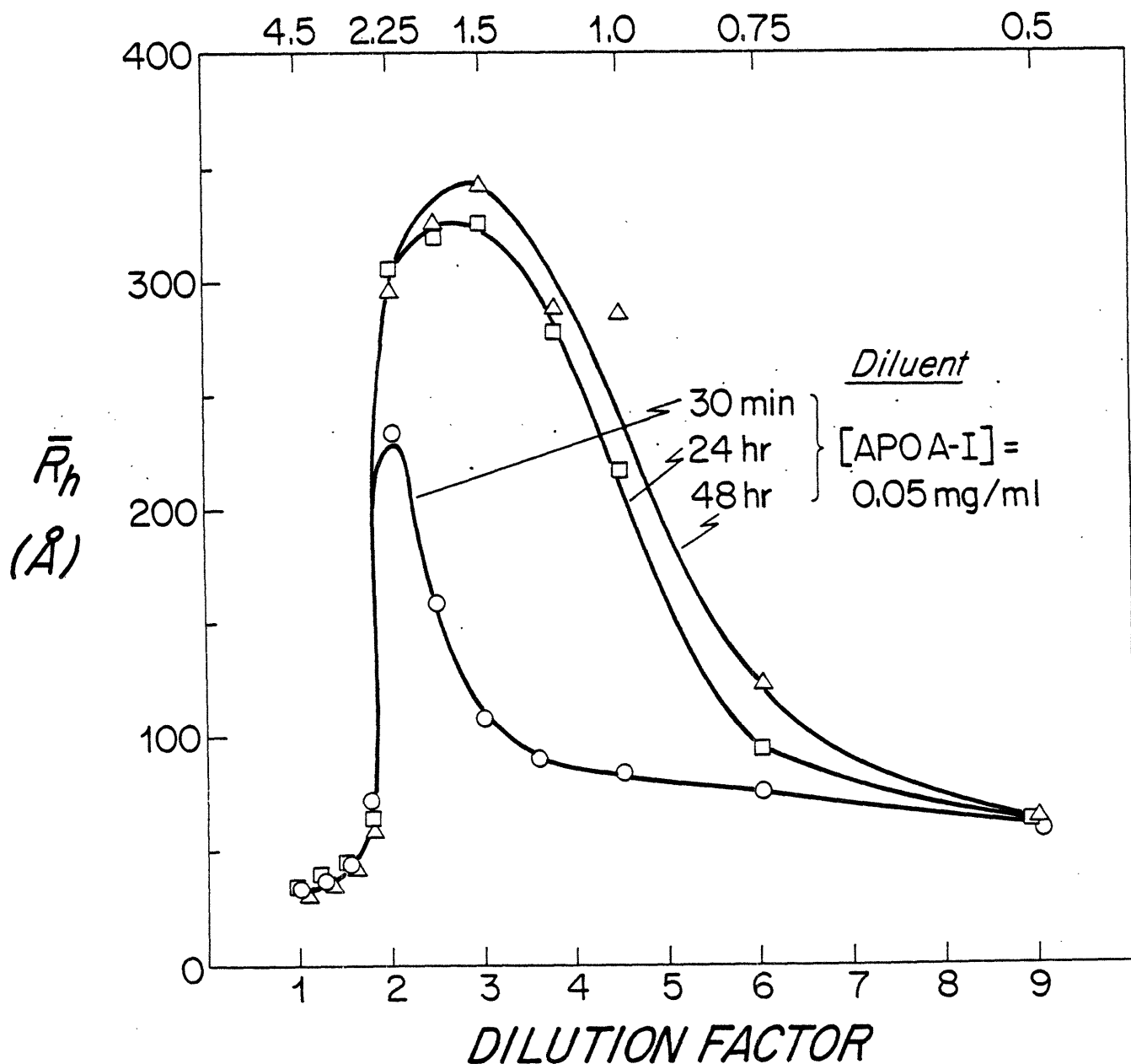


Figure 6d. Diluent contains 0.05 mg/ml apo A-I.

MICELLE TO VESICLE TRANSITION OF TC/EYPC
EFFECTS OF TC AND APO A-I IN DILUENT

TOTAL TC PLUS EYPC CONCENTRATION (mg/ml)

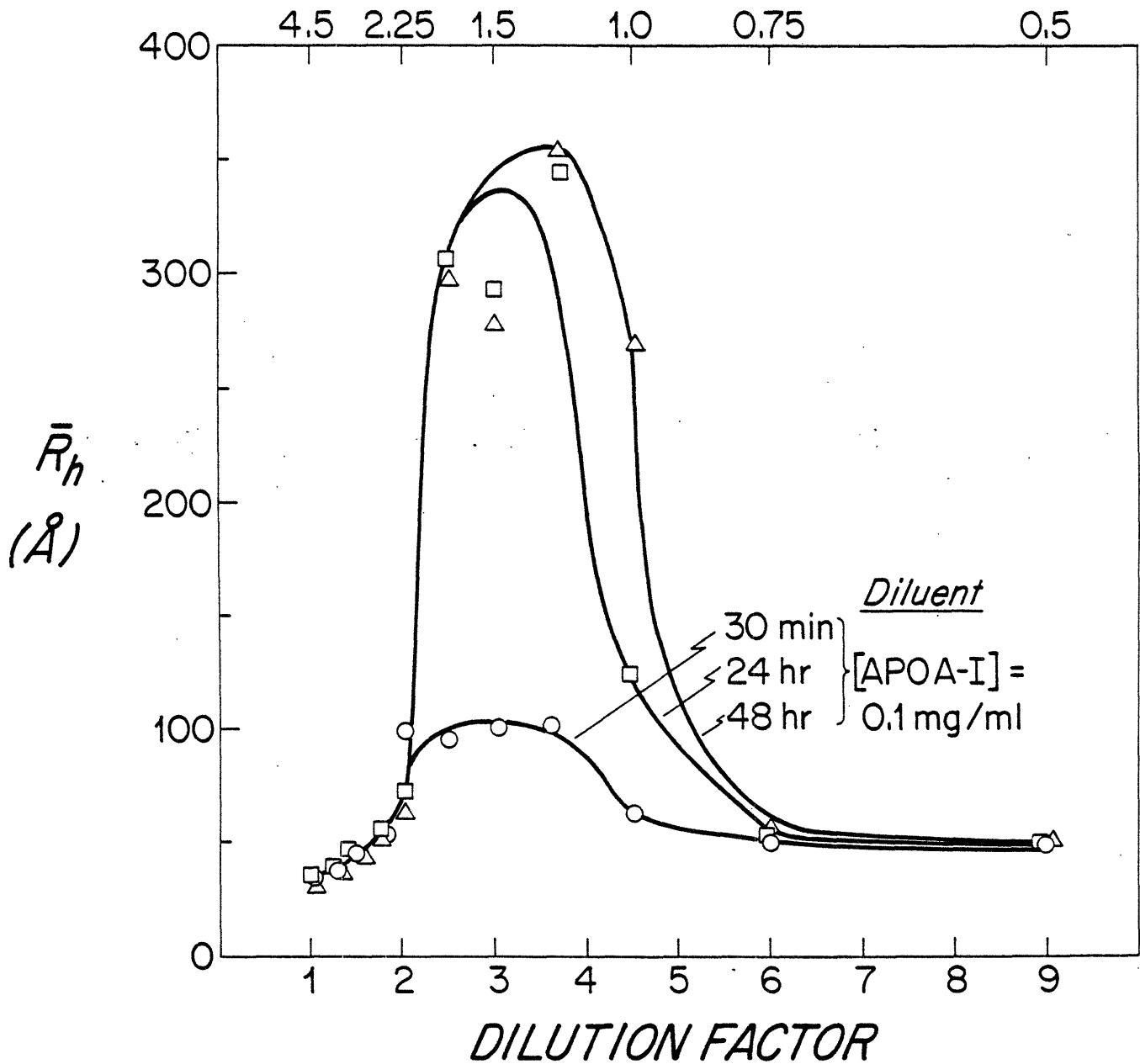


Figure 6e. Diluent contains 0.10 mg/ml apo A-I.

MICELLE TO VESICLE TRANSITION OF TC/EYPC
EFFECTS OF TC AND APO A-I IN DILUENT

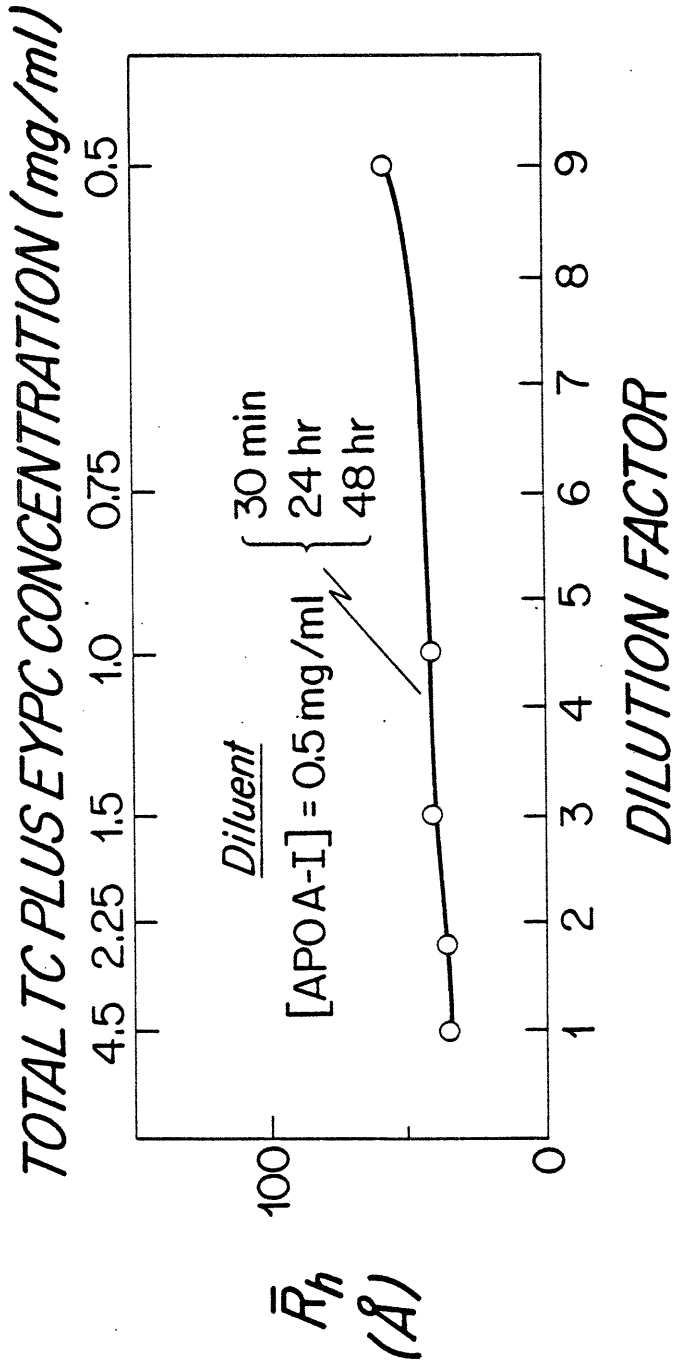


Figure 6f. Diluent contains 0.5 mg/ml apo A-I.

factor by which the initial solution was diluted is also indicated. As the total lipid concentration decreases, \bar{R}_h increases up to the phase limit, at a dilution factor of approximately 2.0. Beyond this point, \bar{R}_h gradually decreases and approaches an asymptotic value of approximately 120 Å. The temporal evolution (at 30 minutes, 24 and 48 hours) of the micelle to vesicle transition is also shown in Figure 6a. Beyond the phase limit achieved by dilution, \bar{R}_h continues to increase from 30 minutes up to 48 hours to values consistent with vesicles.

This micelle to vesicle transition has been shown to be prevented by the presence of an appropriate intermicellar concentration (IMC) of TC in the diluent buffer (Mazer et al., 1980). Figure 6a also shows that \bar{R}_h values remain constant (45 Å) when the initial solution is diluted with buffer containing 2.4 mg/ml TC (30 minutes, 24 and 48 hours).

To determine if dilute apo A-I concentrations had similar effects, we studied the micelle to vesicle transition in the presence of apo A-I. Figures 6b-f show the dependence of \bar{R}_h on the total lipid concentration as an identical EYPC/TC solution (weight ratio 2.7, total concentration 4.5 mg/ml) is diluted with buffer containing various apo A-I concentrations (final concentrations 0.001, 0.01, 0.05, 0.10, and 0.50 mg/ml). As the apo A-I concentration increases, the divergence of \bar{R}_h is shifted to the right, to lower total lipid concentrations, i.e., the EYPC/TC micellar phase was expanded by

apo A-I. At 0.50 mg/ml apo A-I, the sharp increase in \bar{R}_h is entirely abolished and \bar{R}_h does not increase appreciably over the range of total lipid concentrations studied. At final apo A-I concentrations of 0.001 and 0.01 (Figures 6b and 6c), \bar{R}_h of the limiting vesicles increased from 120 Å to values of 150 and 190 Å, respectively. At 0.05 and 0.10 mg/ml apo A-I (Figures 6d and 6e), \bar{R}_h at the lowest lipid concentrations decreased to 60 to 70 Å, values consistent with mixed micelles.

The temporal evolution of the micelle to vesicle transition is also altered in the presence of apo A-I. At the lowest apo A-I concentrations (0.001 and 0.01 mg/ml), (Figures 6b and 6c), \bar{R}_h increased at 30 minutes, and slowly increased further up to 48 hours. In contrast, at apo A-I concentrations of 0.05 and 0.10 mg/ml, \bar{R}_h of some dilute solutions increased minimally to sizes consistent with mixed micelles (approximately 100 Å) at 30 minutes. Over the next 24 to 48 hours, \bar{R}_h increased to values of several hundred Å, values consistent with vesicles (Figures 6d and 6e).

The effect of various low apo A-I concentrations on vesicle size was studied by measuring \bar{R}_h of vesicles formed by diluting a EYPC/TC solution (2.7 weight ratio, 10 mg/ml total lipid concentration) to a final concentration of 0.5 mg/ml with various apo A-I concentrations (method C). Figure 7 shows \bar{R}_h of EYPC/TC/apo A-I vesicles on the vertical axis as a semilogarithmic function of final apo A-I concentration on

DEPENDENCE OF HYDRODYNAMIC RADIUS
OF TC/EYPC/APO A-I VESICLES
ON APO A-I CONCENTRATION

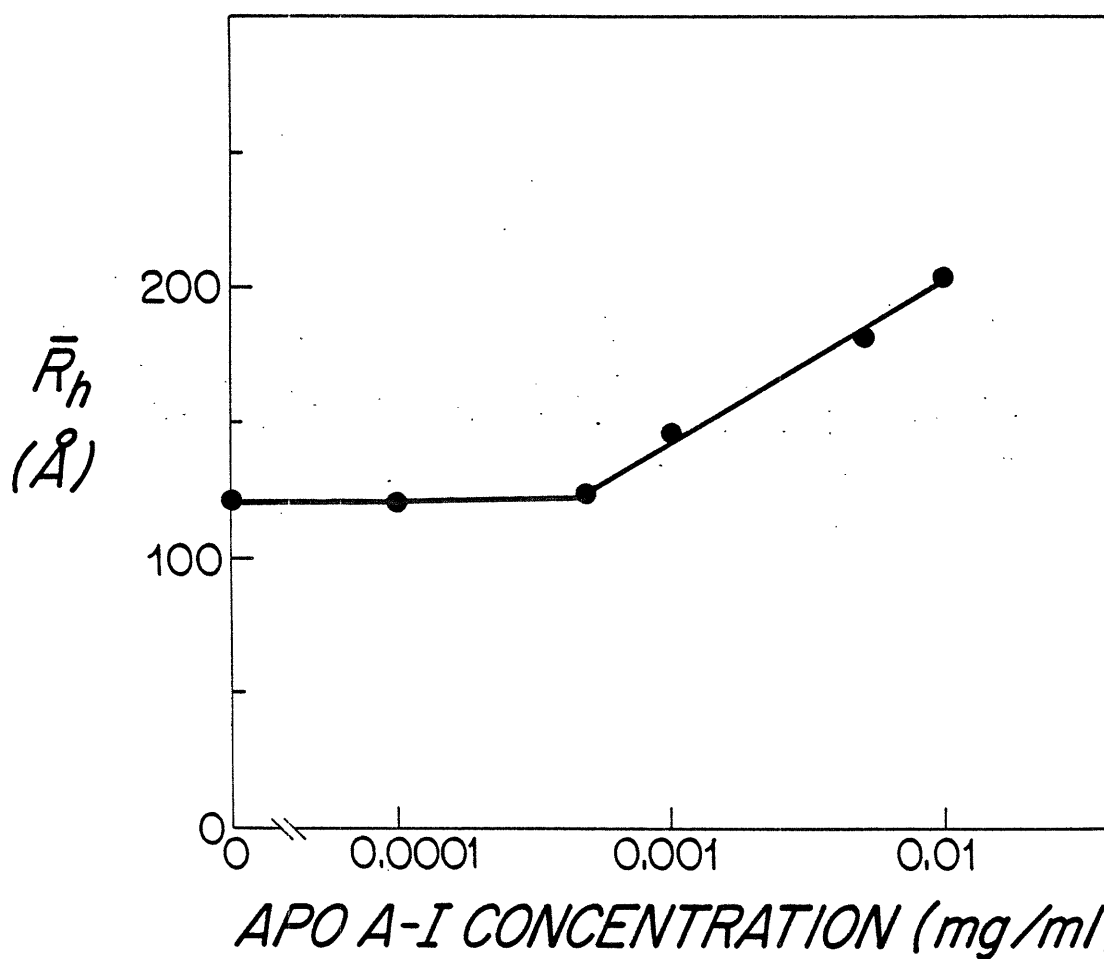


Figure 7. Dependence of \bar{R}_h of TC/EYPC/apo A-I vesicles on apo A-I concentration (TC/EYPC weight ratio 2.7, total lipid concentration 0.5 mg/ml, 37°C.)

the horizontal axis. \bar{R}_h of these vesicles was approximately 120 Å in the presence of up to 0.0005 mg/ml apo A-I. Above this concentration, \bar{R}_h increased linearly with $\log \{\text{apo A-I}\}$ up to 0.01 mg/ml.

E. Apo A-II/DMPC Phase Equilibria. Figure 8 demonstrates the dependence of \bar{R}_h on % DMPC for apo A-II/DMPC solutions at two total solute concentrations (0.5 and 1.0 mg/ml). The general characteristics of the dependence of \bar{R}_h on % DMPC are the same as for apo A-I/DMPC: at low DMPC/apo A-I ratios, \bar{R}_h increases slowly, and then more rapidly as the % DMPC increases and the phase limit is approached. However, the micellar phase limit for apo A-II is consistently observed at a lower DMPC content than the micellar phase limit of apo A-I/DMPC (65% vs. 80%, respectively, at 1 mg/ml). At lower total solute concentrations, \bar{R}_h diverges at a lower DMPC content, similar to the trend observed with apo A-I/DMPC.

DEPENDENCE OF HYDRODYNAMIC RADIUS
OF APO A-II / DMPC MICELLES ON % DMPC
EFFECTS OF CONCENTRATION

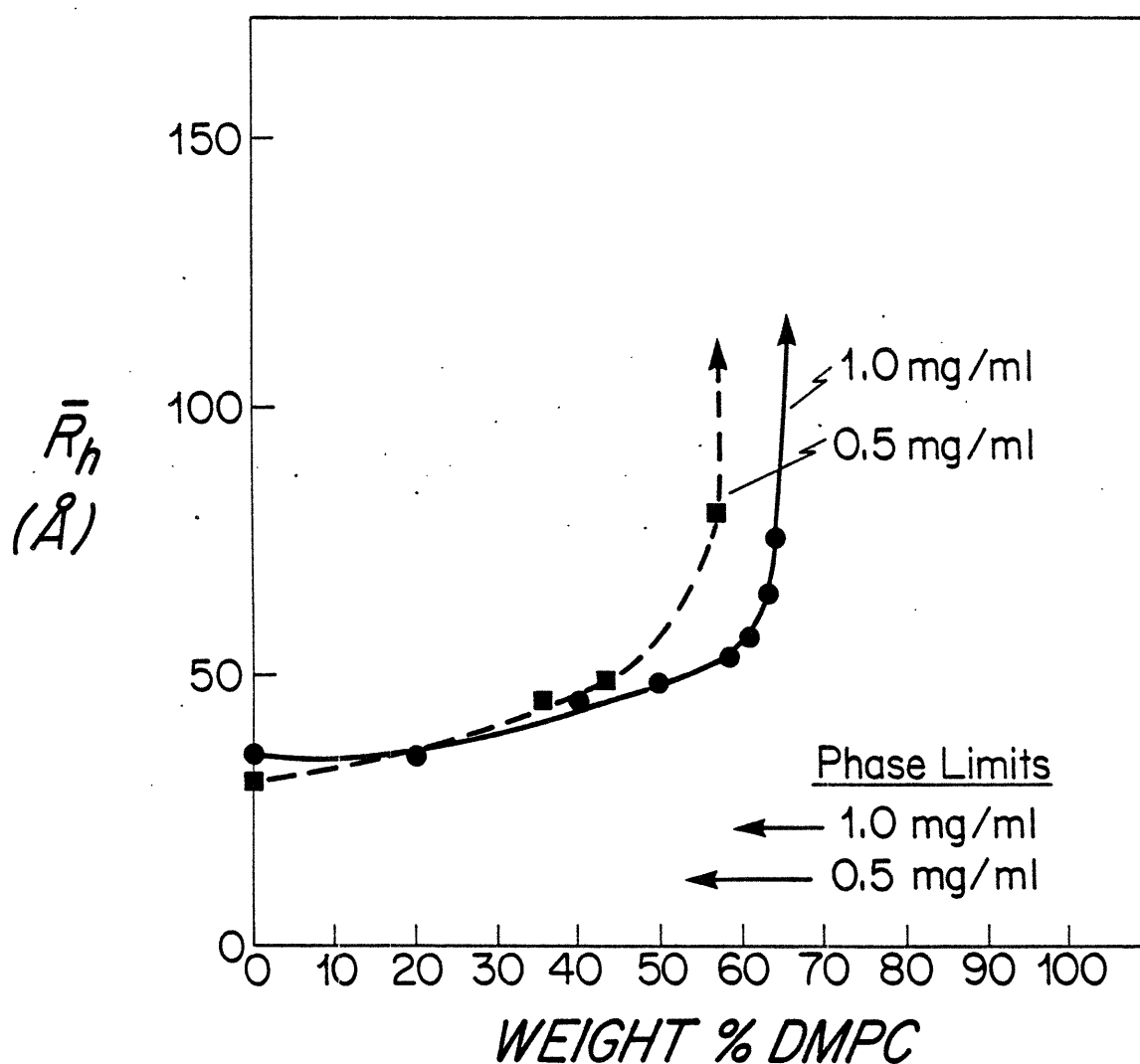


Figure 8. Dependence of \bar{R}_h of apo A-II/DMPC micelles on % DMPC at various total solute concentrations (0.15M NaCl, 25°C): ● 1.0 mg/ml; ■ 0.5 mg/ml. The macroscopic phase limits are also shown.

IV. DISCUSSION

A. Phase Equilibria of Apo A-I and Apo A-II/Lecithin Systems.

The apo A-I and apo A-II/lecithin phase equilibria have striking similarities to the EYPC/TC system. Figure 9 shows the dependence of \bar{R}_h on % EYPC at several total lipid concentrations (taken from Mazer et al., 1980). As the % EYPC increases, \bar{R}_h sharply increases as the phase limit is approached. At lower total lipid concentration, the phase limit is shifted to lower % EYPC. This behavior is consistent with three zones: at low lecithin contents, simple bile salt micelles coexist with lecithin/bile salt mixed micelles. At higher lecithin contents, the lecithin/bile salt mixed micelles are composed of a disc-shaped lecithin bilayer also containing bile salts, surrounded by a perimeter of bile salts. Beyond the phase limit, liquid crystalline vesicles are present. At all points in the phase diagram, a population of bile salt monomers exists in equilibrium with micelles or vesicles. This monomer concentration, called the intermicellar concentration (IMC), varies with the lecithin/bile salt ratio of the mixed micelles (Mazer et al., 1980).

Analogous trends occur in the apo A-I/DMPC phase diagram (see Figure 1). At 1 mg/ml total concentration, \bar{R}_h gradually decreases from 65 Å at 0% DMPC to 57 Å at 50% DMPC. The larger simple micelles present at 0% DMPC dissociate as the lecithin content increases, and the observed \bar{R}_h reflects the average of two populations: simple apo A-I micelles, and apo A-I/DMPC

DEPENDENCE OF HYDRODYNAMIC RADIUS OF TC/EYPC MICELLES ON % EYPC EFFECTS OF TOTAL SOLUTE CONCENTRATION

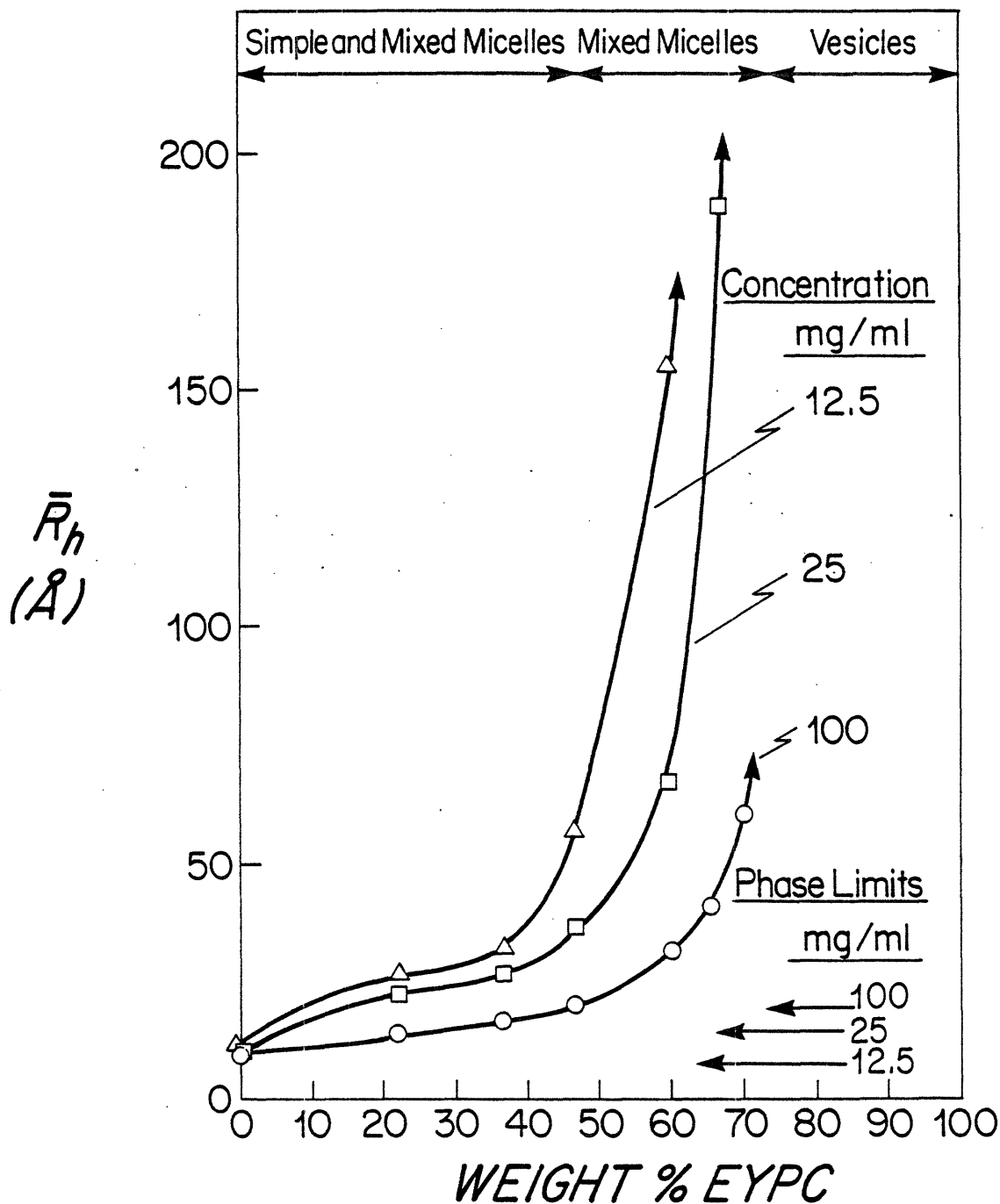


Figure 9. The dependence of \bar{R}_h of TC/EYPC micelles on % EYPC at various total lipid concentrations (0.15M NaCl, 20°C):
 ○ 100 mg/ml; □ 25 mg/ml; △ 12.5 mg/ml. The arrows at the top indicate the species present at 100 mg/ml total lipid concentration. (Taken from Mazer et al., 1980.)

mixed micelles. Since \bar{R}_h is heavily weighted toward higher molecular weight species, from 0 to 20% DMPC, \bar{R}_h does not change, only reflecting the larger apo A-I simple micelles. At 0.25 mg/ml, \bar{R}_h remains about 50 Å up to 50% DMPC. At this concentration, the sizes of the simple apo A-I and the mixed micelles are approximately equal. Therefore, by analogy with the TC/EYPC system, our data suggest that there is a zone between 0 and 50% DMPC where apo A-I monomers, simple apo A-I micelles, and mixed apo A-I/DMPC micelles coexist. Above 50% DMPC, the size of the micelles increases with increasing DMPC content. In this region, mixed micelles coexist with apo A-I/DMPC micelles, and \bar{R}_h is determined by the lecithin/protein ratio within the micelle. Beyond the phase limit, apo A-I monomers and a liquid crystalline vesicle phase coexist.

Our results clearly indicate that the coexistence of apo A-I and apo A-I/DMPC mixed micelles is an equilibrium phenomenon. On the basis of ultracentrifugal density gradient analysis of solutions of various apo A-I/DMPC ratios, three similar zones of composition were proposed by Tall et al. (1977). They conclude that up to 30% DMPC, free apo A-I is present in equilibrium with mixed micelles, and above 80% DMPC, vesicles are present. However, upon reanalysis of the experimental data presented by these authors, we find that their results suggest the presence of free apo A-I up to 54% DMPC, a value consistent with our estimate of the limit of the coexistence zone between simple apo A-I and apo A-I/DMPC mixed micelles.

Other investigators (Jonas et al., 1980, Swaney, 1980) observed the presence of free apo A-I after gel filtration isolation of apo A-I/DMPC complexes with up to 70% DMPC.

The behavior of the apo A-I/DMPC phase diagram in the presence of guanidine HCl is also consistent with these three zones. Up to about 50% DMPC, \bar{R}_h is decreased in 2M guanidine HCl, and above 50% DMPC, \bar{R}_h is essentially unchanged in the presence of 2M guanidine HCl. At low DMPC contents, therefore, \bar{R}_h reflects the dissociated simple apo A-I micelles, and this effect is precisely what we would expect if guanidine HCl affects only the aggregation of apo A-I to form simple but not mixed micelles. From 20 to 50% DMPC, simple micelles coexist with the minimum mixed micelle of $\bar{R}_h = 48 \text{ \AA}$. Since the simple micelles are of much lower molecular weight, the average \bar{R}_h overwhelmingly reflects the \bar{R}_h of the mixed micelles (see the definition of \bar{R}_h in Chapter 2). Above 50% DMPC, the \bar{R}_h of the mixed micelles reflects only the lipid/protein ratio within the micelle, and is largely unaffected by the dissociative effect of guanidine HCl.

These results are consistent with the gel filtration studies of Massey et al., (1981) who found that apo A-I/DMPC mixed micelles in the presence of guanidine HCl were the same size and chemical composition as those formed in the absence of guanidine HCl.

\bar{R}_h of apo A-I/DMPC mixed micelles depends not only on the % DMPC, but also on the total solute concentration (see Figure 1). By analogy to the bile salt/lecithin system, this

implies that there is a monomeric concentration of apo A-I in equilibrium with apo A-I/DMPC mixed micelles. Therefore the total apo A-I concentration is the sum of the monomeric concentration, the IMC and the amount of apo A-I in the mixed micelle:

$$\{\text{apo A-I}\} = \text{IMC} + \{\text{DMPC}\} \times \left(\frac{\text{apo A-I}}{\text{DMPC}}\right) \quad (1)$$

where (apo A-I/DMPC) is the ratio of apo A-I to DMPC within the mixed micelles, and {apo A-I} and {DMPC} are the absolute concentrations of apo A-I and DMPC respectively. If we make the reasonable assumption that the ratio of (apo A-I/DMPC) is the same for all mixed micelles of a given size, then {apo A-I} should be a linear function of {DMPC}. Figure 10 shows the dependence of apolipoprotein concentration on lecithin concentration for several sizes of mixed micelles. This dependence is linear, and estimates of the approximate values of the IMC can be derived. These extrapolated values on the vertical axis are shown in Table 2. The IMC of apolipoprotein in equilibrium with mixed micelles decreases as the \bar{R}_h values increase. The IMC of apo A-I/DMPC mixed micelles decreases as temperature increases from 25 to 37°C. Therefore the shift in the divergence of \bar{R}_h to lower DMPC contents is attributable to an increase in the monomer concentration of apo A-I. As we showed previously, apo A-I is predominantly in the form of monomers and dimers at the IMC concentrations estimated.

DETERMINATION OF IMC OF APO A-I AND A-II / LECITHIN MIXED MICELLES

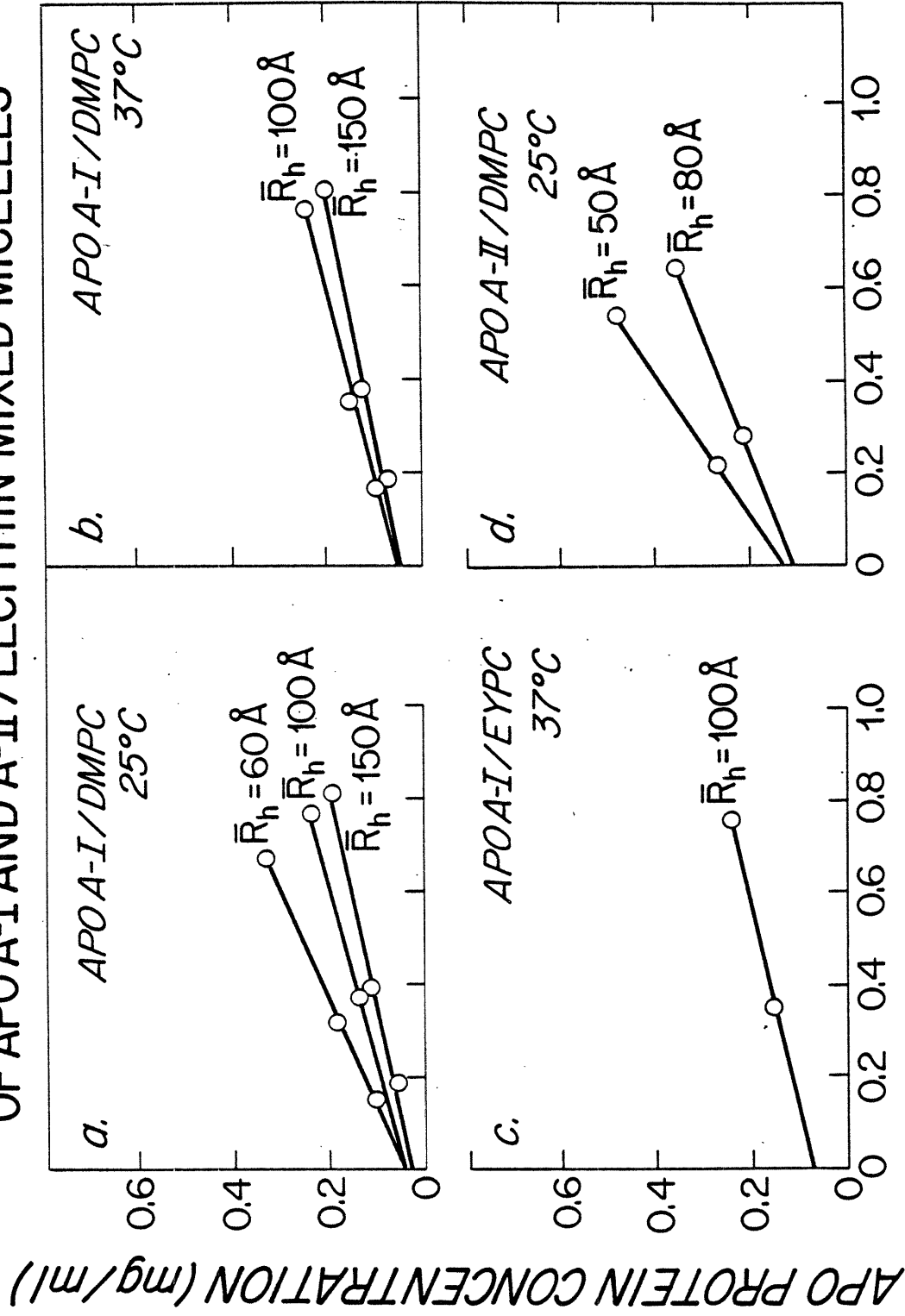


Figure 10. Determination of the IMC of various apoprotein/lecithin mixed micelles, described fully in the text.

TABLE 2

IMC VALUES OF APOLIPOPROTEIN/LECITHIN MIXED MICELLES

Components	T (°C)	\bar{R}_h (Å)	IMC (mg/ml)
Apo A-I/DMPC	25	60	0.05
		100	0.04
		150	0.03
	37	100	0.05
		150	0.045
	Apo A-I/EYPC	37	100
Apo A-II/DMPC	25	50	0.12
		80	0.10

If our observations on the concentration dependence of \bar{R}_h and our values of the IMC are correct, then one should observe an increase in \bar{R}_h upon dilution of mixed micellar solutions. In this case, the IMC will decrease below its equilibrium value, and some of the apo A-I in the mixed micelles will tend to dissociate to restore the IMC. (Since the monomer solubility of DMPC is approximately 10^{-12} , dilution does not significantly decrease the amount of lipid in the mixed micelles.) The increase in lipid/protein ratio in the remaining mixed micelles results in an increase in \bar{R}_h . If the diluent buffer contains apo A-I at the IMC, then there is no tendency for apo A-I to dissociate from the mixed micelles, and \bar{R}_h would not change. If the diluent buffer contains apo A-I at a concentration greater than the IMC, the excess apo A-I and the mixed micelles would reach a new equilibrium, with a lower lipid/protein ratio within the mixed micelles, and \bar{R}_h would decrease. The additional apo A-I would not only prevent the increase in \bar{R}_h , but would effect a decrease in \bar{R}_h . Dilution with buffer containing apo A-I at a concentration equivalent to the IMC should result in no change in \bar{R}_h , as was found in Figure 6f. In Figure 11, the \bar{R}_h data from Table 1 are plotted against apo A-I concentration in the diluent buffer. Two apo A-I/DMPC mixed micellar solutions (80% DMPC with $\bar{R}_h = 135 \text{ \AA}$, and 68% DMPC with $\bar{R}_h = 65 \text{ \AA}$, both 1 mg/ml) were diluted fourfold with buffer only and 3 apo A-I concentrations (0.025, 0.050, and 0.10 mg/ml). Both initial and final \bar{R}_h values are shown (Figure 11). For both solutions \bar{R}_h

DILUTION OF MIXED MICELLAR APO A-I / DMPC SOLUTIONS

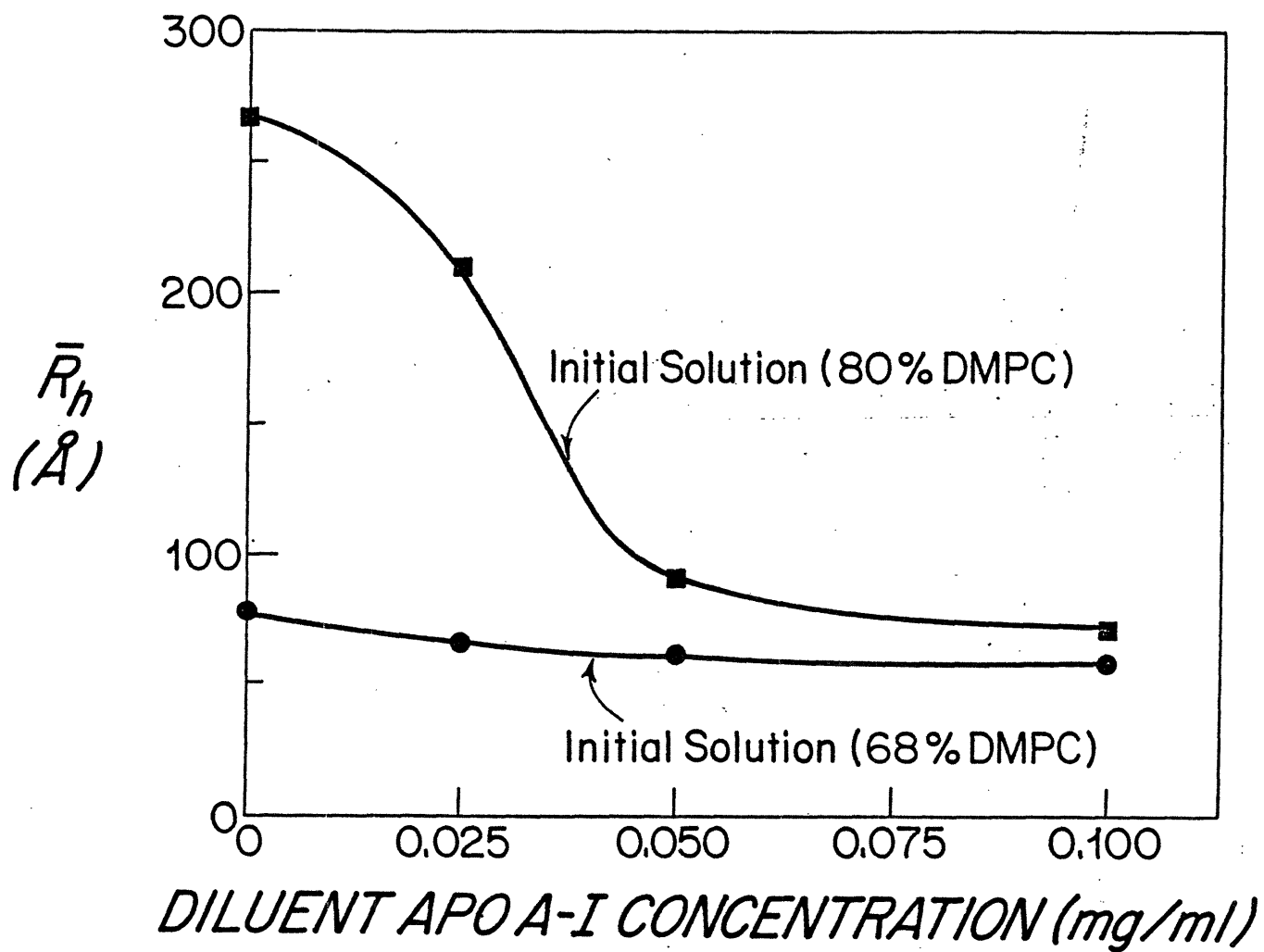


Figure 11. Effect of apo A-I in dilution of apo A-I/DMPC mixed micelles.
Initial solutions: 80% DMPC, 1 mg/ml; 68% DMPC, 1 mg/ml.

increases when the diluent contains only 0.025 mg/ml apo A-I, and decreases when the diluent contains 0.050 mg/ml apo A-I. Therefore we can conclude that the IMC is between 0.025 and 0.050 mg/ml, values consistent with our previous estimates of the IMC. In gel filtration studies of native HDL, Pownall et al. (1978) estimated the apo A-I concentration in equilibrium with mature HDL to be approximately 0.003 mg/ml, a value an order of magnitude smaller than our estimate of the IMC in equilibrium with apo A-I/DMPG mixed micelles. If Pownall's result is correct, it could imply that binding of apo A-I to spherical particles with an apolar core such as native HDL is much stronger than binding to disc shaped mixed micelles.

Two models have been proposed for the structure of apo A-I/lecithin mixed micelles. The most generally accepted model proposes that a perimeter of apolipoprotein surrounds a lecithin bilayer disc (Tall and Small, 1980). The second proposes that lecithin molecules are intercalated between the apolipoprotein α -helices forming an oblate ellipsoid. The first model implies a fixed geometric relationship between the relative lecithin content of the mixed micelles and their radius. This hypothesis will be tested with the present data as follows.

The length of the edge of the disc to be covered with apolipoprotein can be expressed as

$$N_{\text{apo A-I}} L = 2\pi R \quad (2)$$

where $N_{\text{apo A-I}}$ is the number of apo A-I molecules in each

micelle, L is the length of the edge covered per apo A-I, and R is the radius of the lecithin bilayer. L may vary as different amounts of apo A-I is present on the edge of the particle, and the value we derive is an average. The number of lecithin molecules can be expressed in terms of the disc radius:

$$2\pi R^2 = A_L N_L \quad (3)$$

where A_L is the area per lecithin molecule, and N_L is the number of lecithin molecules in each micelle. The area of the disc, πR^2 , must be multiplied by a factor of 2 to account for both faces of the disc. We can now express the disc radius in terms of the lecithin/apolipoprotein ratio in the micelle:

$$R = \frac{A_L}{L} \left(\frac{N_L}{N_{\text{apo A-I}}} \right) \quad (4)$$

We can calculate the relationship between \bar{R}_h and R using a formula for hydrodynamic radius of a disc (Mazer, 1978):

$$R_h = \frac{3}{2} R \left\{ \left(1 + \left(\frac{T}{2R} \right)^2 \right)^{\frac{1}{2}} + \frac{2R}{T} \ln \left[\frac{T}{2R} + \left(1 + \left(\frac{T}{2R} \right)^2 \right)^{\frac{1}{2}} \right] - \frac{T}{2R} \right\}^{-1} \quad (5)$$

where T is the thickness of the disc. For T we chose 50\AA for the DMPC bilayer and 55\AA for the EYPC bilayer. The ratio $N_L/N_{\text{apo A-I}}$ is not simply $N_L/N_{\text{apo A-I}}$ of the solution; the amount of apolipoprotein in the mixed micelles is the total amount in solution less that amount present as monomers (the IMC determined earlier):

$$\frac{N_L}{N_{\text{apo A-I}}} = \frac{C_L}{C_{\text{apo A-I}} - \text{IMC}} \quad (6)$$

Table 3 lists values of \bar{R}_h , R , C_L , $C_{\text{apo A-I}}$ (the weight concentrations of lecithin and apo A-I), IMC and $N_L/N_{\text{apo A-I}}$ for several points on the apo A-I/DMPC phase diagram at total lipid and protein concentrations of 1.0, 0.5 and 0.25 mg/ml (25°C). The dependence of \bar{R}_h (vertical axis) on $N_L/N_{\text{apo A-I}}$ (horizontal axis) is shown in Figure 12a. At R values below 120 Å, there is a linear dependence of R on $N_L/N_{\text{apo A-I}}$, with intercept going through zero. The slope of this line, determined by least squares analysis of the values with \bar{R}_h less than 120 Å, is 1.4. Using a value of 60 Å² for A_L we estimate that L is 84 Å. Above 120 Å, there is a systematic deviation of R : for any value of $N_L/N_{\text{apo A-I}}$, R is greater than is predicted by this model. This implies that at large R , not as much apo A-I is available to cover the lecithin bilayer.

Tall et al. (1977) demonstrated that the diameter of apo HDL/DMPC rouleaux (measured by electron microscopy) depended linearly on the lipid/protein ratio over the range 33 to 63% DMPC. From their results we calculate a value of $L = 90$ Å. Nichols et al. (1983) also employed electron microscopy to measure the mean diameter of apo A-I/EYPC particles. Over the range 73 to 84% EYPC there was a linear relationship between the diameter of these particles and the lipid/protein

TABLE 3
DATA USED FOR DETERMINATION OF L AND α

Components	\bar{R}_h (Å)	R (Å)	C_L (mg/ml)	C_{apo} (mg/ml)	$\frac{N_L}{N_{apo}}$	$\frac{N_{apo}}{N_L}$	JMC (mg/ml)	$\frac{1}{R}$ (Å) ⁻¹
Apo A-I/DMPC	135	164	0.80	0.20	190	0.0052	0.03	0.0061
	85	97	0.75	0.25	144	0.0069	0.04	0.0102
	68	75	0.69	0.31	105	0.0097	0.045	0.0134
	58	61	0.66	0.33	95	0.0105	0.05	0.0163
	178	225	0.39	0.11	196	0.0050	0.03	0.0045
	100	117	0.37	0.13	166	0.0060	0.04	0.0085
	148	181	0.18	0.07	187	0.0055	0.03	0.0055
Apo A-II/DMPC	76	85	0.64	0.36	44	0.0162	0.10	0.0117
	65	71	0.62	0.38	40	0.0181	0.10	0.0141
	53	55	0.58	0.42	34	0.0221	0.10	0.0183
	80	91	0.29	0.21	34	0.0152	0.10	0.0110

TESTS OF APOPROTEIN / DMPC MIXED MICELLE MODELS

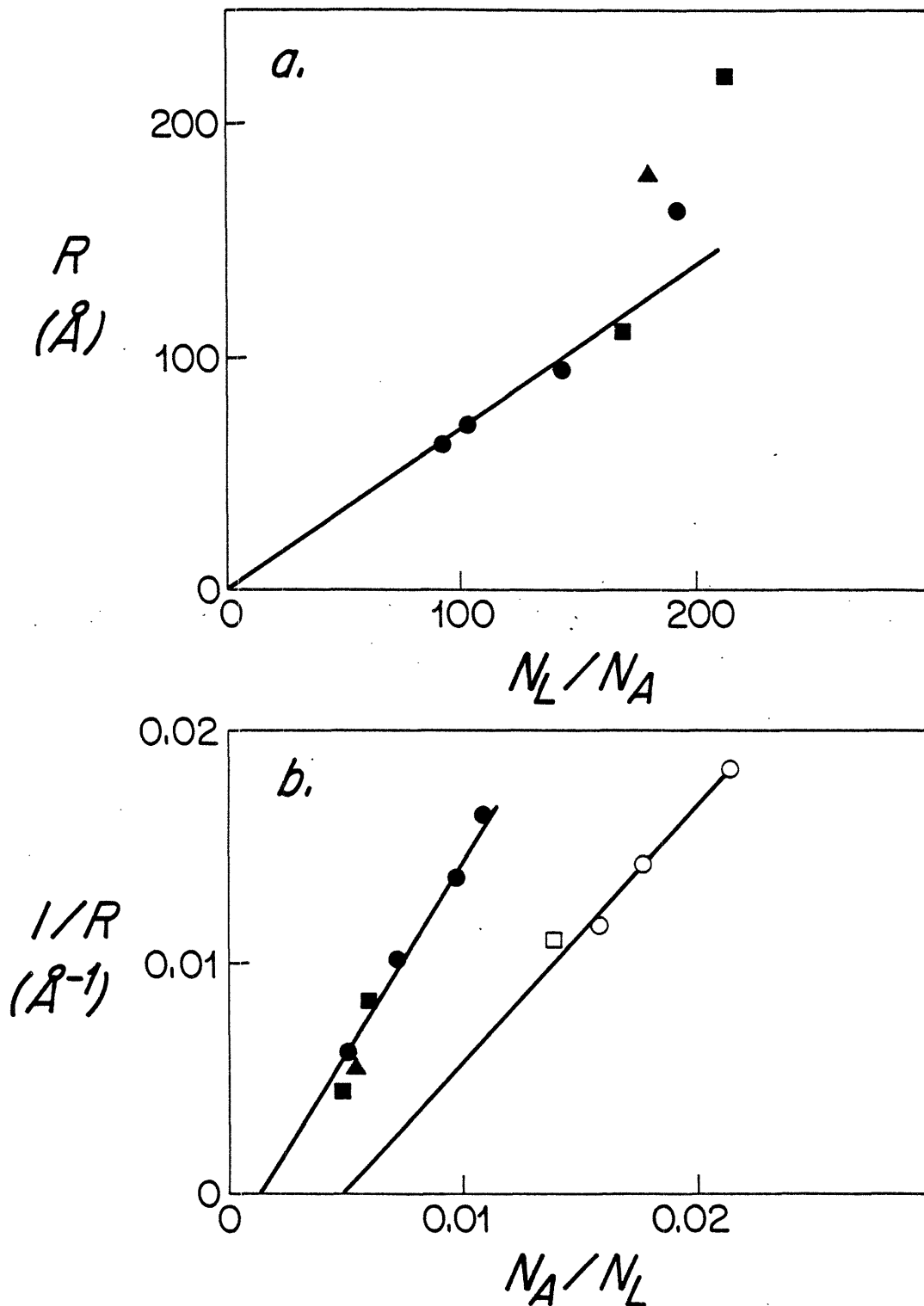


Figure 12. Tests of models for apo A-I and apo A-II/lecithin mixed micelles at total solute concentrations ●○ 1.0 mg/ml; ■□ 0.5 mg/ml; ▲ 0.25 mg/ml. Closed symbols denote apo A-I/DMPC; open symbols, apo A-II/DMPC.

ratio. From their data we calculate a value of $L = 81 \text{ \AA}$. In view of the approximations in measuring particle size by negative staining electron microscopy, it is remarkable that both these values agree well with our value of $L = 84 \text{ \AA}$.

We now modify this model to include the possibility that some of the apo A-I is solubilized in the lipid bilayer and is unavailable to cover the edges of the disc. We will demonstrate that this modification improves the fit of our experimental data to theory at \bar{R}_h values above 120 \AA . An entire apo A-I molecule or 'tails' of several molecules could be solubilized in the lipid bilayer. This model is conceptually similar to that proposed for bile salt/EYPC mixed micelles by Mazer et al. (1980). By assuming that the amount of apo A-I solubilized is proportional to the amount of lipid bilayer present, a quantity α can be defined as the value of $N_{\text{apo A-I}}/N_L$ within the lipid bilayer. Equation 1 must be modified to account for the amount of apo A-I not present on the edge:

$$(N_{\text{apo A-I}} - \alpha N_L) L = 2\pi R \quad (7)$$

As a first approximation, we shall assume that the area the apo A-I occupies is negligible compared to the total area occupied by lecithin, and equation 2 remains unchanged. R can now be expressed as a function of $N_L/N_{\text{apo A-I}}$, the ratio of lecithin to total apo A-I in the mixed micelle:

$$\frac{1}{R} = \frac{L}{A_L} \left(\frac{N_{\text{apo A-I}}}{N_L} - \alpha \right) \quad (8)$$

Values of $1/R$ and $N_{\text{apo A-I}}/N_L$ are presented in Table 3, and the dependence of $1/R$ (vertical axis) on $N_{\text{apo A-I}}/N_L$ (horizontal axis) is shown in Figure 12b. Once again there is a linear dependence of $1/R$ on $N_{\text{apo A-I}}/N_L$ over the entire range of R values. The slope is 1.8, yielding a value of 110 \AA for L . The x intercept is 0.0019, corresponding to a value of approximately 7% by weight apo A-I in the DMPC bilayer. The idea that a small amount of apo A-I is present in the bilayer is also supported by our finding that the insoluble phase present at high DMPC contents is approximately 12% apo A-I by weight.

Several investigators (Brouillette et al., 1984, Nichols et al., 1983) have employed gradient gel electrophoresis to demonstrate that at each lipid/protein ratio there is a distribution of discretely sized complexes. Brouillette hypothesizes that this is due to a different number of amphipathic helices present on the edge of the lecithin bilayer. This is consistent with our proposal that a certain amount of apo A-I is present within the lecithin bilayer since a variable number of helices could be solubilized within the lecithin bilayer.

The absolute size of apo A-I/lecithin recombinants has been measured by several investigators. Figure 13 shows literature values of \bar{R}_h of apo A-I lecithin mixed micelles estimated by gel filtration (Swaney, 1980), or that we have calculated from electron microscopy data (Tall et al., 1977, Nichols et al., 1983, Jonas et al., 1980). Our values of

\bar{R}_h DEPENDENCE OF APOPROTEIN / LECITHIN MIXED MICELLES ON % LECITHIN

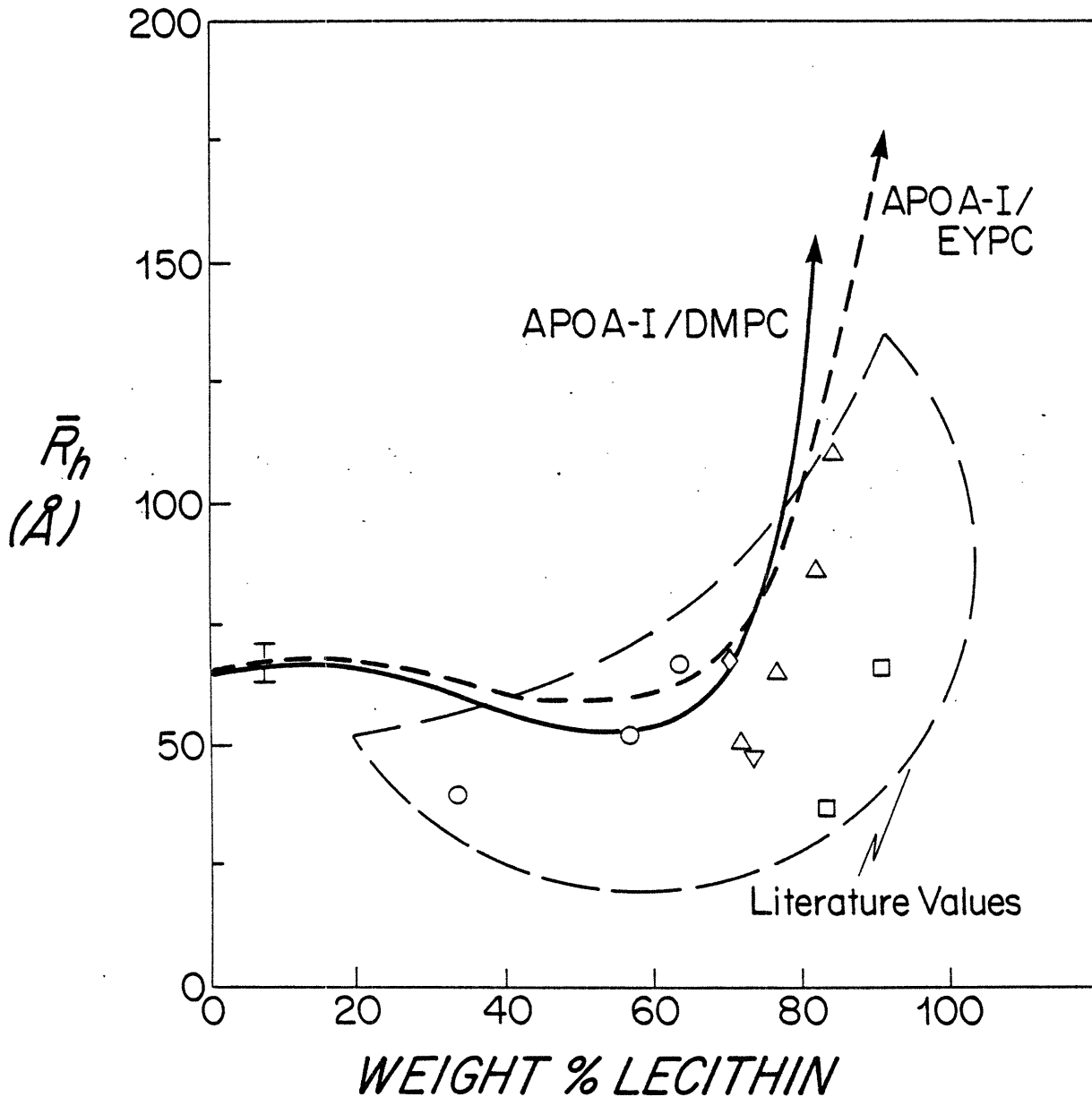


Figure 13. Dependence of \bar{R}_h of apolipoprotein/lecithin mixed micelles on % lecithin: ○ Tall et al., (1977); △ Nichols et al. (1983); □ Swaney (1980); ▽ Matz and Jonas (1982). Dashed and solid lines represent values of \bar{R}_h from the present work for apo A-I/EYPC and apo A-I/DMPC respectively.

\bar{R}_h are similar and show the same trends, except for the values of Swaney, who found a particle with 83% DMPC, with 2 apo A-I molecules per particle. This implies 400 DMPC molecules per particle, which would form a disc of radius 62 Å, a value inconsistent with Swaney's own value of 38 Å (by gel filtration). All these investigators worked at total solute concentrations of greater than 1 mg/ml, a regime where the concentration dependence of \bar{R}_h of mixed micelles is not significant.

The similarity of the apo A-I/DMPC and apo A-II/DMPC phase diagrams suggests that our three zone model also holds for the apo A-II/DMPC phase diagram. The small size of the apo A-II simple micelles does not permit us to distinguish clearly where simple and mixed micelles coexist. The concentration dependence of \bar{R}_h is similar to that observed in the apo A-I/DMPC system, and we can estimate the IMC of apo A-II in equilibrium with mixed micelles in the same fashion, as shown in Figure 10d and Table 2. The IMC of apo A-II is approximately 0.1 mg/ml. This corresponds to twice the value of the IMC of apo A-I.

The dependence of \bar{R}_h of apo A-II/DMPC mixed micelles on the lipid/protein ratio was also analyzed using equations 6 and 7. The data is shown in Table 3 and displayed in Figure 12b. There is a good fit to this model, yielding estimates of 60 Å for L, and 13% apo A-II by weight in the DMPC bilayer. The % DMPC at which \bar{R}_h diverges is lower for

apo A-II than for apo A-I. This difference can be attributed both to the higher IMC of apo A-II, as well as an increase in apo A-II solubility in the DMPC bilayer.

The size of apo A-II/DMPC complexes has been less well characterized. Massey et al. (1980) demonstrated by gel chromatography that three sizes of apo A-II/DMPC complexes are formed with 66, 75, and 91% DMPC, but did not estimate their actual sizes.

B. Apo A-I/EYPC Interactions. Apo A-I alters the phase limits of EYPC/TC solutions. As preformed EYPC/TC mixed micelles are diluted, TC dissociates to maintain the IMC. Since less TC is effectively available to solubilize the hydrocarbon chains of the lecithin, the EYPC/TC ratio within the mixed micelles falls. Therefore the size of the mixed micelles increases and \bar{R}_h diverges. However, in the presence of sufficient concentrations of apo A-I, this increase is diminished or entirely abolished (see Figures 6b-6f). Apo A-I is capable of replacing the TC and preserving the mixed micellar structure. If there is insufficient apo A-I present to form mixed micelles, vesicles are formed. The presence of very low apo A-I concentrations increases the measured \bar{R}_h of these vesicles. The form of the dependence of \bar{R}_h on apo A-I concentration in Figure 7 suggests that apo A-I complexes with vesicles in apo A-I concentrations as low as 0.0005 mg/ml. This concentration is much lower than the values of the IMC (0.08 mg/ml) estimated for apo A-I/EYPC mixed micelles.

The equilibrium binding distribution of apo A-I to preformed unilamellar EYPC vesicles has been studied by Chung et al. (1979) and Yokayama et al. (1980) by preparative ultracentrifugation and rapid gel filtration, respectively. Although their data do not permit direct comparison, the range of apo A-I concentrations over which we see alterations in \bar{R}_h is similar to the range over which binding occurs in their studies.

C. Kinetics of the Interaction of Apo A-I and Apo A-II with Lecithin. Since QLS allow the measurement of the size of mixed micelles at frequent intervals, we have been able to show that apo A-I/DMPC mixed micelles do not reach equilibrium for up to 48 hours. The initial rapid decrease in macroscopic turbidity when apo A-I or apo A-II interacts with DMPC (Jonas and Drengler, 1980) does not imply that equilibrium has been reached, since we observed continuous changes in \bar{R}_h for up to 48 hours. When equilibrium between monomeric apo A-I and apo A-I/DMPC mixed micelles is perturbed, the time required to reapproach equilibrium depends on the free apo A-I concentration. If the IMC of apo A-I is increased above the value in equilibrium with the mixed micelles, some of the free apo A-I associates with the mixed micelles, and \bar{R}_h decreases over a period of several hours. If the IMC of apo A-I is decreased below the equilibrium value (e.g., by dilution with buffer) apo A-I must dissociate from the mixed micelles to

maintain the IMC. However, the resultant increase in \bar{R}_h takes up to 72 hours. This implies that the activation energy of dissociation of an apo A-I molecule from the lecithin hydrocarbon tails must be much higher than the association of apo A-I molecules with a mixed micelle.

Since the reaction of apo A-I with DMPC when monitored by turbidity changes, occurs over minutes to several hours (Jonas and Drengler, 1980, Pownall et al., 1978), investigators have used incubation periods of 24 hours or less to form apo A-I/DMPC complexes. In light of our results we believe that this equilibrium period is insufficient and that at least 48 hours is required.

The temporal evolution of the micelle to vesicle transition is altered in the presence of apo A-I. At final values of % EYPC below 70% (total EYPC plus apo A-I concentration greater than 0.3 mg/ml), stable mixed micelles are formed which change only minimally in size over 48 hours. At final values between 70 and 90% EYPC, after 30 minutes \bar{R}_h increases slightly to values consistent with mixed micelles (less than 100 Å), but after 48 hours \bar{R}_h increases further to 300 to 400 Å. Therefore a metastable zone exists beyond the mixed micellar zone.

D. Pathophysiological Implications. Apolipoprotein/lecithin disc shaped particles and vesicles have been isolated from a variety of sources. Figure 14 demonstrates the dependence

PATHOPHYSIOLOGICAL CORRELATION OF NATIVE AND RECOMBINANT HDL'S WITH APO A-I - LECITHIN PHASE DIAGRAM

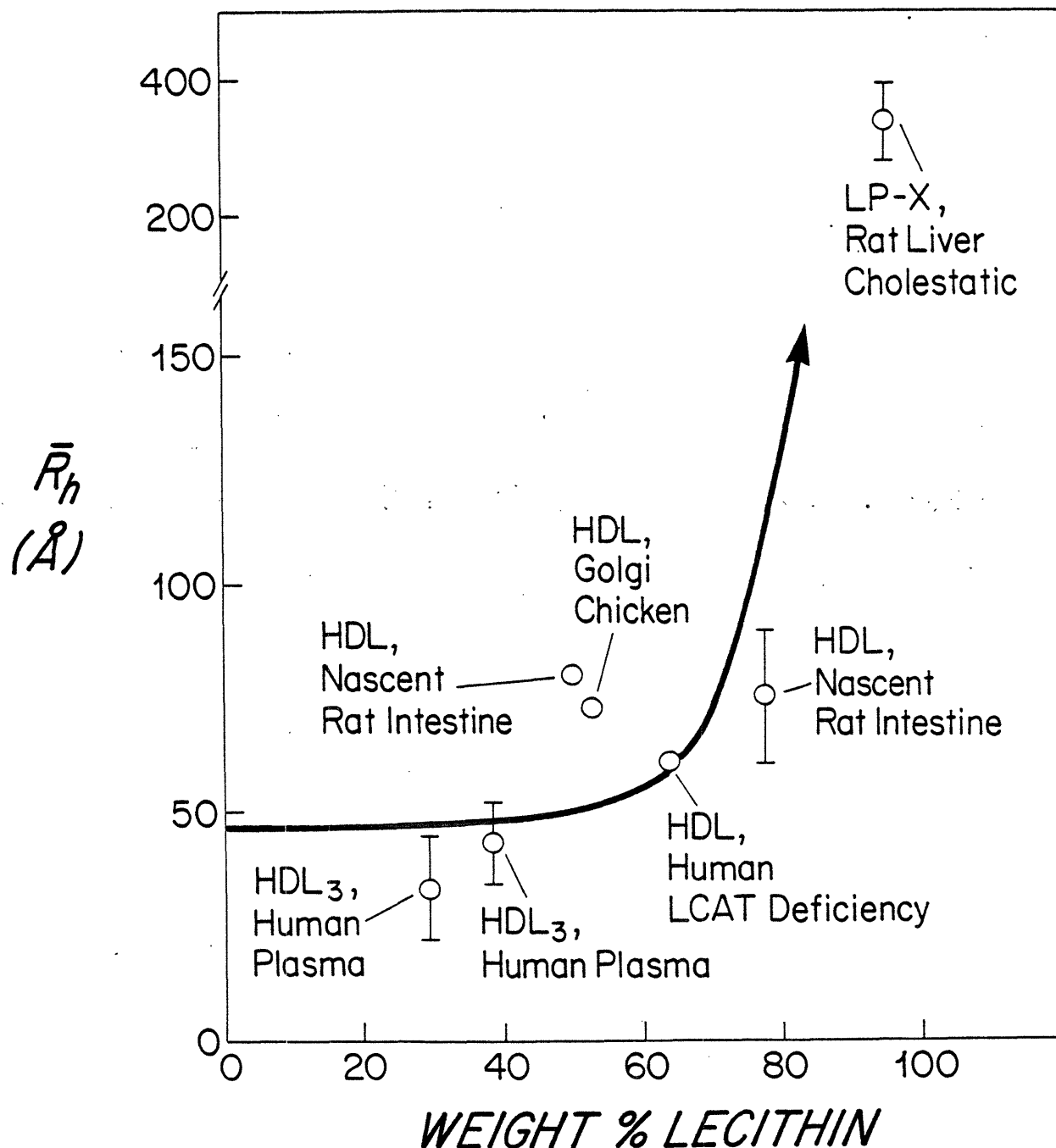


Figure 14. Dependence of \bar{R}_h of various native and model HDL's on % lecithin. Solid curve represents estimate of mixed micellar size of apo A-I/DMPC mixed micelles from this work. Literature values are described fully in the text.

of \bar{R}_h on % lecithin for our model system apo A-I/DMPC and for various HDL like particles described in the literature (calculated from electron microscopy data). In Figure 14 we show data for native HDL₂ and HDL₃ (Scanu et al., 1982); pathological HDL's: Lp-X from cholestatic rat liver (Felker et al., 1978) and HDL from patients with LCAT deficiency (Norum et al., 1971, Forte et al., 1971); nascent HDL's: from rat intestine (Green et al., 1978), and from chicken liver Golgi apparatus (Banerjee and Redman, 1983). Despite the presence of other lipids and apolipoproteins, there is a general trend of increasing size with increases in lecithin content. Therefore the size of HDL particles appears to be determined principally by the lecithin/apolipoprotein ratio of the particle under physiological conditions.

We have demonstrated that the size and stability of biliary lipid vesicles is altered in the presence of apo A-I concentrations found in bile (Figures 6b-6f). Since the formation of liquid crystalline vesicles is hypothesized to be an initial step in the formation of cholesterol gallstones, this suggests apo A-I may act as an antinucleating agent. In contrast to the influence of low apo A-I concentrations on biliary lipids, serum bile salt concentrations (several micromolar) (Carey, 1982) have little effect on the equilibrium interactions between apo A-I and lecithin which occur in serum.

Apo A-I is able to replace bile salts in preformed EYPC/TC mixed micelles. This mechanism implies that bile

salts or other physiological amphiphiles (e.g., lysolecithin, apolipoprotein E) may act as catalysts in the formation of apo A-I/native lecithin mixed micelles.

F. Summary. In conclusion, (1) we have non-invasively established the equilibrium phase diagram of apo A-I and apo A-II with DMPC as functions of concentration and temperature; (2) we have proposed three zones in the phase diagram, with apolipoprotein monomers, simple micelles, and apolipoprotein/lecithin mixed micelles; with apolipoprotein monomers and apolipoprotein/lecithin mixed micelles; and with vesicles and apolipoprotein monomers; and have measured the size and equilibrium concentrations of these species; and (3) we have estimated the monomer concentrations of both apo A-I and apo A-II in equilibrium with mixed micelles and vesicles, the intermicellar concentration; and (4) we have established that apo A-I is important in determining the solution state of biliary lipids at physiological gall bladder concentrations of apo A-I.

REFERENCES

Banerjee, D., and C.M. Redman, Biosynthesis of High Density Lipoprotein by Chicken Liver: Nature of Nascent Intracellular High Density Lipoprotein, *J. Cell Biol.* 96: 651-660 (1983).

Brouillette, C.G., J.L. Jones, T.C. Ng, H. Kercret, B.H. Chung, and J.P. Segrest, Structural Studies of Apolipoprotein A-I/Phosphatidylcholine Recombinants by High-field Proton NMR, Nondenaturing Gradient Gel Electrophoresis, and Electron Microscopy, *Biochemistry* 23: 359-367 (1984).

Carey, M.C., The Enterohepatic Circulation, in (I.M. Arias et al, ed.) The Liver: Biology and Pathobiology, 629-665 (1982).

Chung, J., D.A. Abano, G.M. Fless, and A.M. Scanu, Isolation, Properties and Mechanism of in vitro Action of Lecithin: Cholesterol Acyltransferase from Human Plasma, *J. Biol. Chem.* 254: 7456-7464 (1979).

Felker, T.E., R.L. Hamilton, and R.J. Havel, Secretion of Lipoprotein-X by Perfused Livers of Rats with Cholestasis, *Proc. Natl. Acad. Sci., U.S.A.* 75: 3459-3463 (1978).

Felker, T.E., R.L. Hamilton, J.L. Vigne, and R.J. Havel, Properties of Lipoproteins in Blood Plasma and Liver Perfusion of Rats with Cholestasis, *Gastro.* 83: 652-663 (1982).

Forte, T., K.B. Norum, J.A. Glomset, and A.V. Nichols, Plasma Lipoproteins in Familial Lecithin:Cholesterol Acyltransferase Deficiency: Structure of Low and High Density Lipoproteins as Revealed by Electron Microscopy, *J. Clin. Invest.* 50: 1141-1148 (1971).

Green, P.H.R., A.R. Tall, and R.M. Glickman, Rat Intestine Secretes Discoid High Density Lipoprotein, *J. Clin. Invest.* 61: 528-534 (1978).

Gurantz, D., M.F. Laker, A.F. Hofmann, Enzymatic Measurement of Choline Containing Phospholipids in Bile, *J. Lipid Res.* 33: 373-376 (1981).

Jonas, A., S.M. Drengler, Kinetics and Mechanism of Apolipoprotein A-I Interaction with L-alpha-dimyristoylphosphatidylcholine Vesicles, *J. Biol. Chem.*, 255: 2190-2194 (1980).

Jonas, A., S.M. Drengler, and B.W. Patterson, Two Types of Complexes Formed by the Interaction of Apolipoprotein A-I with Vesicles of L-alpha-dimyristoylphosphatidylcholine, *J. Bio. Chem.* 255: 2183-2189 (1980).

Lowry, O.H., N.J. Rosebrough, A.L. Farr, and R.J. Randall, Protein Measurement with the Folin Phenol Reagent, *J. Biol. Chem.* 193: 265-275 (1951).

Massey, J.B., A.M. Gotto, Jr., and H.J. Pownall, Dynamics of Lipid-Protein Interaction: Interaction of Apolipoprotein A-II from Human Plasma High Density Lipoproteins with Dimyristoylphosphatidylcholine, *J. Biol. Chem.* 255: 10167-10173 (1980).

Massey, J.B., A.M. Gotto, Jr., and H.J. Pownall, Human Plasma High Density Apolipoprotein A-I: Effect of Protein-Protein Interactions on the Spontaneous Formation of a Lipid-Protein Recombinant, *Biochem. Biophys. Res. Commun.* 99 466-474 (1981).

Matz, C.E., and A. Jonas, Micellar Complexes of Human Apolipoprotein A-I with Phosphatidylcholines and Cholesterol Prepared from Cholate-Lipid Dispersions, *J. Biol. Chem.* 257: 4535-4540 (1982).

Mazer, N.A., QLS Studies of Micelle Formation, Solubilization and Precipitation in Aqueous Biliary Lipid Systems, Ph.D. Thesis, M.I.T. (1978).

Mazer, N.A., G.B. Benedek, and M.C. Carey, QLS Studies of Aqueous Biliary Lipid Systems: Mixed Micelle Formation in Bile Salt-Lecithin Solutions, *Biochemistry* 19: 601-615 (1980).

Nichols, A.V., E.L. Gong, P.J. Blanche, and T.M. Forte, Characterization of Discoidal Complexes of Phosphatidylcholine, Apolipoprotein A-I and Cholesterol by Gradient Gel Electrophoresis, *Biochim. Biophys. Acta.* 750: 353-364 (1983).

Norum, K.R., J.A. Glomset, A.V. Nichols, T. Forte, Plasma Lipoproteins in Familial Lecithin: Cholesterol Acyltransferase Deficiency: Physical and Chemical Studies of Low and High Density Lipoproteins, *J. Clin. Invest.* 50: 1131-1140 (1971).

Pownall, H.J., J.B. Massey, S.K. Kusserow, and A.M. Gotto, Jr., Kinetics of Lipid-Protein Interactions: Interaction of Apolipoprotein A-I from Human Plasma High Density Lipoproteins with Phosphatidylcholines, *Biochemistry* 17: 1183-1188 (1978).

Pownall, H.J., Q. Pao, M. Rohde, and A.M. Gotto, Jr., Lipoprotein-Apoprotein Exchange in Aqueous Systems: Relevance to the Occurrence of Apo A-I and Apo C Proteins in a Common Particle, *Biochem. Biophys. Res. Commun.* 51: 408-414 (1978).

Sewell, R.B., S.J.T. Mao, T. Kawamoto, and N.F. LaRusso, Apolipoproteins of High, Low and Very Low Density Lipoproteins in Human Bile, *J. Lipid Res.* 24: 391-401 (1983).

Scanu, A.M., C. Edelstein, and B.W. Shen, Lipid Protein Interactions in the Plasma Lipoproteins. Model: High Density Lipoproteins, in Lipid Protein Interactions (P.C. Jost and O.H. Griffith, eds.), Wiley & Sons, New York, 259-317 (1982).

Swaney, J.B., Properties of Lipid-Apolipoprotein Association Products. Complexes of Dimyristoyl Phosphatidylcholine and Human Apo A-I, *J. Bio. Chem.* 255: 877-881 (1980).

Tall, A.R., D.M. Small, Body Cholesterol Removal: Role of Plasma High Density Lipoproteins, *Adv. Lipid Res.* 17: 1-51 (1980).

Tall, A.R., D.M. Small, R.J. Deckelbaum, and G.G. Shipley, Structure and Thermodynamic Properties of High Density Lipoprotein Recombinants, *J. Biol. Chem.* 253: 4701-4711 (1977).

Yokoyama, S., D. Fukushima, J.P. Kupferberg, F.J. Kedzy, and E.T. Kaiser, The Mechanism of Activation of Lecithin: Cholesterol Acyl Transferase by Apolipoprotein A-I and an Amphiphilic Peptide, *J. Biol. Chem.* 255: 7333-7339 (1980).

ACKNOWLEDGEMENTS

There are many people who have helped in making my experience at M.I.T. and Harvard enjoyable and rewarding, and I would like to take this opportunity to thank them all. In particular, I would like to thank the following.

I would like to thank my thesis advisors, Dr. Martin Carey and Professor George Benedek who have taught me much. I appreciate all the time spent over the years launching me on my career. They have taught me how to think critically, and the time spent with them will stand me in good stead for many years.

My colleagues in Dr. Carey's and Professor Benedek's laboratories, past and present, are due thanks for their helpfulness and companionship throughout the years. Dr. Norman Mazer's work was an inspiration for my own, and his interest in this work, stimulating discussions, helpful suggestions as well as friendship were appreciated. Without Dr. Michael Fisch, the high pressure experiments would have been impossible, and I gratefully acknowledge his help. I would like to thank Professor Mary Roberts for her stimulating ideas and discussions.

I would like to thank Mrs. Grace Ko for her many hours of help. I gratefully acknowledge Ms. Rebecca Ankener for her incredibly fast typing of many drafts of my work throughout the years. The help of Mrs. Patricia Jones is also greatly appreciated. Ms. Esther Simon is due special thanks for her excellent work on the graphical illustrations.

I have been very fortunate to be associated with the Harvard/M.I.T. Health Sciences and Technology program in Medical Engineering. Many people have worked hard to make this program a success, and their efforts are greatly appreciated. I would like to thank Dr. Irving London, Dr. Ernest Cravahlo, Dr. Frederick Bowman, Ms. Keiko Oh, Ms. Carol Cogliani, Dr. Daniel Federman, and Ms. Noreen Koller. Dr. Walter Abelman was a source of support and excellent advice throughout the years. I greatly appreciate the financial support I received from the H.S.T. program. I also am indebted to the Whitaker Fund for a Whitaker Fund Fellowship.

I gratefully express my love and thanks to my parents, the rest of my family, my family-in-law, and my friends who have given me many years of love and support. My daughter Laura also deserves thanks for her hours of sleep, as well as her inspiration. My husband Bob has been an unwavering source of love and support for many years, and without his help, this thesis would not be a reality.

BIOGRAPHY

Joanne Marie Donovan was born May 12, 1956 and is the only child of Barbara J. and D. Joseph Donovan of Brighton, Ma. She attended St. Columbkille Grammar School and was fortunate to be awarded a full scholarship to attend Mount Saint Joseph Academy. There her interest in science was stimulated by the teaching and friendship of Sister Marie Therese Martin. She attended the College of the Holy Cross in Worcester, Ma., and transferred to the Massachusetts Institute of Technology in February, 1975. She began her research career in Dr. Christopher Walsh's laboratory in the Department of Chemistry, and graduated in 1977 with bachelor's degrees in chemistry and biology. She then entered the Department of Chemical Engineering at M.I.T., where she received a master's degree. Her thesis on low density lipoprotein transport in the aortic wall of rabbits was done in the laboratories of Professors Kenneth Smith and Clark Colton, and Dr. Robert Lees.

In 1978, Donovan entered the first class of the Harvard/M.I.T. Health Sciences and Technology doctoral program in Medical Engineering and Medical Physics. Her thesis work was conducted in the laboratories of Professor George Benedek, Department of Physics, M.I.T., and Dr. Martin Carey, Associate Professor of Medicine, Harvard Medical School. She presented her research findings at two national meetings of the American Gastroenterological Association for which she won the Student

Research Prize. She entered Harvard Medical School in 1982, and simultaneously pursued the M.D. and Ph.D. degrees.

In 1977, Donovan was married to Robert Hallett, and on July 12, 1984 gave birth to their first child, Laura. In June, 1984, she began a medical internship and residency at the Brigham and Women's Hospital in Boston, Ma.